USGS
science for a changing world

Prepared in cooperation with California Department of Water Resources

Precipitation-Runoff Processes in the Merced River Basin Central California, with Prospects for Streamflow Predictability, Water Years 1952–2013

Scientific Investigations Report 2020–5150

U.S. Department of the Interior
U.S. Geological Survey

Cover: Yosemite Valley looking eastward towards the upper Merced watershed and the Sierra Nevada crest. Photograph taken by Florence Low, February 5, 2014.

Precipitation-Runoff Processes in the Merced River Basin, Central California, with Prospects for Streamflow Predictability, Water Years 1952–2013

By Kathryn M. Koczot, John C. Risley, JoAnn M. Gronberg, John M. Donovan, and Kelly R. McPherson

Prepared in cooperation with California Department of Water Resources

Scientific Investigations Report 2020–5150

U.S. Department of the Interior
U.S. Geological Survey

U.S. Geological Survey, Reston, Virginia: 2021

Suggested citation:
Koczot, K.M., Risley, J.C., Gronberg, J.M., Donovan, J.M., and McPherson, K.R., 2021, Precipitation-runoff processes in the Merced River Basin, Central California, with prospects for streamflow predictability, water years 1952–2013: U.S. Geological Survey Scientific Investigations Report 2020–5150, 61 p., https://doi.org/10.3133/sir20205150.

Associated data for this publication:
Koczot, K.M., Risley, J.C., Gronberg, J.M., Donovan, J.M., and McPherson, K.R., 2021, Archive of Merced River Basin Precipitation-Runoff Modeling System, with forecasting, climate-file preparation, and data-visualization tools: U.S. Geological Survey data release, https://doi.org/10.5066/F7JH3KFR.

ISSN 2328-0328 (online)

Acknowledgments

This study was conducted by the U.S. Geological Survey (USGS) in cooperation with the California Department of Water Resources (DWR) Cooperative Snow Surveys Program (CCSS). David Rizzardo, formally Chief of Snow Surveys, provided guidance and motivation for this undertaking. Along with the DWR's consultants, John King and Sean de Guzman of the Snow Surveys Section reviewed and provided climate-station datasets used in the Merced River Basin Precipitation-Runoff Modeling System (PRMS). Merced Irrigation District and Steve Nemeth of DWR's Snow Surveys Section provided reconstructed streamflow data used as a calibration target. The authors appreciate the assistance of Steven Markstrom and R. Steven Regan, USGS, Denver, Colorado, who provided modeling direction, troubleshooting guidance, and computer programs as PRMS software evolved to the version used in this study.

Contents

Figures

Tables

Conversion Factors

U.S. customary units to International System of Units

Multiply	By	To obtain
	Length	
inch (in.)	2.54	centimeter (cm)
inch (in.)	25.4	millimeter (mm)
foot (ft)	0.3048	meter (m)
mile (mi)	1.609	kilometer (km)
	Area	
acre	4,047	square meter (m^2)
square mile (mi^2)	2.590	square kilometer (km^2)
	Volume	
cubic foot (ft^3)	0.02832	cubic meter (m^3)
acre-foot (acre-ft)	1,233	cubic meter (m^3)
	Flow rate	
cubic foot per second (ft^3/s)	0.02832	cubic meter per second (m^3/s)
	Solar radiation	
Langley (Ly)	41,868	Joules/square meter (J/m^2)
Langley (Ly)/day	0.484583	Watt/square meter ($Watt/m^2$)

Temperature in degrees Fahrenheit (°F) may be converted to degrees Celsius (°C) as follows:

$$°C = (°F - 32) / 1.8.$$

Datum

Vertical coordinate information is referenced to the North American Vertical Datum of 1988 (NAVD 88).

Horizontal coordinate information is referenced to the North American Datum of 1983 (NAD 83).

Altitude, as used in this report, refers to distance above the vertical datum.

Supplemental Information

Water year constitutes a 12-month period from October 1 through September 30 and designated by the year in which the period ends. For example, water year 1995 begins October 1, 1994, and ends September 30, 1995.

Abbreviations

CBH	climate-by-HRU dataset formatted for PRMS
CDEC	California Data Exchange Center
CNRFC	National Oceanic and Atmospheric Administration's California-Nevada River Forecasting Center
DRI	Desert Research Institute
DWR	California Department of Water Resources
ESP	Ensemble Streamflow Prediction
FNF	full-natural (streamflow) flow, synomous with reconstructed streamflow
GDP	USGS Geo Data Portal
GIS	geographic information system
HEC	U.S. Army Corps of Engineers Hydrologic Engineering Center
HRU	hydrologic response unit
LUCA	Let Us Calibrate
MRC	Merced River near Merced Falls CDEC streamflow station designation
MID	Merced Irrigation District
NOAA	National Oceanic and Atmospheric Administration
NREL	National Renewable Energy Laboratory
NWSRFS	National Weather Service River Forecasting System
OUI	Object User Interface
PET	potential evapotranspiration
PPT	precipitation data
PRISM	Parameter Elevation Regressions on Independent Slopes Model
PRMS	Precipitation-Runoff Modeling System
RMSE	root-mean-square error
TMAX	maximum temperature data
TMIN	minimum temperature data
TNY	Tenaya Lake CDEC climate station designation (also listed on table 1).
USGS	U.S. Geological Survey

Precipitation-Runoff Processes in the Merced River Basin, Central California, with Prospects for Streamflow Predictability, Water Years 1952–2013

By Kathryn M. Koczot, John C. Risley, JoAnn M. Gronberg, John M. Donovan, and Kelly R. McPherson

Abstract

The U.S. Geological Survey, in cooperation with the California Department of Water Resources (DWR), has constructed a new spatially detailed Precipitation-Runoff Modeling System (PRMS) model for the Merced River Basin, California, which is a tributary of the San Joaquin River in California. Operated through an Object User Interface (OUI) with Ensemble Streamflow Prediction (ESP) and daily climate distribution preprocessing functionality, the model is calibrated primarily to simulate (and eventually, forecast) year-to-year variations of inflows to Lake McClure during the critical April–July snowmelt season. The model is intended to become part of a suite of methods used by DWR for estimating daily streamflow from the Merced River Basin, especially during the snowmelt season. This study describes the results of the application of an analysis tool that simulates responses to climate and land-use variations at a higher spatial resolution than previously available to DWR.

A geographic information system was used to delineate the model domain, that is, areas draining to a single outlet at U.S. Geological Survey streamflow-gaging station 11270900, Merced River below Merced Falls Dam, near Snell, CA (also known as California Data Exchange Center station MRC), and subdrainage areas, including four draining to internal gages used as calibration targets. Using this delineation, three contiguous subbasins were recognized and, along with the model domain and nested calibration targets, are the simulation units evaluated in this report.

An auto-calibration tool, LUCA (Let Us CAlibrate), was used for each calibration node, from headwaters to basin outlet, and then parameters were manually adjusted to complete the calibration. The main objective was to match April–July snowmelt seasonal discharge values of simulated streamflow to observed (measured or reconstructed) discharge values. Calibration or validation periods used site-specific streamflows—mostly from October 1, 1988, through September 30, 2013—but differed according to the period-of-record available for the measurements collected at internal gages or reconstructed flows for the single outlet.

The accuracy of the Merced PRMS streamflow simulations varied seasonally, as compared to observed values. Based on statistical results, the Merced PRMS model satisfactorily simulated snowmelt seasonal streamflows. April–July calibrations for all areas had small negative bias (not greater than 7 percent) and low relative error (less than 8 percent). Less satisfactory performance for other seasons was attributed to several factors: (1) high uncertainty in low or zero flows in summer and fall, (2) lack of accounting for basin withdrawals and anthropogenic water use, (3) unavailability and (or) inaccuracy of observed (measured) meteorological input data, and (4) uncertainty in reconstructed streamflow data.

With some additional refinement, the Merced PRMS model may be used for forecasting seasonal and longer-term streamflow variations; evaluating forecasted and past climate and land cover changes; providing water-resource managers with a consistent and documented method for estimating streamflow at ungaged sites within the basin; and aiding environmental studies, hydraulic design, water management, and water-quality projects in the Merced River Basin.

Introduction

The Merced River Basin in Mariposa and Madera Counties, California (fig. 1), is a largely undeveloped, west-facing central Sierra Nevada watershed with headwaters covering the southern half of the majestic Yosemite National Park. Maintained mainly for outdoor recreation, fish-and-wildlife enhancements, national forest conservation, and timber, streamflows from this watershed provide irrigation and municipal water and generate hydropower for use in downstream Merced County. Releases from the controlling reservoir, Lake McClure (near the model-domain outlet; capacity 1,032,000 acre-feet [acre-ft]; California Department of Water Resources, 2020a), and downstream regulating reservoir, Lake McSwain (capacity 9,700 acre-ft; California Department of Water Resources, 2020a), balance hydropower and irrigation demand, reduce flooding risks, and aid in maintaining downstream San Joaquin River water-quality standards. For many decades, water management of this basin has relied on a series of single point statistical models or a lumped physically based model that forecast streamflows into New Exchequer Dam near the basin outlet. To augment these forecasts, it would be a great advantage to account for snowpack formation and streamflows from internal parts of the basin to plan for what may melt in spring and better support reservoir management. The method presented in this study offers a physically based hydrologic model with higher resolution than previously available to (1) better represent both land cover and the effects of climate variation, (2) allow the operator flexibility to simulate and understand streamflow responses to climate variations or land cover changes from internal parts of the basin, and (3) aid in seasonal streamflow forecasting. This improved understanding of how the Merced River responds to changing climate and land-management actions that cause streamflow timing and quantity to change from season to season or year to year will help water managers safeguard this resource.

The climate of the western slope of California's Sierra Nevada is characterized by warm, dry summers and cool, wet winters and springs, with precipitation occurring principally from November through March. This region experiences some of the largest year-to-year climate fluctuations in the United States, and climate is known to vary considerably on interdecadal time scales (Dettinger and others, 2018a, b). Water-resource managers tend to focus on the annual wet period for forecasting streamflow, planning for and managing reservoirs for winter floods, and measuring snowpack accumulation. California Department of Water Resources (DWR) and other managers must also plan for and forecast warm-season streamflow from melting snow. DWR defines snowmelt season as April 1–July 31 and assumes April 1 snowpack accumulations represent annual accumulations (California Department of Water Resources, 2020b; https://cdec.water.ca.gov/snow/bulletin120/index2.html). During the snowmelt season, when flood-generating storms are uncommon, Lake McClure receives about 65 percent of its annual total inflow on average (https://cdec.water.ca.gov/dynamicapp/staMeta?station_id=MRC).

Part of watershed management includes climate (measured as temperature and precipitation trends) and land-cover-related risk assessment as these changes impact resulting streamflows. Therefore, another challenge California watershed managers face is that studies show a warming trend combined with precipitation-pattern shifts in the last decades outside of normal and expected climatic shifts (Dettinger and Cayan, 1995; Peterson and others, 1999, 2000; Cayan and others, 2001; Dettinger and others, 2001, Miller and others, 2001; Schmidt and Webb, 2001; McCabe and Dettinger, 2002; Miller and others, 2003; Simpson and others, 2004; Stewart and others, 2004a, b; Dettinger, 2005a, b; Mote and others, 2005; California Department of Water Resources, 2006; Anderson and others, 2008; Brekke and others, 2009; Lundquist and others, 2009; Intergovernmental Panel on Climate Change, 2014; United States Global Change Research Program, 2017; Dettinger and others, 2018a, b; Thorne and others, 2018). A changing (dryer and warmer) climate has resulted in an increase in forest fires (Westerling and others, 2006; Westerling, 2019). The Sierra Nevada historical average snowline elevation (that is, the elevation that generally differentiates the seasonal snowpack from areas that can have intermittent snow cover) passes through the Merced River Basin model domain at 5,500 feet (ft), making the timing of runoff and streamflows in parts of the model domain especially sensitive to slight changes in temperature. In the future, possibly warmer temperatures may result in more frequent winter high flows, leaving less snowpack in late spring to melt and replenish reservoirs and meet late-summer and fall water demands (Bardini and others, 2001; California Department of Water Resources, 2006; Freeman, 2002; Jeton and others, 1996; Miller and others, 2003). The consequences of these climate trends create additional challenges for longer term (multi-year) watershed management and reservoir operations, as historical records of daily climate used to drive streamflow simulations may no longer be a reasonable indication of future events.

The DWR publishes summaries of warm-season water availability in California each month from February through May (http://cdec.water.ca.gov/snow/bulletin120/). These summaries include streamflow forecasts for the April through July snowmelt season. Forecasts for the Merced River Basin are based on statistical relationships between seasonal (and monthly) inflows to Lake McClure/Lake McSwain and observed previous and expected streamflow, precipitation, and snowpack conditions. The DWR and other water managers use these forecasts to plan summer water deliveries and to schedule releases from reservoirs.

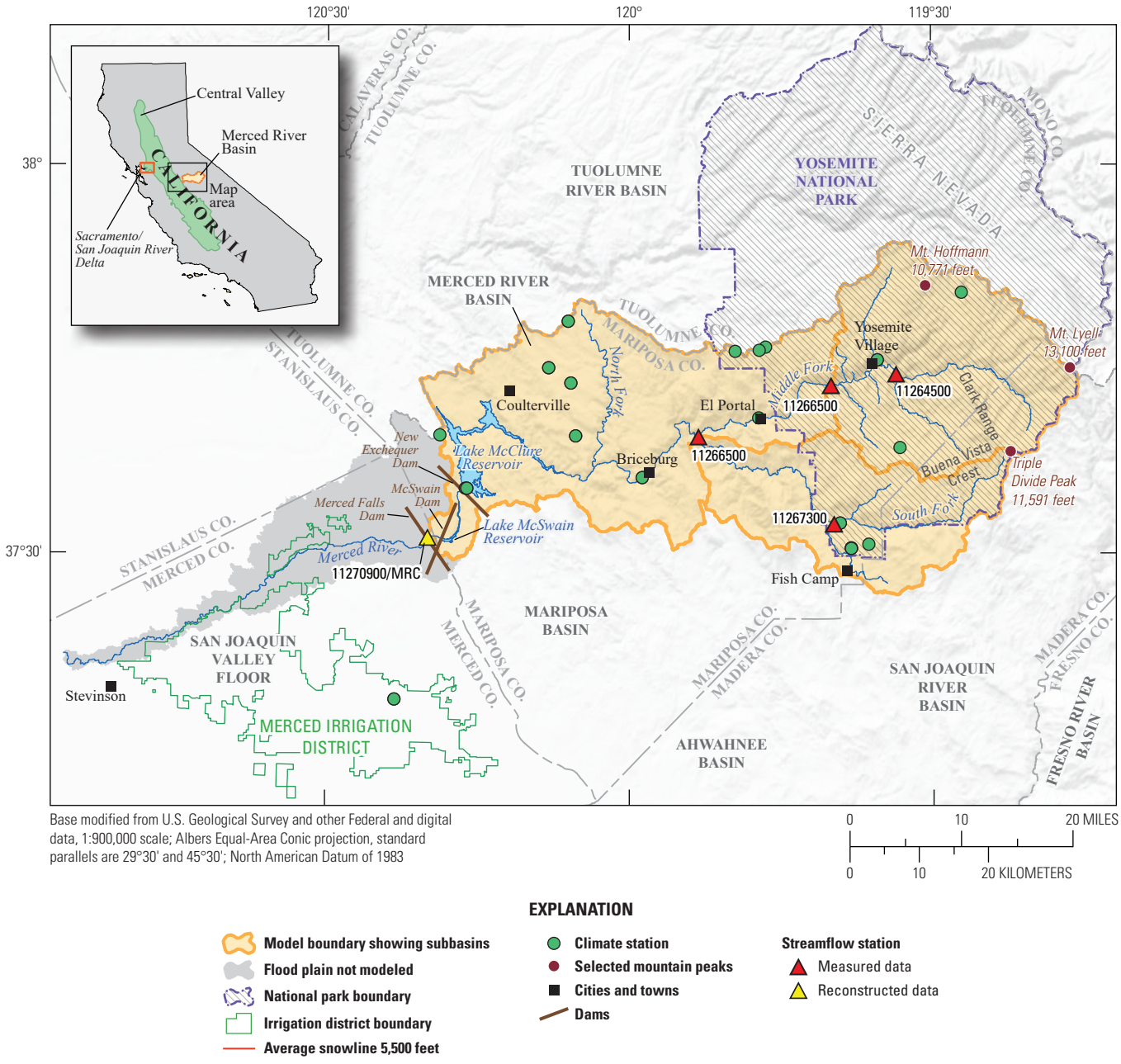

Base modified from U.S. Geological Survey and other Federal and digital data, 1:900,000 scale; Albers Equal-Area Conic projection, standard parallels are 29°30' and 45°30'; North American Datum of 1983

Figure 1. Merced River Basin, California, and the Precipitation-Runoff Modeling System model domain.

In addition to seasonal forecasts, there is a need to improve medium-range (1 week to 1 month) streamflow forecasts. Currently, in the Merced River Basin, DWR makes medium-range forecasts of total streamflow at DWR's station, Merced River near Merced Falls (California Data Exchange Center [CDEC] station MRC; http://cdec.water.ca.gov/staInfo.html), and, also, hydroelectric power operators use their own suite of statistical models to manage power generation. Additionally, agricultural, fishery, logging, recreational, and local user groups may benefit from improved medium-range forecasts.

In cooperation with DWR and with assistance from Merced Irrigation District (MID), the major hydropower operator in the basin who provided calibration data at the basin outlet and general information on climate and streamflow, a physically based distributed-parameter model of the Merced River Basin has been constructed and calibrated using the Precipitation-Runoff Modeling System (PRMS; Markstrom and others, 2015). This model was developed to simulate responses to climate and land-use variation at a higher spatial resolution than existing single-point statistical or lumped models. By incorporating more information about the basin's physical characteristics than is possible in statistical models, this physically based model may improve forecasts and increase understanding of the basin hydrology. The PRMS model presented in this study was designed to simulate streamflow responses to variations of temperature, precipitation, and land cover, and is currently focused on simulating April–July streamflow totals.

Purpose and Scope

This report documents the deterministic, distributed-parameter, physical-process-based PRMS model constructed for the Merced River Basin, California (hereafter referred to as "the model"). Data used for this modeling effort are from October 1, 1948, through September 30, 2013 (water years 1949–2013). The model domain is composed of 19 nested drainage areas delineated from 19 internal stream sites (represented either as nodes or actual physical gages) and one outflow site. These were identified by local stakeholders as points of interest for simulations on stream reaches. Calibrations were conducted at four gages internal to the basin and at the one gaged outlet, for a total of five streamflow-calibration targets. From this configuration, the model has been evaluated in this study as three contiguous subbasins. This report characterizes the Merced River Basin's precipitation, temperature, snowpack evolution, and water and energy balances that determine streamflow rates from and within the basin above outflow site U.S. Geological Survey (USGS) streamflow station 11270900 (physically located at DWR's CDEC station MRC), referred to in this study as 11270900/MRC. This report further documents the functionality of the model to assess the (physically based) predictability of seasonal inflows to Lake McClure.

Previous Modeling Studies

Many different methods have been developed and are used to forecast streamflows past 11270900/MRC. Here we briefly review previous hydrologic modeling studies of the Merced River Basin and other related applications of the PRMS modeling code used here.

At the time of this study, several statistical (regression) models were used by DWR (John King and Steve Nemeth, DWR Snow Surverys Section, written commun., 2015) and MID (Marco Bell, MID, written commun., 2015) to simulate streamflow in the Merced River Basin for various timeframes. A model for forecasting a month ahead (run from about January through August) is used to predict annual streamflow based on antecedent streamflow and on wetness-dependent scenarios of future streamflows (based on historical analogs) to complete the year. The predicted annual totals are then disaggregated into monthly natural streamflow amounts based on historical flow patterns. MID also uses a daily statistical streamflow model that combines recent estimates of daily (natural) flows with 10 days of weather forecasts followed by historical median precipitation rates to predict daily streamflow. The model is calibrated to the existing record by a least-squares fitting technique.

The National Oceanic and Atmospheric Administration (NOAA) California-Nevada River Forecasting Center (CNRFC; https://www.wrh.noaa.gov/cnrfc/) employs the National Weather Service River Forecasting System (NWSRFS) for flood and water-supply forecasting for the Merced River Basin. This system includes the Sacramento Soil Moisture Accounting Model (Burnash and others, 1973) and a snow accumulation and ablation component (Anderson, 1973). The physically based model spatially lumps basin characteristics and hydrologic processes separately for two altitude bands within which snow is expected to accumulate and not accumulate, respectively. Daily, weekly, and seasonal streamflow forecasts are made using the Ensemble Streamflow Prediction (ESP) method (Day, 1985). ESP develops an ensemble of forecast scenarios by combining current model conditions (observed initial conditions) with temperature and precipitation observations from previous years. This procedure yields a probabilistic distribution of possible outcomes that can be analyzed by the forecaster.

The DWR uses statistical models to forecast April through July and water-year volumes of estimated natural inflow past streamflow station 11270900/MRC. These forecasts generally are updated weekly from February through June. Forecasts are issued for probability levels ranging from 10 to 99 percent exceedance levels based on historical distributions of precipitation, snowpack accumulation, and model error subsequent to the forecast date. Snow-water content from snow courses, 10 snow sensors, precipitation gages, and prior streamflow from the Merced River Basin have been regressed against historical streamflow volumes to develop the DWR prediction model. Specifically, data from each station are divided by the historical mean (50-year average), then weighted (in the case of precipitation) by month, averaged for a group of stations for each basin, and raised to a power (if needed) to account for a nonlinear relation with streamflow. The resulting basin indices of precipitation, snowpack, and prior streamflow are used as predictors of streamflow in a linear equation developed as a multiple linear regression. This same technique is used for about 30 other basins within California (J. Pierre Stephens, DWR Resources Hydrology Branch, unpub. data, 2002; Koczot and others, 2005).

The DWR forecasts streamflow for 1 to 20 days with physically based models that use observed and predicted precipitation and temperatures. The physically based models track snow and groundwater in the basin. The models include HED71 (Buer, 1988), which was developed by DWR and the NWSRFS. During the spring snowmelt season, this latter model is operated in ESP mode for forecast leads of 20 or more days by blending 7 days of weather forecasts with historical weather conditions. Previously, flood forecasting was done with other models, including U.S. Army Corps of Engineers Hydrologic Engineering Center (HEC) models and predecessors of the NWSRFS (J. Pierre Stephens, DWR Resources Hydrology Branch, unpub. data, 2002; Koczot and others, 2005).

The USGS has completed two other non-real-time PRMS models that are also referred to as "Merced." The older model was built using 1990s PRMS code (Leavesley and others, 1983, 1996; Leavesley and Stannard, 1995), which contained more basinwide "lumped" parameters and did not include subbasin areas and internal routing that are part of the current version. This 1990s version covers only the upper part of our model domain above the Happy Isles gage, "Merced River at Happy Isles Bridge near Yosemite" (USGS 11264500; fig. 1). It was never formally documented but has been used in climate and streamflow studies (Dettinger and others, 1997; Dettinger and others, 1998; Dettinger and others, 2004; Lundquist and others, 2009; Simpson and others, 2004). The second version was built between 2012 and 2015 to simulate streamflows past Pohono Bridge at "Merced River at Pohono Bridge near Yosemite, CA" (USGS 11266500; fig. 1). The gage is located downstream from Happy Isles gage and covers only the Pohono Subbasin described in this report. This version was developed as a case-study example for the release of the PRMS code (version 4.2; Markstrom and others, 2015). Although similarly discretized as the Pohono Subbasin model described in this report (and borrowed by Markstrom and others, 2015, from our early unpublished work), this 2015 version was developed to illustrate the application of two different climate distribution module options available in PRMS. It is driven by regional, historical climate data. This illustrative PRMS model was not calibrated for the local, real-time datasets used to drive the model that is the focus of this report.

PRMS has been applied in many similar modeling studies for the purposes of simulating snow accumulation, melt, runoff, and streamflow for many alpine basins, including some in the Sierra Nevada, California (Jeton and LaRue Smith, 1993; Jeton and others, 1996; Jeton, 1999, 2000; Wilby and Dettinger, 2000; Koczot and others, 2005; Koczot, USGS, written commun., 2020; Markstrom and others, 2012, 2015; https://wwwbrr.cr.usgs.gov/projects/SW_MoWS/Bibliography.html). PRMS models have been used to explore watershed response to various combinations of climate change (Leavesley and others, 1983; Hay and others, 1993; Leavesley and Stannard, 1995; Jeton and others, 1996; Ryan, 1996; Wilby and Dettinger, 2000; Leavesley and others, 2002; Dettinger and others, 2004; Hay and others, 2011; Markstrom and others, 2015) and land-cover changes (Leavesley and others, 1983; Puente and Atkins, 1989; Risley, 1994; Leavesley and Stannard, 1995; Leavesley and others, 2002; Dettinger and others, 2004 Markstrom and others, 2015). The use of snow depletion curves derived from SNODAS to improve snowmelt forecasts has been tested and described by Driscoll and others (2017).

Knowledge gained in previous work (as cited above), and especially in the construction and implementation of other Sierra Nevada PRMS models (including parameter settings), was built upon to develop the model described in this report.

Physical Characteristics of the Merced River Basin

The PRMS model domain is the drainage area upstream of streamflow station 11270900/MRC, which covers 1,059 square miles (mi^2) of the western slopes of the Sierra Nevada, east of California's Central Valley, between the Tuolumne, Mariposa, Ahwahnee, and San Joaquin River Basins (fig. 1). Altitudes range from about 300 feet just below Merced Falls Dam to about 13,000 feet on the eastern drainage divide at Mount Lyell (fig. 2). Headwaters (about 500 mi^2) cover the southern half of Yosemite National Park (elevations 4,000 to 13,000 feet). Fifty-three percent of the basin lies below the Sierra Nevada historical snowline altitude of 5,500 feet (fig. 2).

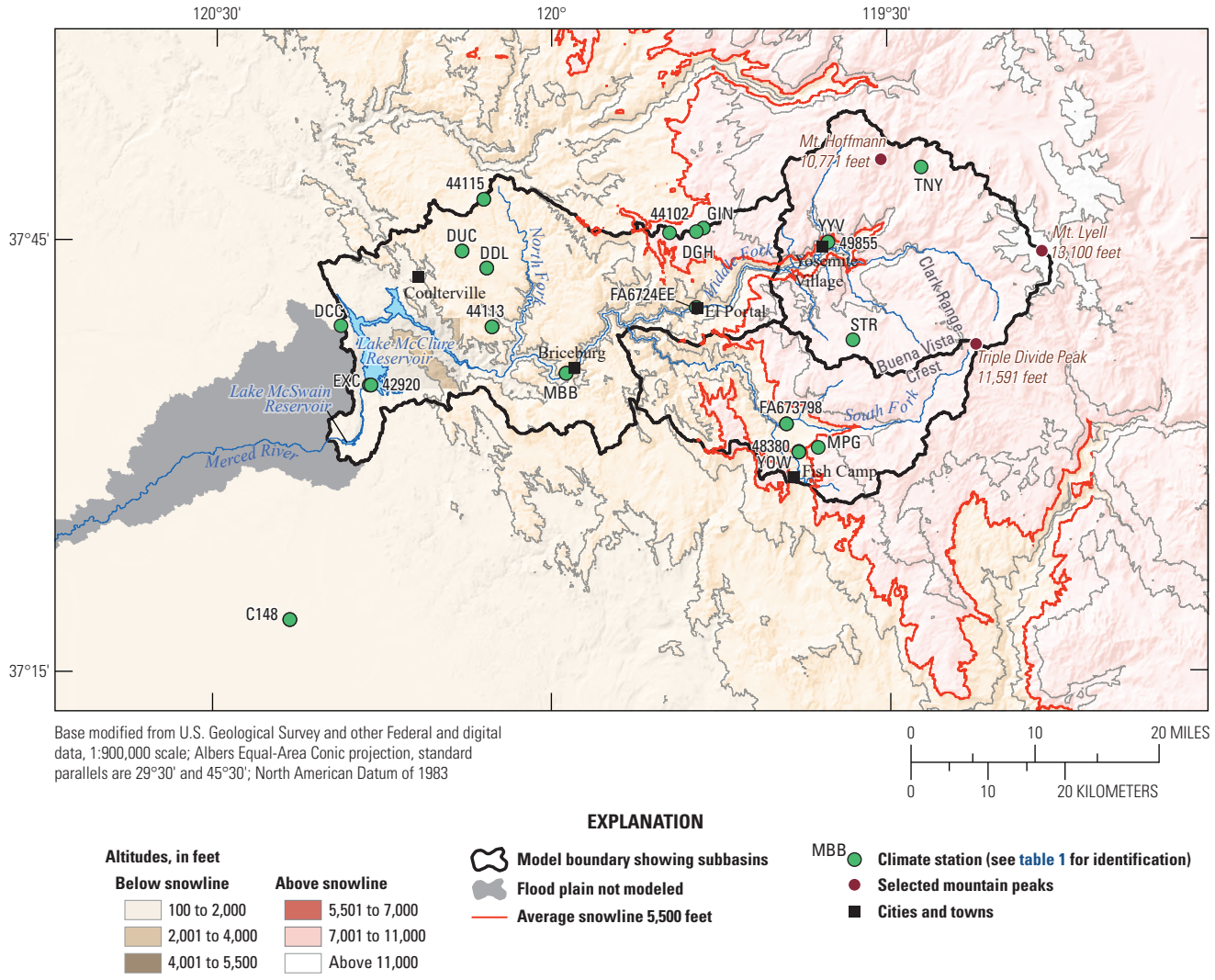

Figure 2. Merced River Basin model domain, showing altitudes above and below the average Sierra Nevada snowline (5,500 feet; North American Vertical Datum of 1988 [NAVD 88]).

Three major tributaries—the North, Middle, and South Fork Merced Rivers—drain into the mainstem of the Merced River, which flows into Lake McClure. The channel is hydrologically engineered downstream of the confluence with the North Fork Merced River, which impedes natural streamflows into the lower flood plain. New Exchequer (forming Lake McClure, also known as Exchequer Reservoir), McSwain, and Merced Falls Dams are part of this system (fig. 1). These are operated by MID (https://mercedirwmp.org/) for irrigation, hydroelectric power production, and downstream streamflow regulation as part of the Merced Falls Hydroelectric Project (http://mercedid.org/; appendix 1; fig. 1.1).

Land cover is primarily natural vegetation, which includes coniferous trees with hardwoods, shrubs, and grasses (fig. 3). Hardwoods are more prevalent at middle and lower elevations of the model domain, and shrubs and grasses are more prevalent at lower elevations. Small agricultural fields exist along the valley floor between Yosemite National Park and Lake McClure. This basin is part of the Stanislaus and Sierra National Forests where timber is harvested. Barren rock outcroppings are present above the tree-line altitude of about 9,500 feet (https://www.us-parks.com/yosemite-national-park/vegetation.html). This model domain is sparsely populated and contains only a few small towns (fig. 1; http://censusviewer.com/county/CA/Mariposa, which lists 18,251 persons as the 2010 population).

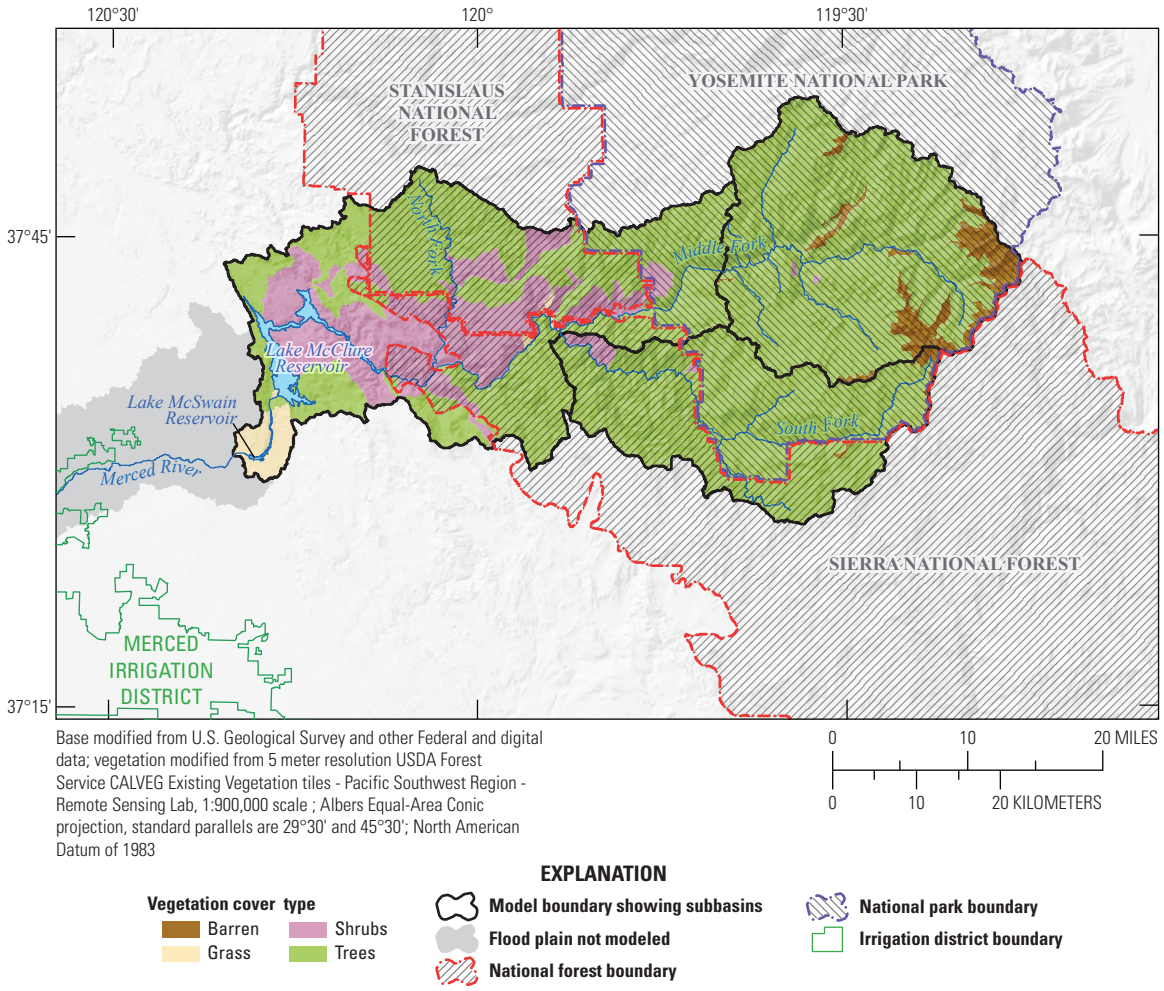

Figure 3. Vegetation cover in the Merced River Basin, California.

The Merced River Basin is composed primarily of pre-Tertiary granitic rocks and separated from the Central Valley by a foothill belt of marine and metavolcanic rocks (Huber, 1989). Higher altitudes are underlain by granitic igneous rock, with some sedimentary rock. Lower altitudes near Lakes McClure and McSwain are underlain by sedimentary and volcanic rocks (figs. 2, 4*A*). In this study, geology (Jennings and others, 1977; fig. 4*A*) is classified according to how it affects surface runoff, soil infiltration, shallow baseflow, and generally, the transmission of water to streams. The classes are (1) volcanic formations (pyroclastic flows and volcanic mudflows); (2) sedimentary formations (marine and non-marine sediments, shales, dolomites, Quaternary sediments such as alluvium, playas, terraces, glacial till, and moraines); and (3) intrusive igneous formations (granites and ultramafics). Volcanic formations have the highest permeability and the potential to contribute the highest amount of groundwater to streams, whereas igneous formations produce the highest surface runoff rates to streams (Freeze and Cherry, 1979, table 2.2). Soil texture, derived from Wieczorek (2014; U.S. Department of Agriculture, 2013; fig. 4*B*) is categorized according to how it affects the transmission of water through the soil profile to streams and how much storage of water it provides for evapotranspiration. In order of decreased percolation rates, the classes are (1) sand, (2) silts and loam, and (3) clay (not shown). The coarser sand is in the upper montane and alpine zones of the basin, coincident with the location of the granitic rock. The finer loam is located lower in the basin. The higher altitude subbasins are predominately sand, whereas the lower altitude subbasin is 25 percent sand and 75 percent loam.

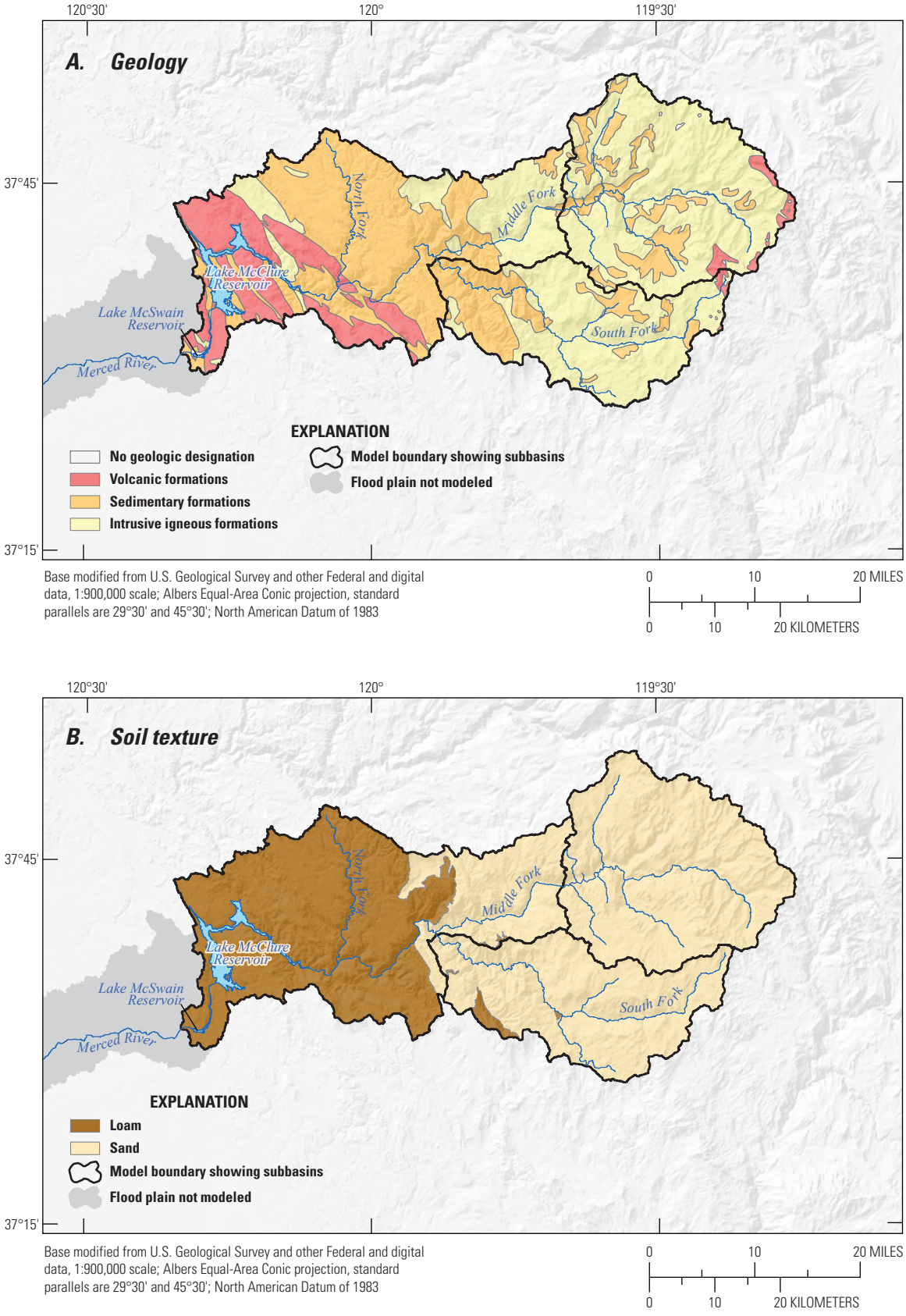

Figure 4. *A*, Geology and *B*, soil texture of the Merced River Basin, California.

The Merced River Basin climate is Mediterranean at lower elevations and alpine at higher elevations (Köppen climate classifications, https://www.blueplanetbiomes.org/climate.htm; Beck and others, 2018), with warm dry summers and cool wet winters and springs. Precipitation occurs mostly during the cool season (winter and spring) and, in the higher altitudes, mostly as snow. The basin receives an average of 41 inches of precipitation per year, varying between 10 (lower altitudes) to 66 inches (high altitudes), with average air temperatures ranging from near 10 degrees Fahrenheit (°F) in winter (high elevations) to summer highs in the 80s (lowland valleys), as interpolated by the Parameter-Elevation Relationships on Independent Slopes Model (PRISM, 30-year mean-average 1981–2010 series; http://www.prism.oregonstate.edu/normals/; Daly and others, 1994, 2008; figs. 5−7). The basin's precipitation and air temperatures follow the classic orographic model of low precipitation/high air temperatures at low altitudes and high precipitation/low air temperatures at high altitudes (figs. 2, 5−7; Strahler and Strahler, 1984, p. 95; Daly and others, 1994, 2008). Most precipitation falls on the north and south drainage divides of the Pohono Subbasin (fig. 5*A*).

Climate data used in this study (water years 1949–2013) are from 21 stations measuring daily precipitation and (or) maximum and minimum air temperatures (table 1; fig. 8) and digital surfaces of mean-monthly precipitation or temperatures as interpolated by PRISM (figs. 5–7). Station data were selected to splice together a long record of observations to increase the opportunity for calibration years, so that not all stations reported during the same timeframe, and many records had missing data. At the close of the study period (2013) only 9 precipitation and 10 temperature stations were active (table 1). Climate stations are located mostly in the lower-to-mid altitudes of the basin domain. Further, data collected at five solar radiation, two evaporation, and four snow-water equivalent stations, which are not required as input to PRMS, were used to gain an understanding of rates in the area (table 2; fig. 8). Precipitation stations 49855 and 48380 have the longest continuous record in the dataset (water years 1949–2002), and stations YYV and YOW (fig. 8; table 1) have the shortest record (water years 2002–13). The earliest temperatures (pre 1967) are measured at only two stations, DDL and 48380. A third temperature station began reporting in 1967 (station 42920, fig. 8; table 1). Therefore, climate estimates in the early period of record may be biased towards data at these few measurement points.

Streamflow data used in this study were either measured or reconstructed as natural, unimpaired streamflows at five stations (table 3; appendix 1). Measured or reconstructed streamflow data are herein referred to as "observed" when they are compared with model simulation values. A snapshot of hydrographs of streamflows from the subbasins modeled and the model domain are shown in figure 9. The time-period shown was selected to illustrate the variability of monthly and seasonal flows, including a 1969 high flow warm-winter event, and to further illustrate what fraction each subbasin contributed to the total combined inflow to Lake McClure (streamflow data reconstructed at CDEC station MRC). The magnitude and timing of streamflows differ based largely on the source of streamflow (snowmelt, rain, or a mix of both). Streamflows into Lake McClure are primarily from snowmelt, followed by mid-altitude rain-on-snow events, and finally, from lower-altitude rainfall-runoff. By July, most snow in the Merced River Basin has melted, so that summer-fall (August–October) streamflow originates from subsurface and groundwater flowpaths. During a 113-year period of streamflow data measured (in early years) or reconstructed at CDEC station MRC (water years 1901–2013; http://cdec.water.ca.gov/), the mean-monthly inflow volumes peaked in May, with maximum inflow in June and minimum monthly inflow in August–September (table 4). During the 113-year record, total-annual volumes exceeded the capacity of Lake McClure (1,032,000 acre-ft) 47 times. For this reason, forecasting spring snowmelt (April–July) is critical to provide water managers time to safely release water from reservoirs and make space for incoming snowmelt runoff.

Streamflow simulations are analyzed in this report according to the seasons defined by DWR forecasts: (1) October–December, during which the primary source of streamflow is from rain and early snowmelt; (2) January–March, during which the basin receives the most precipitation; (3) April–July, during which the main source of streamflow is snowmelt; and (4) August–September, during which the main sources of streamflow are from subsurface and groundwater flows. During the 1901–2013 period, 65 percent of the reconstructed streamflow past 11270900/MRC occurred during the April–July snowmelt period, 26 percent during January through March, 7 percent during October through December, and only about 2 percent during August through September (table 5). Mean monthly streamflow at the model domain outlet CDEC station MRC peaked in May (table 4). For about 64 years of streamflows measured at the Pohono and South Fork Subbasin outlets (table 3), highest monthly flows also were in May.

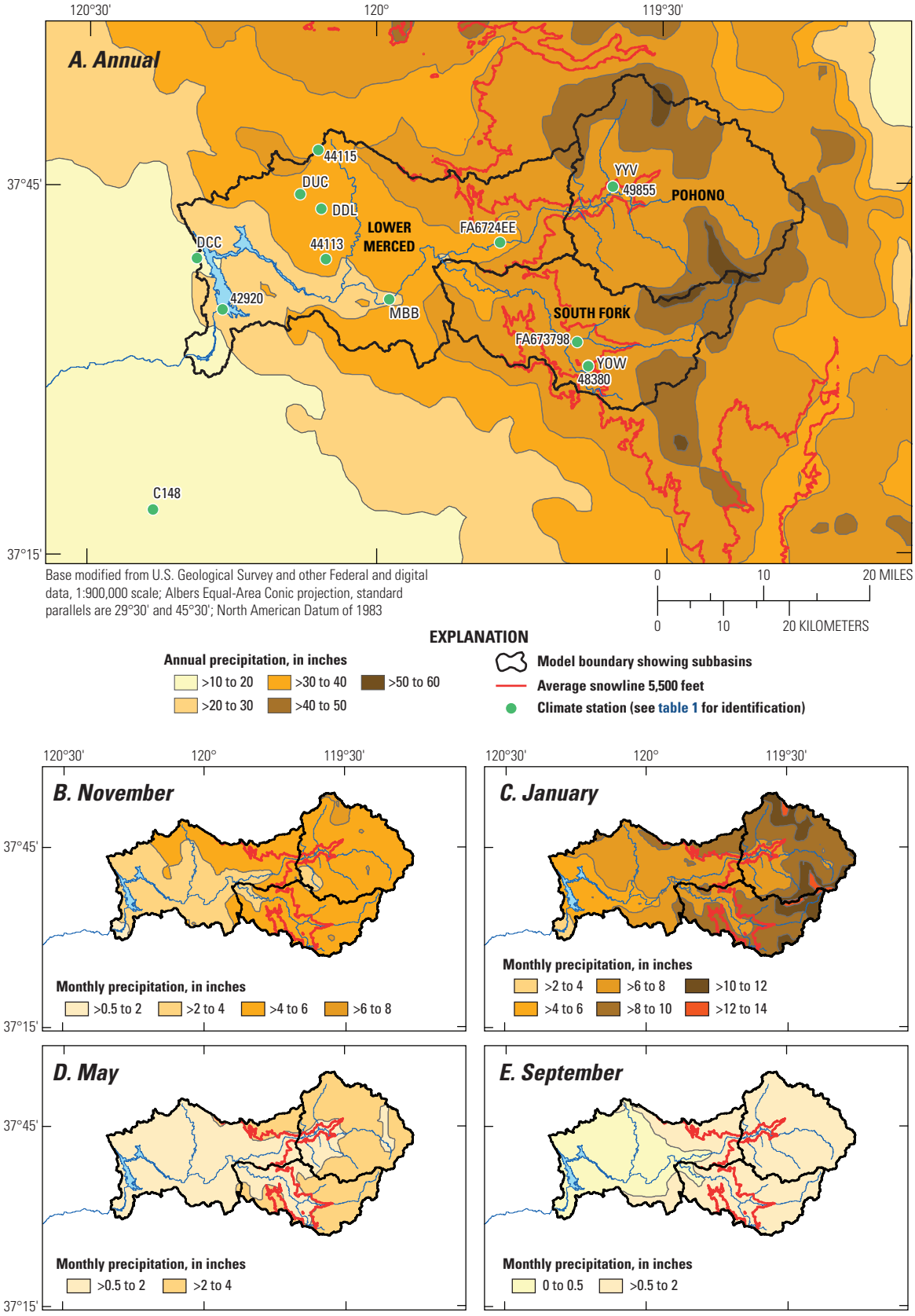

Figure 5. Precipitation over the Merced River Basin, California, including *A*, 30-year mean annual and selected 30-year mean-monthly *B*, November, *C*, January, *D*, May, and *E*, September distributions.

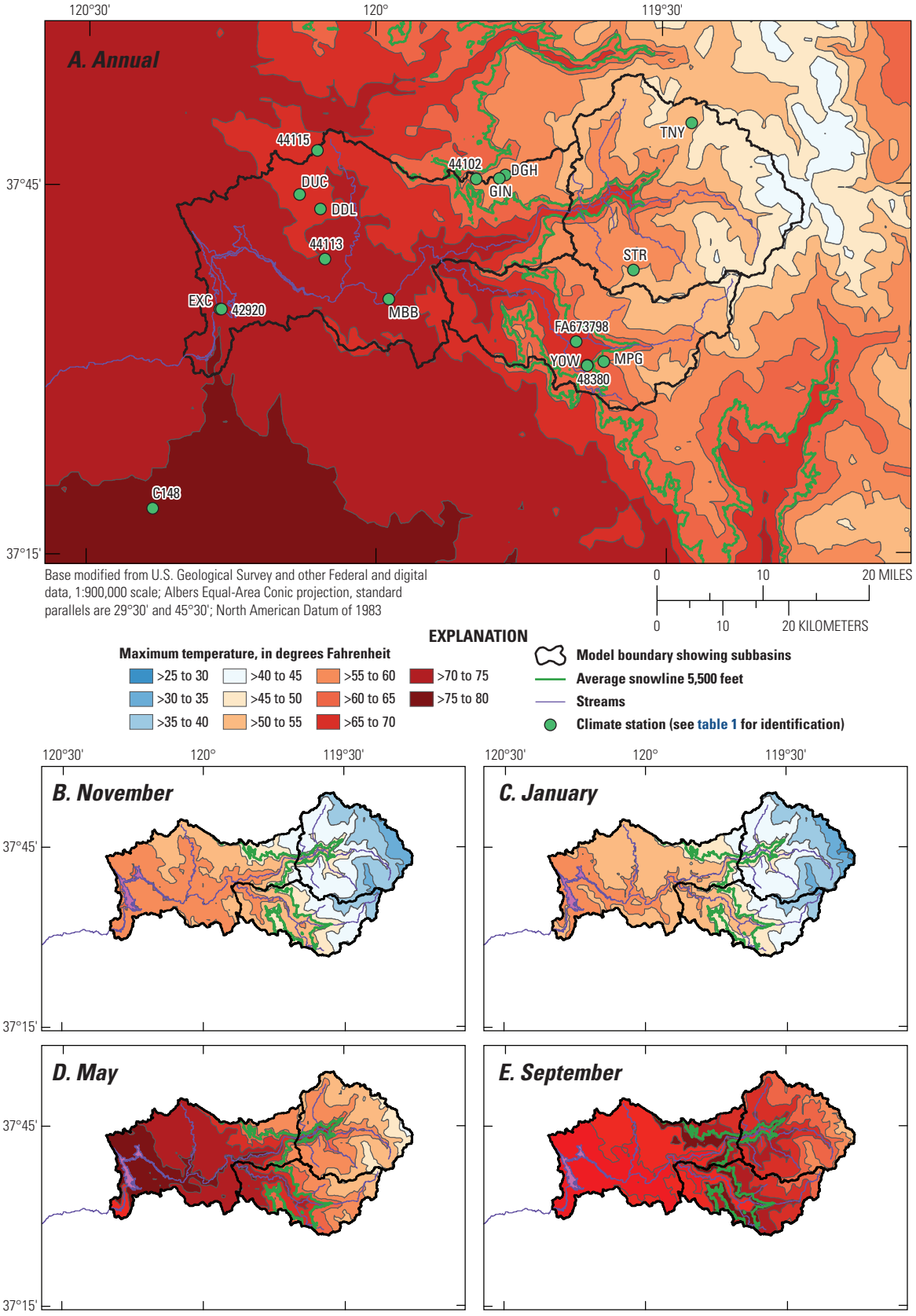

Figure 6. Daily maximum temperatures over the Merced River Basin, California, including *A*, 30-year mean annual and selected 30-year mean-monthly *B*, November, *C*, January, *D*, May, and *E*, September distributions.

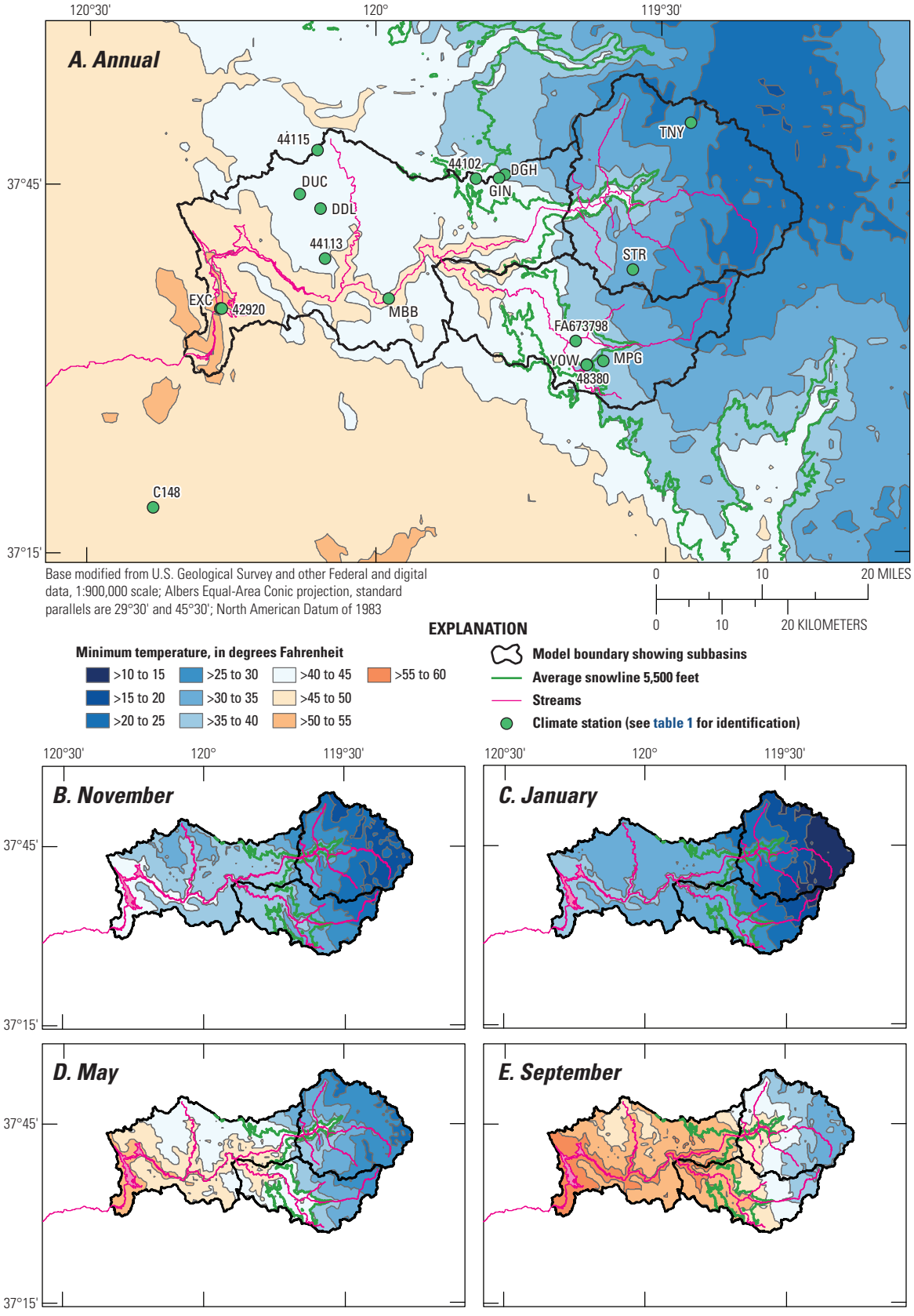

Figure 7. Daily minimum temperatures over the Merced River Basin, California, including *A*, 30-year mean-annual and selected 30-year mean mean-monthly *B*, November, *C*, January, *D*, May and *E*, September distributions.

Table 1. Climate stations used in Precipitation Runoff Modeling System (PRMS) of Merced River Basin, California, during water years 1949–2013.

[CDEC, California Data Exchange Center; CIMIS, California Irrigation Management Information System; DRI, Desert Research Institute; ft, feet; NAVD 88, North American Vertical Datum of 1988; DWR, California Department of Water Resources; MID, Merced Irrigation District; mm/dd/yyyy, month/day/year; NCDC, National Climate Data Center; NESSID, National Environmental Satellite Service Identification; NOAA, National Oceanic and Atmospheric Administration; RAWS, Remote Automatic Weather Stations; WRCC, Western Regional Climate Center; —, no data]

Climate station name	Identifying designation[1]	Altitude[2] (ft)	Precipitation				Temperature			
			Reporting period[3] (mm/dd/yyyy)	Percent missing in reporting period[4]	Percent missing in climate data-set record[5]	Source of data	Reporting period[3]	Percent missing in reporting period[4]	Percent missing in climate data-set record[5]	Source of data
Crane Flat Lookout	44102	6,644	—	—	—	—	11/04/1991–11/20/2007	18	80	DRI-RAWS
Dog House Meadow	DGH	6,100	—	—	—	—	10/01/2005–06/11/2010	3	93	DWR-CDEC
Dry Creek near Coulterville	DCC	728	04/28/1998–09/30/2013	5	77	DWR-CDEC	—	—	—	—
Dudley Ranch below Coulterville	DUC	3,654	12/01/1998–09/30/2013	7	79	DWR-CDEC	01/01/2001–09/30/2013	7	82	DWR-CDEC
Dudleys (McDiarmid Fire Station)[6]	DDL	3,000	10/01/1948–01/31/1976	5	60	DWR-CDEC	10/01/1948–01/31/1976	9	62	DWR-CDEC
El Portal	FA6724EE[7]	2,050	06/09/2004–09/30/2013	11	87	DRI-RAWS	—	—	—	DRI-RAWS
Exchequer Dam[8]	42920	442	12/01/1950–09/30/2002	1	21	DRI-NCDC	08/01/1966–09/30/2005	1	40	MID
Gin Flat[9]	GIN	7,050	—	—	—	—	10/01/1985–09/30/2013	31	70	DWR-CDEC
Mariposa Grove[10]	MPG	6,400	—	—	—	—	09/22/1988–09/30/2013	29	73	DWR-CDEC
Merced #148	C148	200	01/04/1999–09/30/2013	0	77	CIMIS	01/05/1999–09/30/2013	3	78	CIMIS
Merced River	44113	2,600	10/15/1991–11/20/1997	1	91	DRI-RAWS	10/15/1991–11/20/1997	2	91	DRI-RAWS
Merced River near Briceburg	MBB	1,150	06/08/1999–09/30/2013	8	80	DWR-CDEC	10/01/2005–09/30/2013	2	88	DWR-CDEC
New Exchequer- Lk McClure	EXC	879	—	—	—	—	10/01/2005–05/14/2013	1	88	DWR-CDEC
Ostrander Lake	STR	8,200	—	—	—	—	10/24/1989–12/31/2000	18	86	DWR-CDEC
Smith Peak[11]	44115	3,870	06/11/2012–09/30/2013	0	98	DRI-RAWS	06/11/2012–09/30/2013	2	98	DRI-RAWS
South Entr Yosemite	48380	5,137	10/01/1948–09/30/2002	3	20	DRI-NCDC	10/01/1948–09/30/2005	5	17	DRI-NCDC
Tenaya Lake	TNY	8,150	—	—	—	—	10/01/2005–09/30/2013	10	89	DWR-CDEC
Wawona	FA673798	4,052	12/31/2005–09/30/2013	6	89	DRI-RAWS	12/30/2004–09/30/2013	17	89	DRI-RAWS
Yosemite at Yosemite Valley	YYV	4,200	10/01/2002–09/30/2013	1	83	DWR-CDEC	—	—	—	DWR-CDEC
Yosemite near Wawona	YOW	4,957	10/01/2002–09/30/2013	1	83	DWR-CDEC	10/01/2005–09/30/2013	3	88	DWR-CDEC
Yosemite NP	49855	3,966	10/01/1948–09/30/2002	3	20	DRI-NCDC	—	—	—	—

[1]See figure 8 and 11 for location.

[2]Altitudes are from data source and have been converted to or assumed to be measured from NAVD 88. Please see data source for original datums.

[3]Reporting period is the start and end date of daily data collected at this station and used in this study.

[4]"Zero" may include 0–0.5 percent missing from this time series.

[5]"Climate-dataset record" refers to the full daily time series used in this study to equilibrate, calibrate, and validate the model, which is 10/1/1948–9/30/2013.

[6]In August 2013, DDL replaced the discontinued DRI-NCDC station, Dudleys California 42539, which reported from 1948 to 1976.

[7]RAWS NESSID station designation.

[8]MID provides data for Exchequer Dam temperatures and precipitation.

[9]Data series were merged. DRI-WRCC Gin Flat California reported October 1985–2002. GIN began reporting October 2002.

[10]Data series were merged. DRI-RAWS NESSID #FA455664 reported from 1980 to 2012. MPG began reporting October 2005.

[11]Smith Peak is the newest station with a short record, where some months are missing reported measurements.

Figure 8. Subbasins and catchments, streamflow-calibration targets, and climate stations used in Merced River Basin PRMS.

Table 2. Stations measuring solar radiation, evaporation, or snow-water equivalents in or near the Merced River Basin, California, during water years 1981–2013.

[DWR, California Department of Water Resources; CDEC, California Data Exchange Center; CIMIS, California Irrigation Management Information System; DRI, Desert Research Institute; ft, feet; NAVD 88, North American Vertical Datum of 1988; ly, langleys; RAWS, Remote Automatic Weather Stations; SWE, snow-water equivalent; mm/dd/yyyy, month/day/year; —, not applicable]

Station name	Identifying designation[1]	Altitude[2] (ft)	Reporting period (mm/dd/yyyy)	Solar Radiation, summer and winter peak mean-monthly daily rates of high-elevation and low-elevation stations (in ly)	Evaporation mean-total annual rate (in inches)	Range of April 1 SWE[3] (in inches)	Source of data
Solar radiation							
Crane Flat Lookout	44102	6,644	10/16/2000–05/14/2006	June 646 ly; December 241 ly	—	—	DRI-RAWS
El Portal	FA6724EE	2,050	06/09/2004–09/30/2013	July 732 ly; December 238 ly	—	—	DRI-RAWS
Smith Peak[4]	44115	3,870	06/11/2012–09/30/2013	June 800 ly; December 203 ly	—	—	DRI-RAWS
Wawona	FA673798	4,052	12/31/2005–09/30/2013	July 673 ly; November 188 ly	—	—	DRI-RAWS
Merced #148	C148	200	01/04/1999–09/30/2013	July 669 ly; December 150 ly	—	—	CIMIS
Evaporation							
Lake McClure	MCR	867	Mar. 1995–Sep. 2013	—	38.44	—	DWR-CDEC
Merced #148	C148	200	01/04/1999–09/30/2013	—	54.64	—	CIMIS
Snow-water equivalent (SWE)							
Gin Flat	GIN	7,033	10/28/1981–10/04/2011	—	—	9.1–70.9	DWR-CDEC
Snow Flat	SNF	8,700	11/24/1988–10/27/1998	—	—	20.6–73	DWR-CDEC
Ostrander Lake	STR	8,200	12/01/1988–02/17/2012	—	—	13.4–65.4	DWR-CDEC
Tenaya Lake	TNY	8,150	11/01/1998–02/17/2012	—	—	18.3–44.7	DWR-CDEC

[1]See figures 8 and 11 for location.

[2]Altitudes are from data source and have been converted to or assumed to be measured from NAVD 88. Please see data source for original datums.

[3]April 1 is historically the start of the Sierra Nevada snowmelt season. Not every year in the reporting period included measurements on April 1.

[4]Smith Peak has a short record, with some months missing reported measurements. The December average recorded here is computed from 2 months with only 25 and 27 days reporting.

Table 3. Streamflow stations used in watershed modeling of the Merced River Basin, California, during water years 1950–2013.

[DWR, California Department of Water Resources; ft, feet; ID, identifying designation; mi², square miles; mm/dd/yyyy, month/day/year; USGS, U.S. Geological Survey; —, not applicable]

Subbasin index number	Subbasin	Catchment	Area ID	Station name[1]	Station ID[2]	Gaged area (mi²)	Gage altitude[3] (ft)	Source of streamflow data	Collection method	Daily record used in study (mm/dd/yyyy)
—	—	Happy Isles[4]	HI	Merced R A Happy Isles Bridge NR Yosemite	11264500	181	4,030	USGS	Measured[5]	10/01/1949–09/30/2013
1	Pohono	—	PH	Merced R A Pohono Bridge NR Yosemite CA	11266500	322	3,862	USGS	Measured	10/01/1949–09/30/2013
—	—	Wawona[6]	WA	SF Merced R A Wawona CA	11267300	100	4,030	USGS	Measured	10/01/1958–09/30/1968
2	South Fork	—	SF	SF Merced R NR El Portal CA	11268000	241	1,400	USGS	Measured	04/01/1951–10/07/1975
3	Lower Merced[7]	—	LM	—	—	—	—	—	—	—
Model Domain										
Merced River Basin			MB	Merced R NR Merced Falls	11270900/MRC	1,059	311	DWR	Reconstructed[8]	08/01/1966–09/30/2013
Merced River Basin			MB	Merced R NR Merced Falls	11270900/MRC	1,059	311	DWR	Reconstructed	(Monthly) October 1900–September 2013

[1]Station is named in reference to streamflow data used in calibration. For example, streamflow data used to calibrate "Merced River Basin (MB)" is named for the reconstructed data at California Data Exchange Center (CDEC) station "MRC."

[2]See figure 8 and 11 for location.

[3]Some gage altitudes were estimated from a topographic map. Please see data sources for updated information.

[4]Happy Isles is a catchment of Pohono Subbasin.

[5]Measured at each station as noted.

[6]Wawona is a catchment of South Fork Subbasin.

[7]LM flow = MB flow – (PH flow + SF flow). MB low flows are considered unreliable. LM flows are assumed to be near zero during MB low flows.

[8]Provided by DWR and computed using a water-budget approach. Reconstructed from gage data measured on the Merced River below Merced Falls Dam near Snell CA. Please see appendix 1 for details. This site, USGS 11270900, USGS site name is "MERCED R BL MERCED FALLS DAM NR SNELL CA." Zero value represents low negligible streamflow below 500 acre-feet, not necessarily an ephemeral stream.

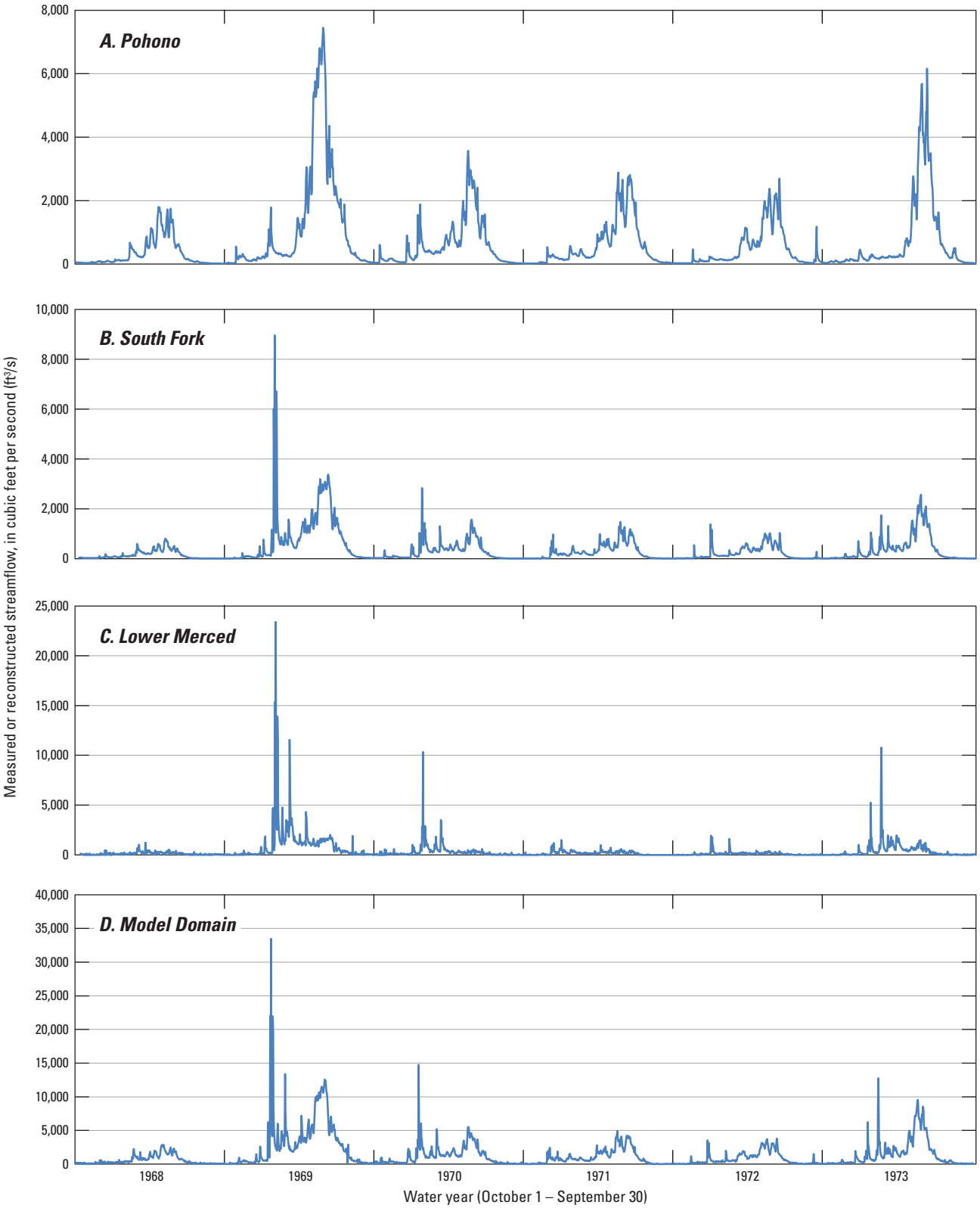

Figure 9. Daily measured or reconstructed streamflow, Merced River Basin, California, water years 1968–73, from *A*, Pohono, *B*, South Fork, and *C*, Lower Merced Subbasins and *D*, the model domain. Lower Merced streamflow was computed by subtracting upper subbasin measured streamflows from data reconstructed at California Data Exchange Center station MRC. Notably, 19 percent of the Lower Merced Subbasin streamflows (computed as negative values) were reset to zero. This was especially true during low flows of late July–mid-October, which is concurrent with error noted by California Department of Water Resources and Merced Irrigation District.

Table 4. Mean monthly reconstructed inflow to Lake McClure, California, water years 1901–2013.

[Based on data from California Data Exchange Center (CDEC) station MRC]

Month	Mean monthly volume, in acre-feet	Maximum monthly volume, in acre-feet	Minimum monthly volume, in acre-feet[1]	Standard deviation, in acre-feet
Oct.	9,165	92,900	500	11,763
Nov.	18,486	258,610	1,200	29,055
Dec.	39,635	372,500	1,020	58,601
Jan.	69,189	633,700	3,340	86,758
Feb.	82,351	362,110	3,142	69,484
Mar.	109,443	458,100	8,040	79,928
Apr.	151,210	428,810	30,890	62,098
May	246,732	565,300	39,170	107,446
June	184,052	656,050	12,600	132,316
July	61,904	384,600	3,800	72,529
Aug.	14,352	97,050	0	15,385
Sep.	6,337	47,500	0	7,236
TOTAL	992,857	—	—	—

[1]Zero value represents low negligible streamflow below 500 acre-feet, not necessarily an ephemeral stream.

Table 5. Mean-seasonal reconstructed inflow volumes to Lake, water years 1901–2013.

[Based on data from California Data Exchange Center (CDEC) station MRC. Rounded to nearest 1,000 acre-feet]

Streamflow season	Mean volume, in acre-feet	Maximum volume, in acre-feet	Minimum volume, in acre-feet[1]	Standard deviation, in acre-feet	Percent of annual volume
October–December	67,000	537,000	5,000	81,000	7
January–March	261,000	852,000	16,000	187,000	26
April–July	644,000	1,587,000	123,000	330,000	65
August–September	21,000	126,000	0	21,000	2
TOTAL	993,000	—	—	—	—

[1]Zero value represents low negligible streamflow below 500 acre-feet, not necessarily an ephemeral stream.

Watershed Modeling

The PRMS configuration developed for this study is coupled with a forecast tool, daily-climate distribution preprocessing functionality, and other supporting tools and is operated through a customized Object User Interface (OUI; Markstrom and Koczot, 2008). Referred to as Merced OUI, this modeling framework was the platform used to operate the Merced River Basin PRMS and perform streamflow simulations and forecasts. This is an extensible format, which is the foundation for future refinement. The Merced OUI, including the Merced River Basin PRMS, supporting tools (forecasting, climate-file preparation, parameter-file editor, and data-visualization tools), data, and documentation, are available as a USGS data release product (Koczot and others, 2021; https://doi.org/10.5066/F7JH3KFR). Supplemental information regarding PRMS modules and source code specific to the PRMS configuration presented in this report is available in the PRMS users manual (Markstrom and others, 2015) and from the USGS PRMS developers site (https://www.usgs.gov/software/precipitation-runoff-modeling-system-prms-0).

PRMS, a deterministic, distributed-parameter, physically based watershed modeling system, was applied to evaluate the response of various combinations of climate and land-use conditions on streamflow and general watershed hydrology (Markstrom and others, 2015). Responses to climatic and land-cover changes are simulated in terms of water and energy balances, streamflow regimes, flood peaks and volumes, soil-water relations, and groundwater recharge (Risley, 1994; Leavesley and Stannard, 1995; Leavesley, 2005; Hay and others, 2011; Markstrom and others, 2012; and Markstrom and others, 2015). In PRMS, the components of streamflow include contributions from surface runoff, subsurface (soils) interflow, and groundwater (shallow baseflow; fig. 10). In PRMS, the basin water budget consists of storage in snowpack, soil moisture, and groundwater; inputs from precipitation and snowmelt; losses to evapotranspiration and recharge to the deeper aquifer system; and outflows to streams from surface, subsurface, and shallow groundwater reservoirs. A schematic diagram of how basinwide and climate inputs are simulated in a typical PRMS model, the conceptual snowpack system, and the components of the snowpack energy-balance equations are shown in figure 10.

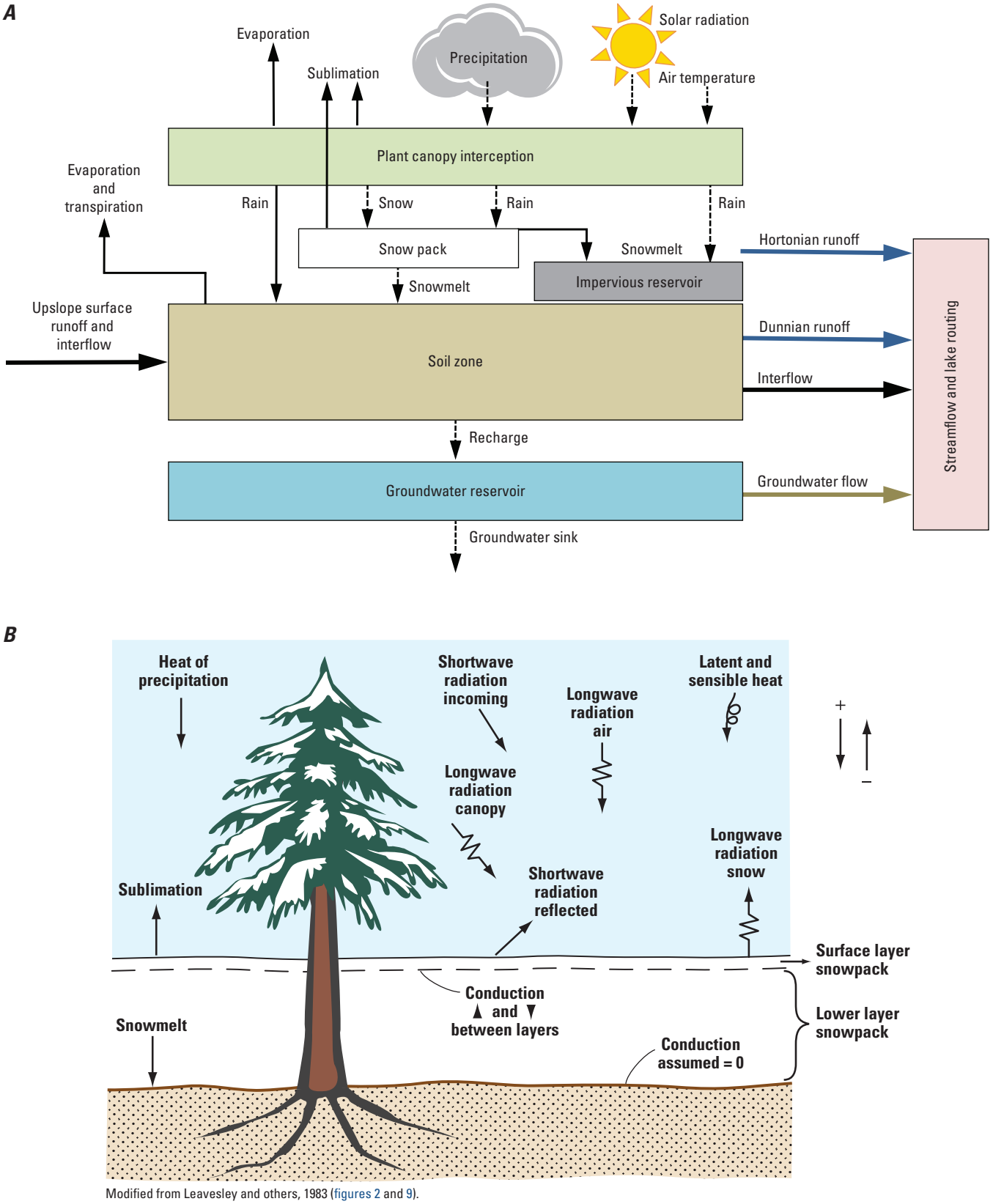

Modified from Leavesley and others, 1983 (figures 2 and 9).

Figure 10. Precipitation-Runoff Modeling System (PRMS) diagrams showing *A*, schematic of the conceptual water system and inputs (Markstrom and others, 2015) and *B*, components of the snowpack energy-balance equations (Koczot and others, 2005).

PRMS version 4.0.2 (Markstrom and others, 2015; hereafter referred to as "PRMS"), used in this study, includes watershed-process algorithms that give the user options to combine a library of subroutine modules to simulate components of the hydrologic system, including water and energy processes. PRMS operates on a fixed daily time-step, with the basic assumption that streamflow travel times from the headwaters of a model domain to its outlet must be less than or equal to the daily time step. When this is not possible, as with the Merced River Basin PRMS, daily streamflows are routed along river channels. For this model configuration, streamflows are routed downstream to a single outlet along 42 stream segments. Hydrologic components of the system, including streamflow, are computed on a daily time step.

Spatially distributed hydrologic properties and responses are represented by dividing a watershed into contiguous model mapping units called hydrologic response units (HRUs). These are the smallest spatial units of the model, defined based on hydrologic and physical characteristics and are as spatially homogeneous as is practical. Hydrologic processes within each HRU, including streamflow generation, are assumed to vary uniformly in response to air temperature and precipitation. For this model, each HRU was sequentially numbered from 1 to 653 and had its own HRU-scale soil zone and shallow groundwater reservoir (fig. 10). The Merced PRMS was configured to be a high-resolution model designed to capture the effects of land use and climate change on streamflows and general hydrogeology from small subareas (catchments) of the model domain. HRU resolution ranged from 1 to 12 mi^2 with an average resolution of 1.6 mi^2. Based on the HRU's physical and hydrologic characteristics and daily weather conditions, water and energy balances and fluxes are computed each day for each HRU, including all surface and subsurface components. These balances represent fluxes through the snowpack, vegetation canopies, land surface, and soil through the root zone of the HRU (fig. 10). The smallest spatial scale at which climatic variation or land-cover changes can be imposed in the model is the HRU scale. The sum of the individual responses of all HRUs, weighted on a unit-area basis, produces the daily watershed response and streamflow for the model domain. Subsets of the sum of these HRUs produce the daily watershed response and streamflows for catchments and subbasins.

Modeled Subbasins

The model is configured as three contiguous subbasins with two nested catchments (table 6; fig. 8). A catchment is a smaller, internal subarea of a subbasin. Subbasins are made up of a subset of the model domain's contiguous HRUs. Catchments contain a subset of the subbasin HRUs. Each subbasin has different topography, land cover, and climate conditions and is similar enough in its internal physical characteristics to stand alone. Each responds differently from the others to precipitation and air temperature forcing. Hydrographs of streamflows from these subbasins illustrate their different responses (fig. 9).

Table 6. Merced River Basin calibrated areas, including modeling period, drainage area, altitude ranges, and average climate (precipitation and temperatures derived from Parameter Elevation Regressions on Independent Slopes Model).

[Precipitation and temperatures as derived from PRISM. **Abbreviations**: ft, feet; mi^2, square miles; PRISM, Parameter-elevation Relationships on Independent Slopes Model; °F, degrees Fahrenheit; —, not applicable]

Subbasin index number	Subbasin	Catchment[1]	Modeling period (water years)	Drainage area (mi^2)	Altitude range[2] (ft)	Average-annual precipitation[3] (inches/year)	Average monthly maximum temperature[3] (°F)	Average monthly minimum temperature[3] (°F)
—	—	Happy Isles	1980–2013	181	4,031–13,100	48	70 (July)	15 (February)
1	Pohono	—	1980–2013	322	3,865–13,100	48	72 (July)	18 (February)
—	—	Wawona	1959–1968	100	3,933–11,614	51	75 (July)	21 (February)
2	South Fork	—	1952–1967	241	1,407–11,614	46	80 (August)	27 (February)
3	Lower Merced	—	2007–2013	496	305–8,980	34	89 (July)	33 (December)
Model Domain								
Merced River Basin			2007–2013	1,059	305–13,100	41	82 (July)	27 (December)

[1]Happy Isles is a catchment of Pohono. Wawona is a catchment of South Fork.

[2]Altitude data are from geographic information system (GIS) topography, not hydrologic response unit (HRU) average-altitudes set in the Precipitation-Runoff Modeling System (PRMS) parameter file.

[3]Derived from PRISM, 30-year average 1981–2010 data, as provided by the PRISM Climate Group (http://www.prism.oregonstate.edu/normals/; Daly and others, 1994, 2008; figs. 5–7).

Pohono

The Pohono Subbasin (30 percent of the model domain) was modeled in two sections: Happy Isles Catchment, at its headwaters, and the remaining area contributing to the subbasin outlet (fig. 8; table 6). Containing the highest altitudes of the three subbasins (Mount Lyell, 13,100 ft, fig. 2), it is topographically steep and bisected by east-west trending Yosemite Valley (at 4,000 ft; fig. 8), where nearly vertical granite cliffs rise 2,000–3,000 feet from the valley floor. Hanging valleys in the Pohono Subbasin terminate at most of Yosemite National Park's waterfall attractions, included in the modeling system as streamflow-simulation nodes. Of the three, this subbasin receives the highest amount of annual precipitation (66 inches at altitude to 39 inches at the outlet; table 6; fig. 5). Precipitation is greatest on the northern divide (Mount Hoffman, 10,771 ft) and along Clark Range on the southern divide (11,500–11,730 ft; fig. 1). Evapotranspiration rates vary considerably over the subbasin due to the extreme altitude range and variety of vegetation, with 75 percent of the area forested, 7 percent covered by shrubs and grasses, and 18 percent barren, mostly above the tree line (fig. 3).

Pohono Subbasin contributes the greatest portion of the total inflows to Lake McClure (fig. 9). Runoff to streams is mostly from spring snowmelt, as most of this subbasin is well within high altitudes that are cold enough to form and retain snowpack until the start of the snowmelt season (around April 1). Twelve percent (mostly Yosemite Valley; fig. 8) is in a lower-altitude zone where air temperatures are warm enough for rain-on-snow or rain-only events, which may result in early wet-season streamflows from that part of the subbasin. Streamflow data used in calibrating the Pohono Subbasin were measured by the USGS at the outlet of Happy Isles Catchment (Merced River at Happy Isle Bridge near Yosemite; 11264500) and the subbasin outlet (Merced River at Pohono Bridge near Yosemite; 11266500; table 3).

South Fork

The South Fork Subbasin (23 percent of the model domain) was modeled in two sections: Wawona Catchment, at its headwaters, and the area below Wawona Catchment to the subbasin outlet (fig. 8; table 6). Contained in Wawona Catchment, Chilnualna Falls is included in the modeling system as a streamflow-simulation node (fig. 8, node 13; table 7). A close second to Pohono, precipitation in this subbasin is greatest on the northeastern drainage divide along Buena Vista Crest (about 65 inches annually), to its highest point, Triple Divide Peak (about 11,600 ft, part of the Clark Range; fig. 2). At the subbasin outlet (about 1,400 ft), about 30 inches of precipitation falls annually (fig. 5). Lower than Pohono, 48 percent of the South Fork drainage is at altitudes in a transitional zone where air temperatures are warm enough for precipitation to fall as rain-on-snow or rain. This subbasin is evenly forested, with the lower altitudes covered by shrubs and grasses (8 percent of the subbasin) and the high altitudes barren (4 percent; fig. 3).

Depending on the source of runoff, streamflows from this lower transitional-altitude subbasin exhibit earlier peak flows and recessions than streamflows from Pohono, with wet-season runoff from rain-on-snow and rainfall events, and later, runoff combined with spring snowmelt (fig. 9). Although discontinued by 1975, streamflow records used in calibrating this subbasin were measured by the USGS at the outlet of Wawona Catchment (South Fork Merced River at Wawona [11267300]) and at the subbasin outlet (South Fork Merced River near El Portal [11268000; table 3; fig. 8]).

Lower Merced

The Lower Merced Subbasin (47 percent of the model domain) is drained by the North Fork Merced River and the mainstem of the Merced River (fig. 8; table 6). Precipitation ranges from 53 inches/year at highest altitudes near Pohono Subbasin (about 9,000 ft) to only 15 inches/year at the outlet (about 300 ft; fig. 5). Unlike other subbasins, soils transition from sand (25 percent of the area) to loam (fig. 4*B*). Mostly forested with shrubs and grasses on the valley floor, this subbasin lies mostly below the historical 5,500-foot snowline (90 percent), with most altitudes (80 percent) below 4,000 feet where air temperatures are warm and precipitation is expected to fall as rain and soon enter streams (figs. 6, 7). Therefore, the streamflow hydrograph exhibits characteristic of mostly rainfall-runoff events, and streamflows from the Lower Merced Subbasin peak earlier in the year (February or March), as compared with the other, higher-altitude subbasins (April–June; fig. 9). Streamflow records used in calibrating the Lower Merced Subbasin were reconstructed at CDEC station MRC, which is physically located at USGS gaging station 11270900, Merced River below Merced Falls Dam near Snell (table 3, fig. 8; appendix 1).

Spatial Features and Parameterization

In this section, the model is described according to its physical architecture and the model parameters which quantify long-term climate and land-surface characteristics. ArcGIS (Environmental Systems Research Institute, Inc., 1992; Viger and others, 1996) was used to delineate physical features of the model. Geographic information system (GIS) processing was also used to manage spatial data and compute estimates of many spatially varying model parameters at the HRU and basinwide scale. The methods employed in this study were like methods described by Battaglin and others (1993), Jeton and LaRue Smith (1993), Frankoski (1994), Viger and others (1996), Ryan (1996), Jeton (1999, 2000), Koczot and others (2005), and Markstrom and others (2015).

Table 7. Summary of the physical architecture of the Merced River Basin Basin Precipitation-Runoff Modeling System, including stream segment and subbasin index numbers, calibration and simulation nodes, drainage areas, and HRU area, altitude, slope and aspect ranges.

[Additional information is provided in https://doi.org/10.5066/F7JH3KFR. **Abbreviations**: ft, feet; ID, identifying designation; mi², square miles; —, not applicable]

Subbasin containing node		Node (stream site)						Drainage area					
									HRU count and ranges for indicated physical characteristics				
Subbasin index number[1]	Subbasin name	Stream segment index number[2]	Calibration node	Simulation node	Name	ID	Altitude[2] (ft)	Area (mi²)	Number of HRUs	Area (acres)	Altitude (ft)	Slope (decimal percent)	Aspect[3] (degrees)
1	Pohono	1	—	1	Merced Lake	ML	7,236	73	72	157–1,776	7,523–12,247	0.126–0.81	74–292
1	Pohono	2	—	2	Nevada Fall	NVWF	5,912	116	104	156–3,451	6,456–12,247	0.126–0.81	74–295
1	Pohono	3	—	3	Vernal Fall	VNWF	5,020	119	108	150–3,451	6,285–12,247	0.126–1.195	74–295
1	Pohono	5	—	4	Illilouette Fall	ILWF	5,825	60	54	139–2,267	6,443–11,200	0.116–0.718	72–286
1	**Pohono**	**7**	**[6]1**	**5**	**Merced R A Happy Isles Bridge NR Yosemite**	**11264500**	**4,033**	**181**	**168**	**59–3,451**	**4,625–12,247**	**0.116–1.195**	**72–295**
1	Pohono	10	—	6	Yosemite Falls	YSWF	6,434	42	34	142–2,778	6,879–10,205	0.143–0.569	87–283
1	Pohono	13	—	7	Sentinel Falls	STWF	7,137	2	2	418–775	7,729–7,801	0.145–0.216	116–247
1	Pohono	16	—	8	Horsetail Fall	HTWF	5,379	0	1	91–91	7,049	0.499–0.499	129–129
1	Pohono	19	—	9	Ribbon Fall	RBWF	6,863	3	4	142–810	7,662–8,289	0.2–0.295	129–217
1	Pohono	22	—	—	—	—	4,620	25	12	137–3,801	6,497–8,436	0.087–0.475	133–258
1	Pohono	9	—	11	Yosemite Creek	YC	7,473	14	12	215–2,778	7,719–10,205	0.227–0.569	115–280
1	**Pohono**	**24**	**[7]2**	**12**	**Merced R A Pohono Bridge NR Yosemite CA**	**11266500**	**3,874**	**322**	**298**	**54–7,917**	**3,930–12,247**	**0.028–1.822**	**72–306**
2	South Fork	26	—	13	Chilnualna Falls	CLWF	6,228	17	8	160–3,375	6,788–9,209	0.208–0.316	173–274
2	**South Fork**	**29**	**[6]3**	**14**	**SF Merced R A Wawona CA**	**11267300**	**3,951**	**100**	**62**	**156–3,470**	**4,230–10,638**	**0.144–0.598**	**87–283**
2	South Fork	30	—	15	Big C Div NR Fish Camp CA	11267350	5,365	12	11	172–1,621	5,722–8,216	0.219–0.379	178–237
2	**South Fork**	**32**	**[7]4**	**16**	**SF Merced R NR El Portal CA**	**11268000**	**1,408**	**241**	**157**	**128–4,264**	**2,652–10,638**	**0.144–0.746**	**74–283**
3	Lower Merced	34	—	17	MID Briceburg	MIDBB	1,136	724	554	54–7,917	1,920–12,247	0.028–1.822	72–306
3	Lower Merced	36	—	18	North Fork	NF	902	124	44	308–3,922	1,885–5,464	0.125–0.541	115–254
3	Lower Merced	39	—	19	New Exchequer-Lk McClure	11270000/EXC	457	1,039	646	54–7,917	766–12,247	0.028–1.822	54–306
3	**Lower Merced[8]**	**42–(24+32)**	**—**	**—**	**—**	**—**	**—**	**496**	**198**	**130–7,701**	**393–8,373**	**0.018–0.835**	**40–280**
Model Domain													
Merced River Basin		42	5	20	Merced R NR Merced Falls	11270900/MRC	323	1,059	653	54–7,917	393–12,247	0.018–1.822	40–306

[1]This number identifies the Merced PRMS subbasin used to access streamflow simulations from the subbasin area of interest.

[2]This number identifies the Merced PRMS stream segment used to access streamflow simulations from drainage areas to the node of interest.

[3]See figure 11 for location.

[4]Data derived from Digital Elevation Model.

[5]Aspect is the slope direction on a terrain surface, measured clockwise, starting north as zero degrees to 360 degrees north again. Flat areas are given a value of –1 or zero degrees.

[6]Calibrated catchment.

[7]Calibrated Subbasin.

[8]The Lower Merced Subbasin was calibrated solely to balance flows at the model domain after headwater subbasins were calibrated.

Geospatial Fabric

Within the context of PRMS, geospatial fabric means the geo-referenced features that are of importance to the model. Concretely, this means the maps of the modeling units that the model uses (in other words the HRU map, stream segment map, nodes of interest map, and sub-area maps). These geo-referenced features have meaning to the model and are used to define the model's physical architecture. The geospatial fabric was delineated from spatial subdivisions of the model domain, which were based on the locations of the stream network, nodes of interest on streams (which may or may not include actual streamgages), subbasins, catchments (subdivisions of subbasins), and other nested areas draining to node locations. HRUs were defined primarily from topography, land cover, and left and right stream banks. Natural streams, which form the basis of the Merced River Basin PRMS streamflow routing network, were partitioned into PRMS features called "stream segments." Stream segments were defined by bisecting the natural streams at confluences and lake boundaries, at node locations, at boundary-intersections with subbasins and catchments, and at the boundaries of areas defined as draining to nodes (also known as "drainage areas"). A summary of information about the model domain, subbasins, calibration and simulation nodes, and streamflow-routing segments is presented in table 7 and illustrated in figure 11. For additional information regarding specifics of the Merced River Basin PRMS physical architecture, please also see the USGS data release product; https://doi.org/10.5066/F7JH3KFR (Koczot and others, 2021).

Parameters

Long-term climate and land-surface characteristics are quantified by many model parameters. Spatial variations of these characteristics are represented by HRU-specific and reservoir-specific parameters. Other properties that are homogeneous over the whole model area are quantified by non-distributed parameters. Parameters are specified as constants or monthly values. All parameters are independent of daily fluctuations of the air temperature and precipitation inputs. In the southern and central Sierra Nevada, the most important parameters were those that are determined from topography, those that describe how much precipitation falls onto the HRUs, the air temperature thresholds that determine precipitation form (snow, rain, or a mix of both), and the prevailing air temperatures at the HRUs during the snowmelt season.

Sources and ranges of key model parameters are presented in table 8. The designation "calibrated" means that the initial estimates of the parameter values were adjusted during iterative model runs to minimize differences between simulated and observed streamflows. "Computed" values were first derived from the literature (Black, 1996; Markstrom and others, 2015) and then revised prior to calibration to reflect conditions specific to the Merced River Basin. "GIS derived" parameters are estimated directly from spatial data and were not altered during calibration. PRMS parameters describing radiation planes, interception conditions, infiltration and subsurface-flow conditions, and the distribution of precipitation and air temperatures within the basin (by HRU) were estimated based on combinations of experience with other models in the Sierra Nevada (Jeton and LaRue Smith, 1993; Jeton, 1999, 2000; Koczot and others, 2005; Markstrom and others, 2016), values reported in the scientific literature, and as noted in table 8, further calibrated. In the model, default snow depletion curves were applied for areas below and above the tree line of 9,500 ft, and a static time/space HRU-scale land surface and plant canopy was assumed throughout the calibration and simulation periods.

Model Input

The most significant limitations in the practice of snowmelt-runoff modeling are (1) the scarcity of climate data and the need to extrapolate point measurements to areal values and (2) that the distribution and temperature-dependent form of precipitation are the most important factors in producing accurate estimates of runoff volume (Koczot and others, 2005). Meteorological input data needed to run the model are daily HRU-scale inputs of precipitation and maximum and minimum air temperatures, but these were not readily available. As part of this study, an existing technique was modified and enhanced (Koczot and others, 2005) to distribute climate from data measured at stations and gridded surfaces to HRU centroids and create the daily time-series datasets needed to run the model.

Precipitation measurements from 14 stations and maximum and minimum air temperatures from 17 stations, reported sometime during water years 1949–2013, were assembled and reviewed by DWR from local and national databases and supplied to USGS (table 1; fig. 8; Fazel and others, 2013; John King, DWR Snow Surverys Section, written commun., 2015). To allow for future real-time forecasting applications (the subject of this study), stations that reported daily measurements in or near the Merced Basin model domain were preferred, but concessions were made to find data to match the available streamflow calibration-target time frames (table 3). Climate stations that reported real-time data at the close of the study are indicated in table 1 with an ending reporting-period date of September 30, 2013. To update model inputs for purposes of forecasting after September 30, 2013, at the time of this publication, data could be retrieved from CDEC (http://cdec.water.ca.gov), MID, or from the Desert Research Institute (DRI). CDEC is intended to provide access to provisional data for immediate use, but most data are not reviewed. For our study, the task of screening data was performed by DWR.

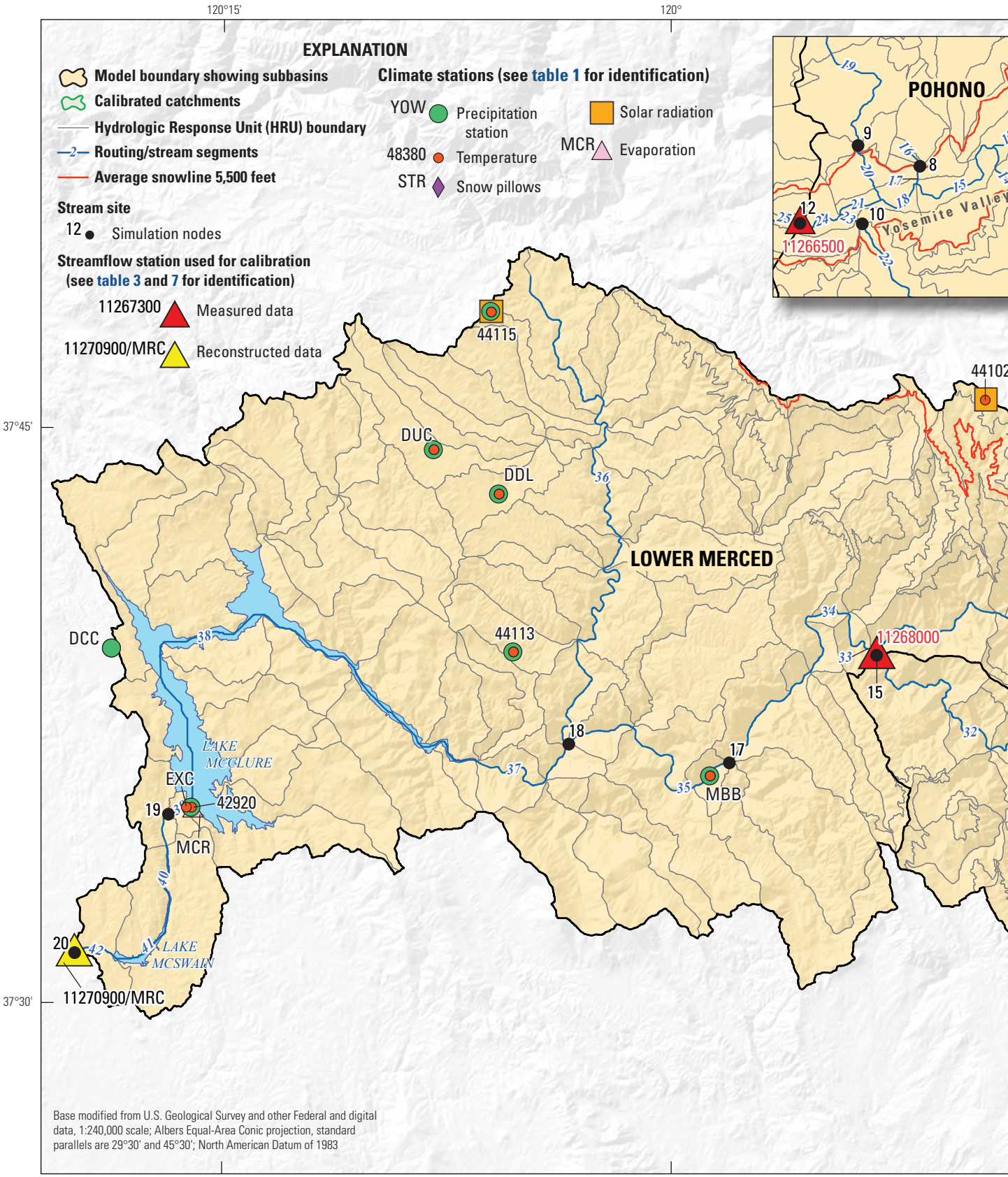

Figure 11. Physical architecture of the Merced River Basin Precipitation-Runoff Modeling System, including calibration and simulation nodes, stream segments used in routing, subbasins and catchments, and hydrologic response units.

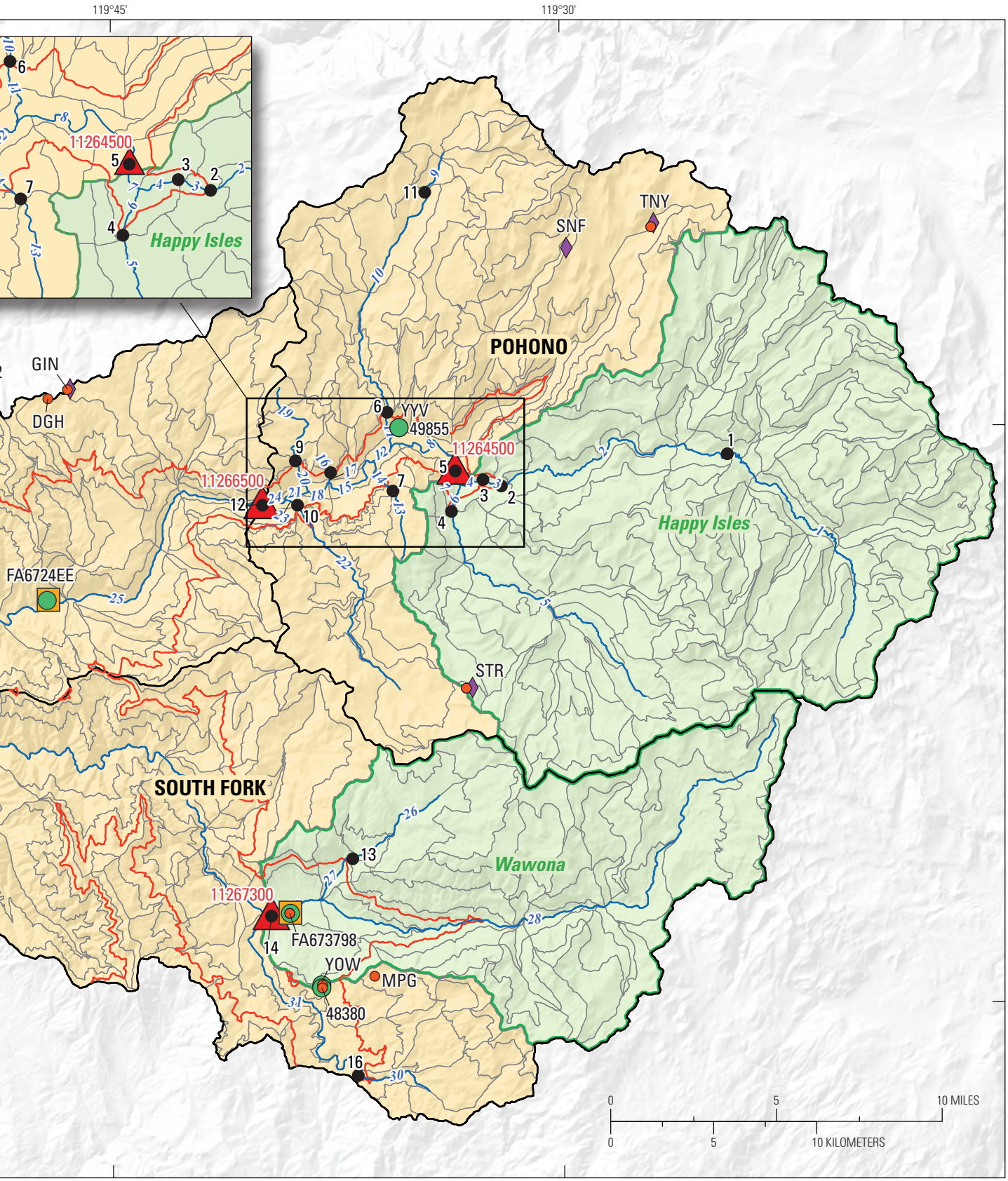

See table 1 for identification of climate stations, tables 3 and 7 for identification of streamflow stations used for calibration and validation.

Table 8. Source of parameter values for hydrologic response units, routing, two-dimensional, and whole-model parameters for the Merced River Basin Precipitation Runoff Modeling System.

[Source(s) of parameter data is indicated by "X" character. **Abbreviations**: ET, evapotranspiration; GIS, geographic information system; nhru, number of HRUs; nmonths, number of months; nsegment, number of stream segments; PRMS, Precipitation-Runoff Modeling System; —, not applicable]

Model parameter	Module	Description of parameter (PRMS version 4.0.2)	Range of values	Source of parameter value					
				GIS derived	Assigned value	Computed	Literature	Default value	Calibrated
HRU (distributed) parameters (nhru = 653)									
carea_max	srunoff_smidx	Maximum possible area contributing to surface runoff expressed as a portion of the HRU area (decimal percent).	[1]0.6	X	—	—	—	—	—
cov_type	basin	Vegetation cover type for each HRU (0=bare soil; 1=grasses; 2=shrubs; 3=trees).	0–3	X	—	—	—	—	—
covden_sum	basin	Summer vegetation cover density (decimal percent) for the major vegetation type in each HRU.	0–0.75	X	—	—	—	—	—
covden_win	basin	Winter vegetation cover density (decimal percent) for the major vegetation type in each HRU.	0–0.75	X	—	—	—	—	—
emis_noppt	snowcomp	Emissivity of air on days without precipitation (decimal fraction). Average emissivity of air on days without precipitation.	0.83607–1	—	—	—	—	—	X
fastcoef_lin	soilzone	Linear preferential-flow routing coefficient (fraction/day). Linear coefficient in equation to route preferential-flow storage down slope for each HRU.	0.00106–0.79939	—	—	—	—	—	X
fastcoef_sq	soilzone	Non-linear preferential-flow routing coefficient. Non-linear coefficient in equation used to route preferential-flow storage down slope for each HRU (no units).	0.8–0.83	—	—	—	—	X	—
freeh2o_cap	snowcomp	Free-water holding capacity of snowpack (fraction/day). Free-water holding capacity of snowpack expressed as a decimal fraction of the frozen water content of the snowpack (variable: pk_ice).	0.01001–0.19806	—	—	—	—	—	X
gwflow_coef	gwflow	Groundwater routing coefficient (fraction/day). Linear coefficient in the equation to compute groundwater discharge for each groundwater reservoir.	0.01573–0.09984	—	—	—	—	—	X
gwsink_coef	gwflow	Groundwater sink coefficient to compute the seepage from each reservoir to a groundwater sink (fraction/day).	0–0.00855	—	X	—	—	—	—
gwstor_init	gwflow	Initial storage in each groundwater reservoir. Storage in each groundwater reservoir at the beginning of a simulation (in inches).	0.966–2	X	—	—	—	—	—
hru_area	basin	Area of each HRU (acres).	54–7917	X	—	—	—	—	—
hru_aspect	soltab	Aspect of each HRU (angular degrees).	40–306	X	—	—	—	—	—
hru_deplcrv	snowcomp	Index number for the snowpack areal depletion curve associated with each HRU.	1–2	X	—	—	X	—	—

Table 8. Source of parameter values for hydrologic response units, routing, two-dimensional, and whole-model parameters for the Merced River Basin Precipitation Runoff Modeling System.—Continued

[Source(s) of parameter data is indicated by "X" character. **Abbreviations**: ET, evapotranspiration; GIS, geographic information system; nhru, number of HRUs; nmonths, number of months; nsegment, number of stream segments; PRMS, Precipitation-Runoff Modeling System; —, not applicable]

Model parameter	Module	Description of parameter (PRMS version 4.0.2)	Range of values	Source of parameter value					
				GIS derived	Assigned value	Computed	Literature	Default value	Calibrated
HRU (distributed) parameters (nhru = 653)—Continued									
hru_elev	basin	Mean elevation for each HRU (feet).	393–12,247	X	—	—	—	—	—
hru_lat	basin	Latitude of each HRU.	37.45846–37.88779	X	—	—	—	—	—
hru_percent_imperv	basin	HRU impervious area as a decimal percent of the total HRU area.	0–0.999	X	—	—	—	—	—
hru_segment	basin	Segment index to which an HRU contributes lateral flows (surface runoff, interflow, and groundwater discharge).	1–42	—	X	—	—	—	—
hru_slope	soltab	Slope of each HRU, specified as change in vertical length divided by change in horizontal length (decimal fraction).	0.018–1.822	X	—	—	—	—	—
hru_subbasin	subbasin	Index of subbasin assigned to each HRU.	1–3	—	X	—	—	—	—
hru_type	basin	Type of each HRU (0=inactive; 1=land; 2=lake; 3=swale).	[1]1	—	X	—	—	—	—
imperv_stor_max	srunoff_smidx	Maximum impervious area retention storage for each HRU (in inches).	0–0.2	—	—	X	—	—	—
jh_coef_hru	potet_jh	Air temperature (°F) coefficient used in Jensen-Haise potential ET computations for each HRU.	9.84–21.6945	—	—	X	—	—	X
potet_sublim	intcp	Fraction of potential ET that is sublimated from snow in the canopy and snowpack for each HRU (decimal fraction).	0.11447–0.74891	—	—	—	—	—	X
pref_flow_den	soilzone	Fraction of the soil zone in which preferential flow occurs for each HRU (decimal fraction).	0.00003–0.099997	—	—	—	—	—	X
rad_trncf	snowcomp	Transmission coefficient for short-wave radiation through the winter vegetation canopy (decimal fraction).	00000.14–0.95	—	—	X	—	—	—
sat_threshold	soilzone	Soil saturation threshold, above field-capacity threshold. Water holding capacity of the gravity and preferential-flow reservoirs; difference between field capacity and total soil saturation for each HRU (in inches).	1.00132–13.99712	—	—	—	—	—	X
segment_type	routing	Segment type (0=segment; 1=diversion; 2=lake; 3=replace inflow).	[1]0	—	—	—	—	X	—
slowcoef_lin	soilzone	Linear gravity-flow reservoir routing coefficient. Linear coefficient in equation to route gravity-reservoir storage down slope for each HRU (fraction/day).	0.00144–0.48198	—	—	—	—	—	X
slowcoef_sq	soilzone	Non-linear gravity-flow reservoir routing coefficient in equation to route gravity-reservoir storage down slope for each HRU (no units).	0.05036–0.29937	—	—	—	—	—	—

Table 8. Source of parameter values for hydrologic response units, routing, two-dimensional, and whole-model parameters for the Merced River Basin Precipitation Runoff Modeling System.—Continued

[Source(s) of parameter data is indicated by "X" character. **Abbreviations**: ET, evapotranspiration; GIS, geographic information system; nhru, number of HRUs; nmonths, number of months; nsegment, number of stream segments; PRMS, Precipitation-Runoff Modeling System; —, not applicable]

Model parameter	Module	Description of parameter (PRMS version 4.0.2)	Range of values	Source of parameter value					
				GIS derived	Assigned value	Computed	Literature	Default value	Calibrated
HRU (distributed) parameters (nhru = 653)—Continued									
smidx_coef	srunoff_smidx	Coefficient in contributing area computations. Coefficient in non-linear contributing area algorithym for each HRU (decimal fraction).	0.001–0.00225	—	—	—	—	—	X
smidx_exp	srunoff_smidx	Exponent in contributing area computations. Exponent in non-linear contributing area algorithym for each HRU (in 1.0/inch).	0.218–0.3	—	—	—	—	—	X
snarea_thresh	snowcomp	Maximum threshold snowpack water equivalent below which the snow-covered-area curve is applied; varies with elevation (inches).	0–57.976	—	—	X	—	—	—
snow_intcp	intcp	Snow interception storage capacity for the major vegetation type in each HRU (inches).	0–0.35	—	—	—	X	—	—
snowinfil_max	srunoff_smidx	Maximum snow infiltration per day for each HRU (in inches/day).	2–5	—	—	—	—	X	—
soil2gw_max	soilzone	Maximum value for capillary reservoir excess to groundwater reservoir. Maximum amount of the capillary reservoir excess that is routed directly to the groundwater reservoir for each HRU (inches).	0.00001–0.3694	—	—	—	—	—	X
snowpack_init	sonwcomp	Initial snowpack water equivalent in each HRU (in inches). Storage of snowpack in each HRU at the beginning of a simulation.	1 0	—	X	—	—	—	—
soil_moist_init	soilzone	Initial value of available water in capillary reservoir for each HRU (inches).	0.2–4.97077	X	—	—	—	—	—
soil_moist_max	soilzone	Maximum value of water for soil zone. Maximum available water holding capacity of capillary reservoir from land surface to rooting depth of the major vegetation type of each HRU (inches).	2.03737–9.99996	—	—	—	—	—	X
soil_rechr_init	soilzone	Initial storage for soil recharge zone (upper part of capillary reservoir where losses occur as both evaporation and transpiration) for each HRU; must be less than or equal to soil_moist_init (inches).	0.05–1.24269	X	—	—	—	—	—
soil_rechr_max	soilzone	Maximum storage for soil recharge zone (upper portion of capillary reservoir where losses occur as both evaporation and transpiration); must be less than or equal to soil_moist_max (inches).	0.48963–2.49137	—	—	—	—	—	X

Table 8. Source of parameter values for hydrologic response units, routing, two-dimensional, and whole-model parameters for the Merced River Basin Precipitation Runoff Modeling System.—Continued

[Source(s) of parameter data is indicated by "X" character. **Abbreviations**: ET, evapotranspiration; GIS, geographic information system; nhru, number of HRUs; nmonths, number of months; nsegment, number of stream segments; PRMS, Precipitation-Runoff Modeling System; —, not applicable]

Model parameter	Module	Description of parameter (PRMS version 4.0.2)	Range of values	Source of parameter value					
				GIS derived	Assigned value	Computed	Literature	Default value	Calibrated
HRU (distributed) parameters (nhru = 653)—Continued									
soil_type	soilzone	Soil type of each HRU (1=sand; 2=loam; 3=clay).	1–2	X	—	—	—	—	—
srain_intcp	intcp	Summer rain interception storage capacity for the major vegetation type in each HRU (inches).	0–0.35	—	—	—	X	—	—
ssr2gw_rate	soilzone	Linear coefficient in equation used to route water from the gravity reservoir to the groundwater reservoir for each HRU (fraction/day).	0.05003–0.08351	—	—	—	—	—	X
tmax_allsnow	climate_hru	Maximum temperature in degrees Fahrenheit (°F) when precipitation is all snow. Maximum air temperature when precipitation is assumed to be snow; if HRU air temperature is less than or equal to this value, precipitation is snow.	30.00431–38.57192	—	—	—	—	—	X
tmax_cbh_adj	climate_hru	HRU maximum temperature adjustment in degrees Fahrenheit (°F) to HRU temperture, basd on slope an daspect of HRU.	–5–(–2.5)	—	—	—	—	—	X
tmin_cbh_adj	climate_hru	HRU minimum temperature adjustment in degrees Fahrenheit (°F) to HRU temperture, basd on slope and aspect of HRU.	–5–(–2.5)	—	—	—	—	—	X
transp_beg	transp_tindex	Month to begin summing the maximum air temperature for each HRU; when sum is greater than or equal to transp_tmax, transpiration begins.	0–4	—	—	—	X	—	—
transp_end	transp_tindex	Month to stop transpiration computations; transpiration is computed thru end of previous month.	0–11	—	—	—	X	—	—
transp_tmax	transp_tindex	Temperature index to determine the specific date of the start of the transpiration period; the maximum air temperature (°F) for each HRU is summed starting with the first day of month transp_beg; when the sum exceeds this index, transpiration begins.	1–500	—	—	—	—	X	—
wrain_intcp	intcp	Winter rain interception storage capacity for the major vegetation type in each HRU (inches).	0–0.35	—	—	—	X	—	—
Selected routing (distributed) parameters (nsegment = 42)									
k_coef	muskingum	Muskingum storage coefficient. Travel time of flood wave from one segment to the next downstream segment; enter 1.0 for reservoirs, diversions, and segment(s) flowing out of the basin (in hours).	1–6.02032	—	—	—	—	—	X
segment_flow_init	muskingum	Initial flow in each stream segment.	1 0	—	—	—	—	X	—

Table 8. Source of parameter values for hydrologic response units, routing, two-dimensional, and whole-model parameters for the Merced River Basin Precipitation Runoff Modeling System.—Continued

[Source(s) of parameter data is indicated by "X" character. **Abbreviations**: ET, evapotranspiration; GIS, geographic information system; nhru, number of HRUs; nmonths, number of months; nsegment, number of stream segments; PRMS, Precipitation-Runoff Modeling System; —, not applicable]

Model parameter	Module	Description of parameter (PRMS version 4.0.2)	Range of values	Source of parameter value					
				GIS derived	Assigned value	Computed	Literature	Default value	Calibrated
Two-dimensional (distributed) parameters (nhru = 653, nmonths = 12)									
adjmix_rain	climate_hru	Monthly (January to December) factor to adjust rain proportion in a mixed rain/snow event. Adjustment factor for rain in a rain/snow mix (decimal fraction).	1–1.4	—	—	—	—	—	X
cecn_coef	snowcomp	Monthly (January to December) convection condensation energy coefficient for each HRU (in calories per degree Celsius above 0).	3.55161–9.75294	—	—	—	—	—	X
dday_intcp	ddsolrad	Monthly (January to December) intercept in temperature degree-day equation used in solar radiation computations.	(–30)–(–10)	—	—	—	—	—	X
dday_slope	ddsolrad	Monthly (January to December) slope in temperature degree-day equation used to compute solar radiation computations.	0.0855–0.9119	—	—	—	—	—	X
jh_coef	potet_jh	Monthly (January to December) air temperature coefficient used in Jensen-Haise potential ET computations (air temperature coefficient used in the Jensen-Haise (1963) potential evapotranspiration computations) for each HRU (per °F).	0.0031–0.0523	—	—	—	—	—	X
rain_cbh_adj	climate_hru	Monthly (January to December) adjustment factor to measured precipitation determined to be rain on each HRU to account for differences in elevation, and so forth. Rain adjustment factor, by month for each HRU (factor to adjust precipitation [rain]) to each HRU (decimal fraction).	0.6–1.2	—	—	—	—	—	X
snow_cbh_adj	climate_hru	Monthly (January to December) adjustment factor to measured precipitation determined to be snow on each HRU to account for differences in elevation, and so forth. Snow adjustment factor, by month for each HRU (factor to adjust precipitation [snow]) to each HRU (decimal fraction).	0.6–1.1	—	—	—	—	—	X
tmax_allrain	climate_hru	Precipitation is rain if HRU max temperature >= this value. Monthly (January to December) maximum air temperature (°F) when precipitation is assumed to be rain; if HRU air temperature is greater than or equal to this value, precipitation is rain.	34–48.76898	—	—	—	—	—	X
Selected whole-model (non-distributed) parameters									
melt_look	snowcomp	Julian date to start looking for spring snowmelt.	[1]60	—	—	—	—	—	X
melt_force	snowcomp	Julian date to force snowpack to spring snowmelt.	[1]90	—	—	—	—	—	X

[1]For this parameter, a single parameter value was assigned to all HRUs.

Precipitation stations are located below the historical 5,500-foot snowline so that measurements were not recorded in areas where snow is likely to form (table 1; fig. 8). An evaluation of mean-monthly measurements showed that November through March is the wet season, with December–January being the wettest months (table 9). Notably, two sets of precipitation stations are co-located so that the representation of local measurements is continued from one station to the next, transiting at the start of water year 2003 (Yosemite Valley stations 49855 and YYV at about 4,000 feet and South Fork stations 48380 and YOW at about 5,000 feet).

It is especially important to understand the spatial and temporal distribution of daily air temperatures when studying and simulating streamflows, as PRMS uses daily air temperatures to compute heat balances, solar radiation, precipitation form (rain only, snow only, or rain-snow mixture), snowmelt and accumulation, sublimation, evapotranspiration, and other critical elements (Markstrom and others, 2015). The measurements collected at the 17 air temperature stations used in this study (table 1) may not be entirely representative of conditions throughout the model domain, but other stations that might improve the coverage of daily measurements of the basin, especially at higher attitudes, were not yet reporting at the time of this study on a real-time basis. Further, localized environmental conditions influenced the measurements collected at stations. In particular, the steep, 2,000–3,000 ft elevation gains of the granite cliffs surrounding Yosemite Valley proved challenging. A typical orographic lapse rate for basins in the Sierra Nevada has been estimated to be about 3.6 °F per 1,000 ft of altitude change (Jeton, 2000; Koczot and others, 2005). In this study, lapse rates between Yosemite Valley air temperature stations, compared with ridgeline or Lower Merced Valley climate stations, were found to change as much as 10 degrees per 1,000 feet. Therefore, Yosemite Valley produces its own microclimate, effectively on occasion operating as a freezer in winter or warming oven in summer in relationship to neighboring climate stations. Through trials of model runs and comparisons of simulated to observed streamflows, it was determined that these stations biased the climate inputs to unrealistic extremes and created poor simulations, so these stations (YYV and 49855) were dropped from the dataset of measured temperatures used in this study.

To get a sense of the character and limitations of measurements of air-temperature time-series data used in this study, mean-monthly measurements of observed daily air temperatures from the 17 stations (table 1) were evaluated from months missing no more than 3 days of record. Locations are shown on figure 8. As expected, January and February are the coldest months. Only 5 stations are located at or above the historical 5,500-ft snowline, but none above 8,200 ft (fig. 2). As with precipitation records, temperature data collected at nearby stations continue the local records of offline sites (record-pairs include stations 42920 and EXC, and 48380 and YOW (this set was later dropped from this study). Three air temperature stations, 44102, DGH, and GIN, simultaneously reported near one another on the northern model-domain ridgeline, although 44102 and DGH were offline by June 2010. Therefore, nearby temperature measurements serve to continue the local record, though there can be differences between paired temperature records owing to differential exposure to localized climatic effects or instrument calibration. Differences play a part in the climate inputs that drive the model and were evaluated using a climate distribution tool (Donovan and Koczot, 2019; see the section "Climate Data Distribution Methodology").

To determine the form precipitation is likely to take and when and where snowpack is likely to form in the basin based on air temperatures recorded for a day, the percentage of days when air temperatures were measured to be above and below freezing were compiled by month from stations using only months missing no more than three daily measurements. Because most of the temperature stations in this dataset are located below the snowline, we focused this analysis on the six higher-altitude stations (above 6,000 ft), with two at about 8,000 feet (table 1). Four temperature stations are in the transitional altitudes where precipitation may fall as rain on snow. Tenaya Lake (TNY; 8,150 ft) is the coolest and highest altitude station reporting during expected months of precipitation (October–April). In all cases, during the months when precipitation is expected to fall, daily maximum temperatures are warmer than freezing as much as 80 percent of the time, and minimum temperatures were at or below freezing about 50–100 percent of the time.

Table 9. Mean-monthly (total) precipitation, in inches, measured at stations in or near the Merced River Basin, California, during water years 1949–2013.

[Values are computed from mean-monthly total precipitation, in inches, from months missing no more than three daily measurements. **Abbreviations**: ft, feet; mm/dd/yyyy, month/day/year]

Precipitation station	Identifying designation[1]	Altitude[2] (ft)	Reporting period[3] (mm/dd/yyyy)	Oct.	Nov.	Dec.	Jan.	Feb.	Mar.	Apr.	May	June	July	Aug.	Sep.
Dry Creek near Coulterville	DCC	728	04/28/1998–09/30/2013	0.81	1.37	2.24	2.59	2.54	1.96	1.77	0.91	0.22	0.27	0.30	0.25
Dudley Ranch below Coulterville	DUC	3,654	12/01/1998–09/30/2013	1.94	3.25	6.82	6.12	6.24	3.93	2.68	1.16	0.51	0.06	0.12	0.11
Dudleys (McDiarmid Fire Station)[4]	**DDL**	**3,000**	**10/01/1948–01/31/1976**	**1.17**	**4.42**	**6.09**	**6.83**	**5.27**	**5.54**	**3.64**	**1.05**	**0.38**	**0.03**	**0.11**	**0.41**
El Portal	FA6724EE	2,050	06/09/2004–09/30/2013	2.92	2.37	5.27	5.50	4.85	4.62	2.03	1.56	0.63	0.02	0.01	0.22
Exchequer Dam[4]	**42920**	**442**	**12/01/1950–09/30/2002**	**0.96**	**2.29**	**2.99**	**3.68**	**3.23**	**3.24**	**1.86**	**0.58**	**0.22**	**0.04**	**0.05**	**0.32**
Merced #148	C148	200	01/04/1999–09/30/2013	0.79	1.09	2.19	1.99	2.18	1.62	1.41	0.48	0.17	0.00	0.00	0.07
Merced River	44113	2,600	10/15/1991–11/20/1997	1.63	2.39	6.20	8.22	4.53	4.04	1.82	1.18	0.57	0.17	0.00	0.06
Merced River near Briceburg	MBB	1,150	06/08/1999–09/30/2013	2.03	2.47	5.59	4.38	4.38	3.57	2.06	1.07	0.37	0.00	0.01	0.20
Smith Peak[5]	44115	3,870	06/11/2012–09/30/2013	0.49	6.97	9.97	0.77	0.61	2.13	1.12	0.68	0.27	0.00	0.01	0.10
South Entr Yosemite[4]	**48380**	**5,137**	**10/01/1948–09/30/2002**	**1.88**	**4.98**	**6.34**	**8.54**	**7.22**	**6.56**	**3.72**	**1.57**	**0.64**	**0.14**	**0.07**	**0.79**
Wawona	FA673798	4,052	12/31/2005–09/30/2013	3.31	3.39	7.58	4.43	5.34	4.12	2.25	1.48	0.57	0.01	0.09	0.23
Yosemite at Yosemite Valley	YYV	4,200	10/01/2002–09/30/2013	2.56	3.27	9.22	5.46	5.68	5.97	3.32	1.91	0.35	0.29	0.10	0.45
Yosemite near Wawona	YOW	4,957	10/01/2002–09/30/2013	3.21	4.18	10.16	6.06	6.64	5.85	4.40	2.36	0.46	0.17	0.19	0.30
Yosemite NP[4]	**49855**	**3,966**	**10/01/1948–09/30/2002**	**1.67**	**4.55**	**5.59**	**6.84**	**6.12**	**5.34**	**2.91**	**1.43**	**0.62**	**0.42**	**0.20**	**0.77**

[1]See figures 6, 8, and 11 for location.

[2]Altitudes are from data source and have been converted to or assumed to be measured from North American Vertical Datum of 1988 (NAVD 88). Please see data source for original datums.

[3]Mean-monthly values are computed from data in the reporting period. The reporting period may have had a day or two of records missing from this time series.

[4]Records cover the early part of the study period.

[5]Smith Peak, 44115, mean-monthlys computed from a short record of only 15 months of data, especially during water year 2013.

Climate Data Distribution Methodology

PRMS provides various methods of distributing data from a meteorological station to an HRU. In this study, the configuration of the Merced River Basin PRMS executable included a module (climate_hru) that read climate-by-HRU (CBH) input as time series data; every HRU has its own individual daily precipitation and air temperature time series. These time series datasets are prepared externally to PRMS and can be created using gridded meteorological datasets, such as PRISM (http://www.prism.oregonstate.edu/normals/; Daly and others, 1994, 2008), Daymet data (https://daymet.ornl.gov/; Thornton and others, 2018), and GIS technology to compute a weighted average time series for each HRU. This approach was not used to construct and calibrate the model because gridded daily meteorological datasets were not available in real time at the time of this study, which is essential for real-time streamflow forecasting. Therefore, to distribute real-time climate data measurements collected at meteorological stations (table 1) to individual HRUs, the Draper Climate-Distribution Software (Draper) was used (Koczot and others, 2005; Donovan and Koczot, 2019). Draper-constructed climate-by-HRU (CBH) data (precipitation and minimum/maximum air temperatures) files are formatted for PRMS input. The period of record for these data included enough spin-up time to equilibrate the model (typically three years or more) up to the current date when the forecast is made.

Long-term mean-monthly climate-data estimates from the PRISM method—30-year means for 1981–2010 data—were used as input to Draper, along with daily climate data measured at meteorological stations (table 1) to compute the estimates at each HRU centroid (for examples of PRISM surfaces, please see figs. 5–7). A detailed description of the Draper methodology is presented in the Draper user's manual (Donovan and Koczot, 2019), which includes the Merced River Basin PRMS time-series file preparation as a case study.

Distribution Method Limitations

A significant limitation encountered with the chosen climate data distribution method was that only 4–5 precipitation and 2–3 temperature stations for the South Fork model were online prior to 1986, and their records exhibit intermittent gaps before becoming completely inactive in later years (fig. 8; table 1). We examined each station's daily record for the average of percent missing values in a year and found that the precipitation dataset is more comprehensive than the temperature dataset (table 10).

We further examined the percentage of time Draper used each of its three estimation methods (described by Donovan and Koczot, 2019). The preferred method is Method I, which requires three or more stations reporting on a given day; the second preference is Method II, which requires one or two stations reporting; and the fallback method is Method III, which simply uses the PRISM monthly surface if no stations are reporting. Table 11 indicates how often each method was used for precipitation and temperature for three different time periods. Because too few temperature stations consistently reported in the early part of the record, the temperatures used for the South Fork calibration/validation were mostly derived from scaled averages of the PRISM 1981–2010 data without the benefit of Draper Method I and, therefore, may not be entirely representative of the South Fork climate during the time periods selected. Draper also reverted to Method II or Method III if the preferred method generated any values outside of the allowable range specified in the RANGE file. For precipitation (PPT) and minimum temperature data (TMIN), this happened on a negligible number of days. For maximum temperature data (TMAX), Method III was used only once, but Method II was used on 140 days, mostly between 1967 and 1975.

To get a sense of how well the PRISM data initially represented local conditions without improvement by Methods I or II, mean-monthly values were computed from station data and compared to values sampled from digital surfaces of the PRISM mean-monthly 1981–2010 series used in this study. The PRISM mean-monthly precipitation values were generally found to be within 1–2 inches of measured precipitation, with stations 44115 and FA673798 differing the most from PRISM during November–March by about 2.5–6 inches. In the cool season, November–April, the mean-monthly maximum temperatures were generally found to be within a few degrees Fahrenheit of the PRISM values, but with stations EXC and 42920 cooler by 4–7 degrees. Mean-monthly minimum temperatures were generally found to be within a few degrees Fahrenheit of the PRISM values, with 44113 and 44115 considerably cooler by as much as 9 °F and stations DDL and 48380 warmer by as much as 5 °F.

Table 10. Climate stations mean-yearly percentage of missing data during water years 1949–2013, Merced River Basin, California.

[ft, feet; ID, identification mm/dd/yyyy, month/day/year; —, not applicable]

Station name	ID	Altitude[1] (ft)	Reporting period (mm/dd/yyyy)	Number of years	Mean-annual percent missing in reporting period[2]	Standard deviation
Precipitation stations						
Dry Creek near Coulterville	DCC	728	04/28/1998–09/30/2013	15	8.8	16.9
Dudley Ranch below Coulterville	DUC	3,654	12/01/1998–09/30/2013	14	8.2	15.3
Dudleys (McDiarmid Fire Station)	DDL	3,000	10/01/1948–01/31/1976	28	7.6	20.8
El Portal	FA6724EE	2,050	06/09/2004–09/30/2013	9	18.5	30.7
Exchequer Dam	42920	442	12/01/1950–09/30/2002	52	1.0	3.4
Merced #148	C148	200	01/04/1999–09/30/2013	14	1.9	7.0
Merced River	44113	2,600	10/15/1991–11/20/1997	7	13.5	32.0
Merced River near Briceburg	MBB	1,150	06/08/1999–09/30/2013	14	12.5	25.7
Smith Peak	44115	3,870	06/11/2012–09/30/2013	1	69.4	—
South Entr Yosemite	48380	5,137	10/01/1948–09/30/2002	54	3.4	10.6
Wawona	FA673798	4,052	12/31/2005–09/30/2013	7	10.1	25.4
Yosemite at Yosemite Valley	YYV	4,200	10/01/2002–09/30/2013	10	0.5	0.4
Yosemite near Wawona	YOW	4,957	10/01/2002–09/30/2013	10	1.0	1.4
Yosemite NP	49855	3,966	10/01/1948–09/30/2002	54	3.2	7.7
Temperature stations						
Crane Flat Lookout	44102	6,644	11/04/1991–11/20/2007	17	22.3	25.0
Dog House Meadow	DGH	6,100	10/01/2005–06/11/2010	5	8.9	13.7
Dudley Ranch below Coulterville	DUC	3,654	01/01/2001–09/30/2013	12	9.4	17.4
Dudleys (McDiarmid Fire Station)	DDL	3,000	10/01/1948–01/31/1976	28	10.7	21.7
Exchequer Dam	42920	442	08/01/1966–09/30/2005	40	3.2	13.0
Gin Flat	GIN	7,050	10/01/1985–09/30/2013	26	29.3	22.7
Mariposa Grove	MPG	6,400	09/22/1988–09/30/2013	25	31.3	36.2
Merced #148	C148	200	01/05/1999–09/30/2013	14	4.6	7.4
Merced River	44113	2,600	10/15/1991–11/20/1997	7	14.5	31.6
Merced River near Briceburg	MBB	1,150	10/01/2005–09/30/2013	7	2.3	4.9
New Exchequer- Lk McClure	EXC	879	10/01/2005–05/14/2013	7	1.1	1.0
Ostrander Lake	STR	8,200	10/24/1989–12/31/2000	12	23.3	21.2
Smith Peak	44115	3,870	06/11/2012–09/30/2013	1	69.4	—
South Entr Yosemite	48380	5,137	10/01/1948–09/30/2005	57	5.3	11.9
Tenaya Lake	TNY	8,150	10/01/2005–09/30/2013	7	8.7	3.8
Wawona	FA673798	4,052	12/30/2004–09/30/2013	8	21.5	39.4
Yosemite near Wawona	YOW	4,957	10/01/2005–09/30/2013	7	2.6	1.5

[1]Altitudes are from data source and have been converted to or assumed to be measured from North American Vertical Datum of 1988 (NAVD 88). Please see data source for original datums.

[2]"Zero" may include 0–0.5 percent missing from this time series.

Table 11. Summary of the frequency of days that used Draper methods I, II, and III, by data type and time-period, Merced River Basin, California.

[<, less than]

Data type	Water years	Days using method I		Days using method II		Days using method III		Total days
		Number of days	Percent of total days reporting	Number of days	Percent of total days reporting	Number of days	Percent of total days reporting	
Precipitation	1949–1975	9,787	99	72	<1	2	<1	9,861
Precipitation	1976–1988	4,317	91	432	9	0	0	4,749
Precipitation	1989–2013	9,094	99	37	<1	0	0	9,131
Temperature	1949–1975	2,171	22	7,671	78	19	<1	9,861
Temperature	1976–1988	2,406	51	3,939	49	11	<1	4,749
Temperature	1989–2013	9,050	99	81	<1	0	0	9,131

Calibration

A preliminary calibration of the model has been completed and is presented in this report. Additional calibration refinement may be needed depending on the application. The most important use of the model is to simulate (and eventually, forecast) year-to-year variations of inflows to Lake McClure (at the model domain outlet) during the critical April–July snowmelt season. Therefore, calibration focused primarily on simulating flows during this season, secondly on monthly simulations, and finally on daily flow characteristics. Annual-flow calibrations were also considered. The calibration and validation periods (table 12) were chosen from the available streamflow records with an effort to represent a balance of wet and dry years. The calibration and validation periods selected for the South Fork were especially limited by the short streamflow record (water years 1952–75). Calibrations were performed at four U.S. Geological Survey streamflow gage locations within the basin and at a single outlet point at U.S. Geological Survey streamflow-gaging station 11270900 (also known as CDEC station MRC; tables 2, 11; fig. 11). Simulations from Pohono and South Fork Subbasins were evaluated against measured streamflow, whereas simulations from the entire model domain were evaluated against reconstructed streamflow data. The calibration/validation periods for the various areas were between water years 1952–2013 (table 12).

Target Data

PRMS is a natural flow model and minimally requires natural, unimpaired daily time-series streamflow data as model-calibration and validation targets. Solar radiation, potential evaporation, and snow-water equivalents are not required as calibration targets or as input to PRMS because they are computed within the model, but, if adequate long-term station observations that are distributed over the model domain are available, these may be useful in either calibrating or forecasting. This was not the case for this study. Instead, solar radiation and potential evaporation were calibrated using data sampled from mean-monthly digital surfaces as calibration targets.

Streamflows

Streamflow measurements collected by the USGS and used in this study as calibration targets were considered in this study to be “unimpaired natural flows” (U.S. Geological Survey, 2020; https://waterdata.usgs.gov/nwis; table 3; figs. 8, 9). The USGS rates the accuracy of its streamflow records based on (1) the stability of the stage-discharge relation, (2) the accuracy of measurements of stage and discharge, and (3) the interpretation of records (Bonner and others, 1998). Accuracy levels of “good” indicate that about 95 percent of the daily discharges are within 10 percent of their true values. “Fair” indicates that 95 percent of the daily discharges are within 15 percent (Bostic and others, 1997). The accuracy of USGS streamflow records at streamgages used here has been historically good to excellent, except for those with a period of no gage height, or estimated daily discharges, which are considered fair. For accuracy ratings, please see the USGS Water-Data Reports (https://ca.water.usgs.gov/data/waterdata). Conditions not accounted for in data supplied by USGS are summarized here for completeness. Small diversions upstream of the Happy Isles gage are used for Yosemite Valley’s water supply. A small amount of treated sewage effluent is returned between Happy Isles and Pohono streamgages. Small diversions above the South Fork gages are sent for use in the Fresno River Basin or for local irrigation and domestic water supply.

Table 12. Merced River Basin PRMS model calibration and validation periods, water years 1952–2013.

[HRU, hydrologic response unit; ID, identification; mi², square miles; —, not applicable; USGS, U.S. Geological Survey]

Area name	Calibration node[1] and station name	Station ID[2]	Drainage area (mi²)	Calibration period (water year)	Validation period (water year)	Number of HRUs	Stream segment index number[3]
Happy Isles	1. Merced R A Happy Isles Bridge NR Yosemite	11264500	181	1989–2006	1980–1988; 2007–2013	168	7
Pohono	2. Merced R A Pohono Bridge NR Yosemite CA	11266500	322	1989–2006	1980–1988; 2007–2013	298	24
Wawona	3. SF Merced R A Wawona CA	11267300	100	1959–1963	1964–1968	62	29
South Fork	4. SF Merced R NR El Portal CA	11268000	241	1956–1967	1952–1955; 1968–1975	157	32
Lower Merced	—	—	—	—	—	—	—
Model Domain	5. Merced R NR Merced Falls	11270900/ MRC[4]	1,059	1989–2006	2007–2013	653	42

[1]For more information about calibration nodes, see table 7.

[2]For more information about the stations, see table 3. See figures 6, 8, and 11 for location.

[3]This number identifies the Merced PRMS stream segment used to access streamflow simulations from drainage areas to the node of interest.

[4]Reconstructed streamflow data provided by California Department of Water Resources (DWR) and computed using a water-budget approach. Reconstructed from gage data measured on the Merced River below Merced Falls Dam near Snell CA. Please see appendix 1 for details. This site is co-located with USGS 11270900, USGS site name is "MERCED R BL MERCED FALLS DAM NR SNELL CA."

The source of the reconstructed natural streamflow data (also known as full natural flows, FNF) at CDEC station MRC used in this study as a calibration target is Merced Irrigation District, who has proprietary knowledge of Merced River Hydroelectric Project operations (table 3; figs. 8, 1.1). After applying inhouse automated tools, DWR further smoothed MID's daily reconstructed streamflow for use in this study by visually scanning data for irregularities and making manual corrections. Reconstructed streamflow at CDEC station MRC was computed from USGS gage data measured at 11270900 using mass-balance calculations cross-referenced against nearby measured natural flows. Daily flows were estimated, from measured daily changes in lake storage and outflow, as apparent inflows to the lakes. FNFs were accumulated in downstream directions and corrected for intervening diversions and impoundments to reconstruct natural flow at MRC. Any moderate error in the Lake McSwain storage (capacity 9,730 acre-ft) would likely have a negligible effect on a calculation of reconstructed natural streamflow given the storage capacity of Lake McClure (capacity 1,032,000 acre-ft). The calculation of the monthly FNF assumes that the evaporative losses from Lake McClure and Lake McSwain are a constant for a given month regardless of the storage for that month. The inflow to Lake McClure is considered unimpaired. Low flows in the reconstructed record are considered unreliable. DWR estimates the accuracy is based on the accuracy of the gage measurements used in the reconstructions; uncertainty of these reconstructions has not been quantified (Steven Nemeth, DWR Snow Surveys Section, unpub. data, 2014). A summary of terms used to compute reconstructed flow is presented in appendix 1.

Solar Radiation, Evaporation, and Snow-Water Equivalents

Calibration targets included gridded solar radiation data from the National Renewable Energy Laboratory (1980; grid-cell size resolution of 10 kilometers [km; 6.2 miles (mi)]) and evaporation data from Farnsworth and others (1982) and Farnsworth and Thompson (1982) with a grid-cell size of 10.25 mi (16.5 km). Typically, solar radiation measured at the Earth's surface increases with altitude and proximity to the equator, and less evaporation occurs at higher altitudes as compared with lower altitudes. The solar radiation daily peak, as a mean-monthly rate, computed from the basinwide digital surfaces ranges from about 700 langleys (ly) in June–July to 190 ly in December–January (data series 1998–2009). The mean annual rate of total evaporation as computed from the basinwide digital surfaces is 48.35 inches (data series 1956–70). Further, a few point measurements of data collected at stations in or near the model domain were available for comparison with estimates from the gridded data (table 12; fig. 8). With exception of an outlier of station 44115 (also known as Smith Peak, measuring high rates of solar radiation for its altitude of 3,870 ft), the comparison of estimates from the gridded data to local observations showed that gridded values fall within a reasonable range for the model area.

Methodology

Calibration of this model, or any watershed model, is an iterative process where, after each adjustment of model parameters, simulated daily streamflows are compared with observed daily streamflows visually (by graphing simulations against observations) and (or) statistically. After initial parameters are set, the model is run, and the simulated hydrograph is compared with observed flows. The model was further calibrated using a combination of manual and automated optimization techniques. A rough initial manual calibration was first performed, followed by calibration of solar radiation and evapotranspiration-process parameters. Next, LUCA, an automated calibration tool (Hay and others, 2006; Hay and Umemoto, 2007) was used to calibrate streamflows from each catchment and subbasin (table 12), and finally manual modifications were made to selected parameter values to complete the calibration. The automated calibration was performed in an upstream to downstream progression (fig. 11; table 7) by incorporating parameter settings from upstream calibrated HRUs into their immediate downstream subbasin. These previously calibrated HRU parameters were held constant, and the calibration was continued on the remaining HRUs in the downstream direction. This process was repeated until no further model improvement was seen.

Another important step in building the model was to first verify that daily HRU temperature data estimated using the Draper method (as described in the "Model Input" section above) were appropriate. These values are very important to the integrity of the model because minimum and maximum daily air temperatures are inputs to the solar radiation, evapotranspiration, and snowpack-formation module algorithms. In trial model runs, it was determined that some estimates of these values were too warm, suggesting that data from air temperature stations used in the Draper method did not adequately represent actual air temperatures in all HRUs, especially at higher altitudes. This was especially problematic because verification is difficult where no site measurements exist. The fits of the simulated to observed streamflows were improved by applying an HRU-based parameter correction factor for all months to adjust temperatures downward. Different values were applied above and below the snowline (5,500 ft altitude) of 5 °F and 2.5 °F, respectively (table 8, tmax_cbh_adj and tmin_cbh_adj). This is normal procedure for an analytical model such as PRMS where limited ground-truth data are available.

Next, solar radiation was manually calibrated against mean-monthly regional- and HRU-resolution data (National Renewable Energy Laboratory, 1980). Daily potential solar radiation was computed using the degree-day method described in Markstrom and others (2015, p. 87). The two parameters **dday_slope** and **dday_intcp** are arrays, both dimensioned by month and HRU, that were manually calibrated against mean-monthly normal incident solar radiation data from National Renewable Energy Laboratory (NREL), area-weighted for the five calibration areas and HRUs using the USGS Geo Data Portal (GDP; https://cida.usgs.gov/gdp/). To calibrate, the PRMS model was run for water years 1949–2013 to simulate daily short-wave solar radiation output. Mean-monthly values of the simulated daily solar radiation were then computed and compared with mean-monthly values of NREL normal incident solar radiation data. The parameters were iteratively adjusted to calibrate them until a best agreement of simulated values with NREL observations was found. The final simulated values show close agreement with observed (fig. 12*A*).

Next, a parameter used to simulate potential evapotranspiration (PET) was manually calibrated against mean-monthly regional and HRU-scale data. As described by Jensen and Haise (1963), Jensen and others (1970), and Markstrom and others (2015, p. 90), daily PET is computed as a function of air temperature, solar radiation, and two coefficients, parameters **jh_coef** and **jh_coef_hru**, using the Jensen-Haise method. The air temperature coefficient parameter, **jh_coef_hru**, was computed (and not subject to further calibration) using equation 1–53 described in Markstrom and others (2015, p. 91). The parameter **jh_coef**, dimensioned by month and HRU, was calibrated using mean area-weighted monthly potential evapotranspiration targets from Farnsworth and Thompson (1982) and Farnsworth and others (1982), acquired using the USGS GDP (https://cida.usgs.gov/gdp/). Mean-monthly potential evapotranspiration values for all HRUs were then computed from simulated daily potential evapotranspiration output for water years 1969–2013. Differences between simulated and observed values were then minimized to determine the appropriate values of the monthly **jh_coef** coefficients for each HRU. The simulated mean-monthly values show close agreement with observed (fig. 12*B*).

Next, areas of the PRMS model were individually calibrated for water balance and streamflows using the LUCA computer program (Hay and others, 2006; Hay and Umemoto, 2007). LUCA has a graphical user interface that provides a simple, systematic way of implementing a multiple-objective, stepwise calibration of the PRMS model parameters, using the Shuffled Complex Evolution global search algorithm (Duan and others, 1993) to optimize and calibrate model parameters. LUCA has been used by researchers to calibrate other PRMS models (Hay and others, 2006; Dudley, 2008; Goode and others, 2010; Christiansen, 2012; LaFontaine and others, 2013; Haj and others, 2014, 2015; Risley, 2019; Koczot, USGS, written communs., 2020).

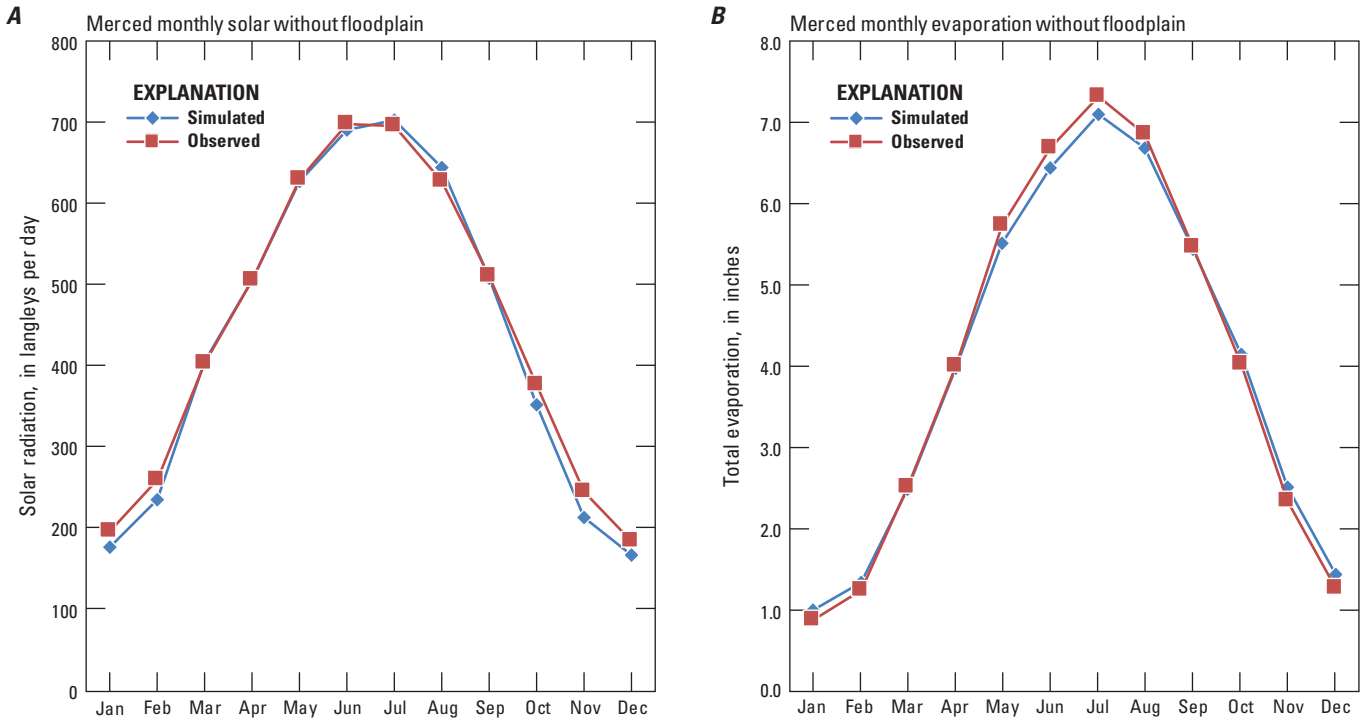

Figure 12. Observed and simulated mean-monthly *A*, solar radiation and *B*, potential evapotranspiration, Merced River Basin Precipitation Runoff Modeling System, water years 1949–2013.

The LUCA runs for the Merced River Basin catchments and subbasins used different calibration periods (table 12). LUCA performs parameter optimization using a series of steps and rounds. During each step, a group of parameters are optimized simultaneously. After a step is completed, the program goes to the next step and optimizes another group of parameters. When it has completed all the specified steps, the program starts a new round by returning to the first step. For this study, LUCA calibration runs were configured to optimized groups of parameters in four steps and six rounds (table 13; Lauren Hay, U.S. Geological Survey, written commun., 2017). The parameters used in the LUCA calibration process are considered to be the sensitive parameters in this model (Markstrom and others, 2016). In each step, an objective function defined as the normalized root mean square error (NRMSE) statistic is used with four separate parameter groups depending on the calibration goal (water balance, timing, high flows, or low flows). Low-flow parameters describe the slower flow paths through soils and the vertical transmission of water into the shallow groundwater reservoir and slower pathways to streams (fig. 10A). Minimum and maximum ranges for the parameter values were also preset. The daily high- and low-flow timing steps were optimized using subdivided observed daily streamflow datasets of either high or low flow, respectively. For each model area (table 12; fig. 11), in addition to the calibration steps shown in table 13, additional LUCA optimization runs were made to improve low flows by further optimizing the parameters ***gwflow_coef, soil2gw_max, ssr2gw_rate, soil_moist_max, and slowcoef_sq*** using a single step and six rounds strategy, employing three equally weighted objective functions (monthly mean, mean monthly, and annual mean). These two LUCA run configurations were repeated several times, by narrowing the parameter ranges and (or) by removing parameters from the group until model performance stopped improving. Parameters that were auto adjusted using LUCA for calibration are shown in table 13. A summary of the final parameter data used by the model is presented in table 8.

Table 13. Let Us Calibrate (LUCA) automated calibration steps and parameters calibrated during the LUCA operation for the Merced River Basin Precipitation Runoff Modeling System, California.

[Table is based on written communication from Lauren Hay, USGS, 2017. **Abbreviations**: PRMS, Precipitation-Runoff Modeling System; Min, minimum; max, maximum; NRMSE, Normalized Root Mean Square Error; ET, evapotranspiration]

Calibration dataset	Objective functions	PRMS parameter	Dimensions	Parameter range		Parameter description
				Min	Max	
			Step 1			
Water balance	NRMSE	rain_cbh_adj	nhru, nmonths	0.6	1.4	Rain adjustment factor
	1. Monthly mean	snow_cbh_adj	nhru, nmonths	0.6	1.4	Snow adjustment factor
	2. Mean monthly					
	3. Annual mean					
			Step 2			
Daily all-flow timing	NRMSE	adjmix_rain	nhru, nmonths	0.6	1.4	Adjustment factor for rain in a rain/snow mix
	1. Daily	cecn_coef	nhru, nmonths	2	10	Convection condensation energy coefficient
	2. Monthly mean	emis_noppt	nhru	0.757	1	Emissivity of air on days without precipitation
		freeh2o_cap	nhru	0.01	0.2	Free-water holding capacity of snowpack
		K_coef	nsegment	1	24	Muskingum storage coefficient
		potet_sublim	nhru	0.1	0.75	Fraction of potential ET that is sublimated from snow
		slowcoef_lin	nhru	0.001	0.5	Linear gravity-flow reservoir routing coefficient
		soil_moist_max	nhru	2	10	Maximum value of water for snow zone
		soil_rechr_max	nhru	0.1	5	Fraction of capillary reservoir with evaporation and transpiration losses
		tmax_allrain	nhru, nmonths	34	50	Offset to determine if precipitation is all rain
		tmax_allsnow	nhru	30	40	Maximum temperature when precipitation is all snow
			Step 3			
Daily high-flow timing	NRMSE	fastcoef_lin	nhru	0.001	0.8	Linear preferential-flow routing coefficient
	1. Daily	pref_flow_den	nhru	0	0.1	Fraction of the soil zone in which perferential flow occurs
	2. Monthly mean	sat_threshold	nhru	1	15	Soil saturation threshold above field-capacity threshold
		smidx_coef	nhru	0.001	0.06	Coefficient in contributing area computations
			Step 4			
Daily low-flow timing (slower pathways through soils to the shallow groundwater reservoir and streams)	NRMSE	gwflow_coef	ngw	0.001	0.1	Groundwater routing coefficient
	1. Daily	soil2gw_max	nhru	0	0.5	Maximum value for capillary reservoir excess
	2. Monthly mean	ssr2gw_rate	nssr	0.05	1.0	Cofficient to route water from gravity reservoir

Streamflow Simulations: Results and Performance Assessment

Performance statistics were computed from simulated and observed streamflow values for annual, seasonal, monthly, and daily time frames, paying special attention to April–July seasonal calibrations and evaluated for each calibration area. No single set of parameter values from calibration of the model will simulate all flow regimes with equal accuracy. Simulations using the final parameter set should have (1) little to no bias, (2) small simulation errors of volume and timing, and (3) realistic parameter values reflecting the environmental conditions being modeled (Leavesley and others, 1983). In watershed modeling, some common measures of simulation error are the sum of errors (for bias), the sum of the absolute values of the errors, and the sum of the squared errors. Absolute errors and errors squared tend to be dominated by a few large events (Haan and others, 1982; Troutman, 1985), unless normalized by the observed flows to form "relative error" measures. The unnormalized root-mean-square error (RMSE) provides a common measure of the magnitude of variation of simulation errors in the original units of measure that complements the relative measures provided by the bias and relative errors. The goal of the calibration process was to maintain a good visual fit between the simulated and observed hydrographs and at the same time keep biases and relative errors below 10 percent (established as an acceptable fit in previous work; Jeton, 1999, 2000; Koczot and others, 2005).

Percent ***Bias***, percent ***Relative error***, and root-mean-square error (***RMSE)*** are defined as

$$Bias = \frac{\sum(s-o)}{\sum o} x\ 100 \quad (1)$$

$$Relative\ Error = \frac{\sum\left[\frac{(s-o)}{o}\right]}{N} x\ 100 \quad (2)$$

$$RMSE = \sqrt{\frac{\sum(s-o)^2}{N}} \quad (3)$$

where

s is simulated mean streamflow, in cubic feet per second (ft^3/s),
o is observed (measured or reconstructed) mean streamflow, in ft^3/s, and
N is the number of streamflow values.

Therefore, Percent ***Bias*** describes the tendency of simulated values to be larger or smaller than observed values. A ***Bias*** of 0.0 is ideal performance (no bias). A positive or negative ***Bias*** indicates an over- or underestimation, respectively. Percent ***Relative Error*** is a measure of the error between simulated and observed values that has been normalized with the observed values. ***Relative Error*** of 0.0 is also ideal performance (errors average to zero), and positive or negative ***Relative Error*** indicates an over- or underestimation, respectively. ***RMSE*** provides a measure of the magnitude of variation of the simulation errors in the original units of the data (that is, not normalized). These were the objective functions used in this study. Note that while individual errors were measured using the daily values of streamflow, the model performance was evaluated for longer time periods (monthly, seasonal, or annual values of the objective functions).

Statistics at each time scale (annual [water year], seasonal, monthly, and daily) were computed from the difference between mean simulated and observed (measured or reconstructed) flows. Model biases, relative errors, and RMSEs computed during the calibration and validation periods for the five calibrated areas are given in table 14. During the season of most interest to water managers, April–July, a good agreement was achieved, indicating acceptable simulations for this seasonal calibration. During this season, the model slightly underestimates streamflows for the interior of the domain and, during the validation period only, overestimates flows at the outlet. However, simulations from the Pohono Subasin underestimate streamflows during the validation period. This difference must originate from the calibration adjustments of the Lower Merced Subbasin, which has different soils and land cover characteristics as compared with other subbasins and is solely calibrated against reconstructed flows. Because the object of this study was to match mid-to-higher flows, during the low-flow seasons of October–December and August–September, not surprisingly, the performance statistics indicate larger errors or biases at the model domain outlet.

The streamflow simulations of the January–March season computed during these periods show considerable over- and underestimation for most of the basin subareas, with the best agreement reached at the outlet of the model domain, based on bias and relative error statistics (table 14). This disparity on accuracy in the calibration of the interior parts of the basin may be due to a couple of factors: (1) different storm types and storm tracks during the January–March season, that were not accounted for in this study, and (2) in some years, the temperatures used to drive the model simulations during the January–March season may still be too warm to represent actual climatic conditions. To test improvements, temperature corrections would have to be performed on the preprocessed CBH data used to drive the model. Refinement of the climate inputs for the January–March season may correct the underestimation of flows in the interior of the model domain during the April–July season and aid in developing a more robust calibration for the Lower Merced Subbasin area calibrated above the domain outlet.

Table 14. Calibration and validation statistics, Merced River Basin Precipitation Runoff Modeling System, water years 1952–2013.

[ID, identification; acre-ft, acre-foot; RMSE, root-mean square error; ft³/s, square foot per second; —, not applicable]

Area[1]	Period of record used (water-years)	Annual (water years)				Seasonal												Monthly			
						Oct.–Dec.			Jan.–Mar.			Apr.–July			Aug.–Sept.						
		N[2]	Bias (percent)	Relative error (percent)	RMSE (ft³/s), except for MRC (acre-ft)	Bias (percent)	Relative error (percent)	RMSE (ft³/s), except for MRC (acre-ft)	Bias (percent)	Relative error (percent)	RMSE (ft³/s), except for MRC (acre-ft)	Bias (percent)	Relative error (percent)	RMSE (ft³/s), except for MRC (acre-ft)	Bias (percent)	Relative error (percent)	RMSE (ft³/s), except for MRC (acre-ft)	N[2]	Bias (percent)	Relative error (percent)	RMSE (ft³/s), except for MRC (acre-ft)
Calibration statistics: water years 1956–2006																					
Happy Isles	1989–2006	18	1.0	–0.9	64.0	11.1	7.6	33.4	–3.0	13.5	104.3	–1.2	–3.5	162.7	56.7	11.6	128.9	216	0.9	14.5	217.3
Pohono	1989–2006	18	3.0	2.5	96.6	27.9	19.0	88.0	30.6	54.2	272.5	–5.1	–7.7	216.8	66.2	18.7	195.1	216	3.1	22.8	377.4
Wawona	1959–1963	5	2.0	3.2	10.8	–26.1	–46.9	4.9	42.5	60.6	47.2	–6.8	–7.8	38.8	42.4	73.8	9.7	60	2.1	21.2	66.8
South Fork	1956–1967	12	3.9	8.1	43.7	–26.0	–16.4	96.8	30.0	46.3	126.0	–3.5	–3.3	77.6	165.5	202.2	54.4	144	4.1	56.2	159.8
Lower Merced[3]	—	—	—	—	—	—	—	—	—	—	—	—	—	—	—	—	—	—	—	—	—
Model Domain	1989–2006	18	5.3	9.8	187.9	15.1	37.8	125.9	12.2	30.3	543.5	–2.8	–1.5	378.8	160.9	358.0	386.9	216	5.3	128.6	775.3
Validation statistics: water years 1952–2013																					
Happy Isles	1980–88, 2007–2013	18	0.3	–2.9	48.4	19.0	19.5	72.7	23.9	17.4	170.8	–5.6	–7.3	124	22.2	25.5	161.5	216	0.3	10.5	222
Pohono	1980–88, 2007–2013	18	0.1	0.4	62.2	10.7	12.0	104.9	50.2	52.6	348.8	–11.0	–10.0	285.7	18.3	11.8	169.0	216	0.1	12.7	370.1
Wawona	1964–68	5	–10.7	–13.0	23.5	–40.1	–43.4	45.1	–13.7	–8.1	40.3	–7.2	–10.9	57.2	70.4	31.1	16.0	60	–10.7	–7.0	94.4
South Fork	1952–55, 1968–75	12	8.0	10.5	45	6.2	3.2	28.6	25.7	37.2	126	–2.6	–1.8	79	229.0	232.5	78	144	8.0	64.0	190
Lower Merced[3]	—	—	—	—	—	—	—	—	—	—	—	—	—	—	—	—	—	—	—	—	—
Model Domain	2007–2013	18	8.4	13.7	188	–25.5	–0.6	229.5	17.4	24.6	367	4.5	8.5	287	216.2	272.4	373	216	8.3	106.5	616

[1]See tables 3 and 7 for details about the streamflow stations and data used in this study for calibration and validation targets.

[2]In relative error and RMSE equations, N is the number of observations for the time scale of interest.

[3]Model parameters for this area were adjusted solely to improve calibrations at the model outlet. No statistics are provided for this area.

Daily

After calibrations were completed on parameters of the upper subbasins (Pohono and South Fork) and saved in the master parameter file, parameters of the Lower Merced Subbasin (tables 8 and 13; fig. 11) were calibrated solely to balance reconstructed inflows to Lake McClure (tables 3, 4, and 5). To best match the lower-flow MRC reconstructions (noting low flows were considered unreliable in many cases), daily streamflow simulations from the Lower Merced Subbasin were reduced to near zero in different water years spanning as many months as July–December. Daily statistics (fig. 13 insets) indicate simulations are similar to observed data. South Fork Subbasin statistics are computed from a different time period, based on available data (water years 1952–75). Because no observed data exist for the Lower Merced Subbasin area, simulations are graphed only for comparison with other areas. The daily calibration at the model outlet (MRC) was further evaluated by removing reconstruced records with low flows (below 100, 200, and 500 ft^3/s). Bias improved from −6.0 to +1.9, with relative error and RMSE showing more variability (21.7 and 1,620.3, respectively).

Mean-Monthly

Mean-monthly percentages (water years 1989–2013) of annual streamflows, showing simulated and observed values, are graphed for each subbasin and the whole model domain (figs. 14*A–D*). As graphed in figure 14*B*, the South Fork Subbasin was calibrated/validated on data from a different climatic period (water years 1952–75). For comparison with the model domain calibration/validation period, the South Fork simulation for water years 1989–2013 is also included in the graph (fig. 14*B*). From Pohono and the model domain, streamflows peak in May (1989–2013). Streamflows from the South Fork calibration and validation periods (water years 1952–75; table 12) also peak in May, but during water years concurrent with calibration/validation of the model domain (water years 1989–2013), streamflows peak a little later (May–June), indicating possible climatic differences between the earlier and latter time periods. Streamflows from the Lower Merced peak in March, corresponding with the rainy season at lower altitudes below the snowline. Although statistically sound as a calibration, visual inspection of the graphs indicates that simulations using the calibrated parameter values result in overestimation of simulated inflows during February–March and July−August (especially for the South Fork Subbasin) and an underestimation for May inflows at the model domain outlet (fig. 14*D*). The primary sources of peak annual streamflow are from the Pohono and South Fork Subbasins. The computed overall RMSEs for monthly inflows from these subbasins and the model domain ranged from 1.9 to 2.5 percent.

The mean-monthly percentage of simulated inflow to Lake McClure for water years 1989–2013 was compared with MRC reconstructions (fig. 15). Figure 15 illustrates the contribution of each individual subbasin model (Pohono, South Fork, and Lower Merced) to the total simulation of Lake McClure inflow, compared with the reconstructed flows computed for the MRC location. For this period of record, the model undersimulates in May and oversimulates in July and August. Table 14 indicates that the temperatures used to drive the model in the February and March months may have been too warm, as too much runoff occurred during those months and not enough snowmelt was left to runoff during April and May. Further, in some cases temperatures may have been too cool in April and May, as too much snowpack was left to melt in July and August (fig. 15). The examples of the comparisions of simulated to observed streamflows presented here suggest that a compromise was struck during calibration to match the average of streamflows from historical climatic extremes represented in the calibration periods.

Wet-Season Inflows to Lake McClure

Model simulations of annual seasonal streamflow-volumes were compared graphically with measurements at the basin outlet for the wettest seasons (January–March and April–July; water years 1989−2013; fig. 16). A comparison of the January–March simulations to MRC reconstructions yields a positive bias of +15 percent and relative error of +31.2 percent, with flow volumes ranging from about 70,400 to 843,200 acre-ft (fig. 16*A*). A comparison of April–July simulations to MRC reconstructions yields a good statistical agreement with an overall slight negative bias of –0.9 percent and relative error of +0.8 percent, with flow volumes ranging from 152,400 to 1,375,700 acre-ft (fig. 16*B*). During the January–March season, the model simulations tend to overestimate streamflows in several years, but well underestimated the high reservoir inflow for 1997, the wettest such season simulated. Simulated streamflows more closely match MRC reconstructions in the April–July season, although there is a slight tendency in April–July towards underestimation, most notably for 1995.

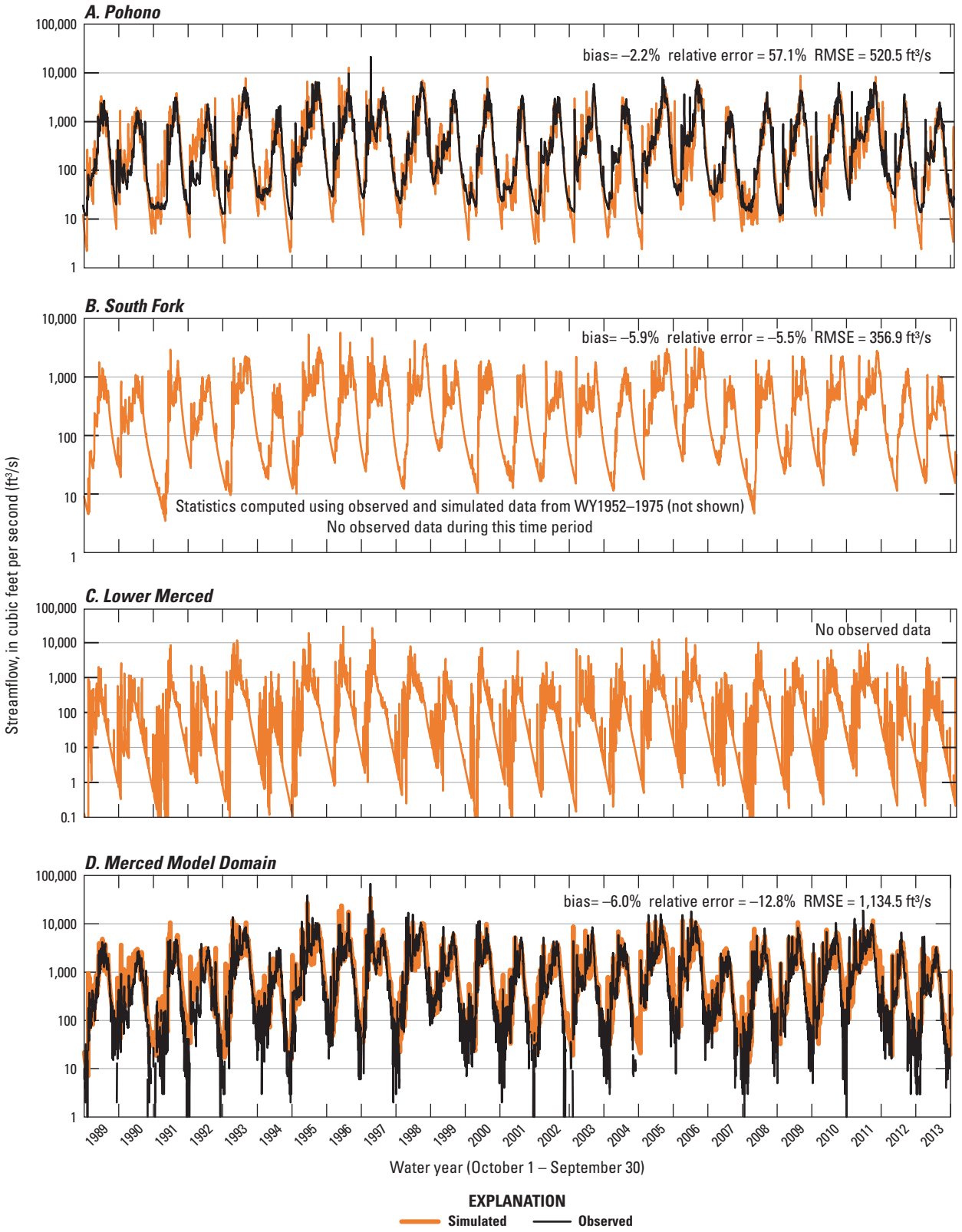

Figure 13. Daily streamflow showing model simulations and observed (measured or reconstructed) streamflow, water years 1989–2013, from *A*, Pohono, *B*, South Fork, and *C*, Lower Merced Subbasins, and *D*, the model domain. (Range of vertical axes vary. Model performance statistics computed from full record of observed data. RMSE, root-mean-square error.)

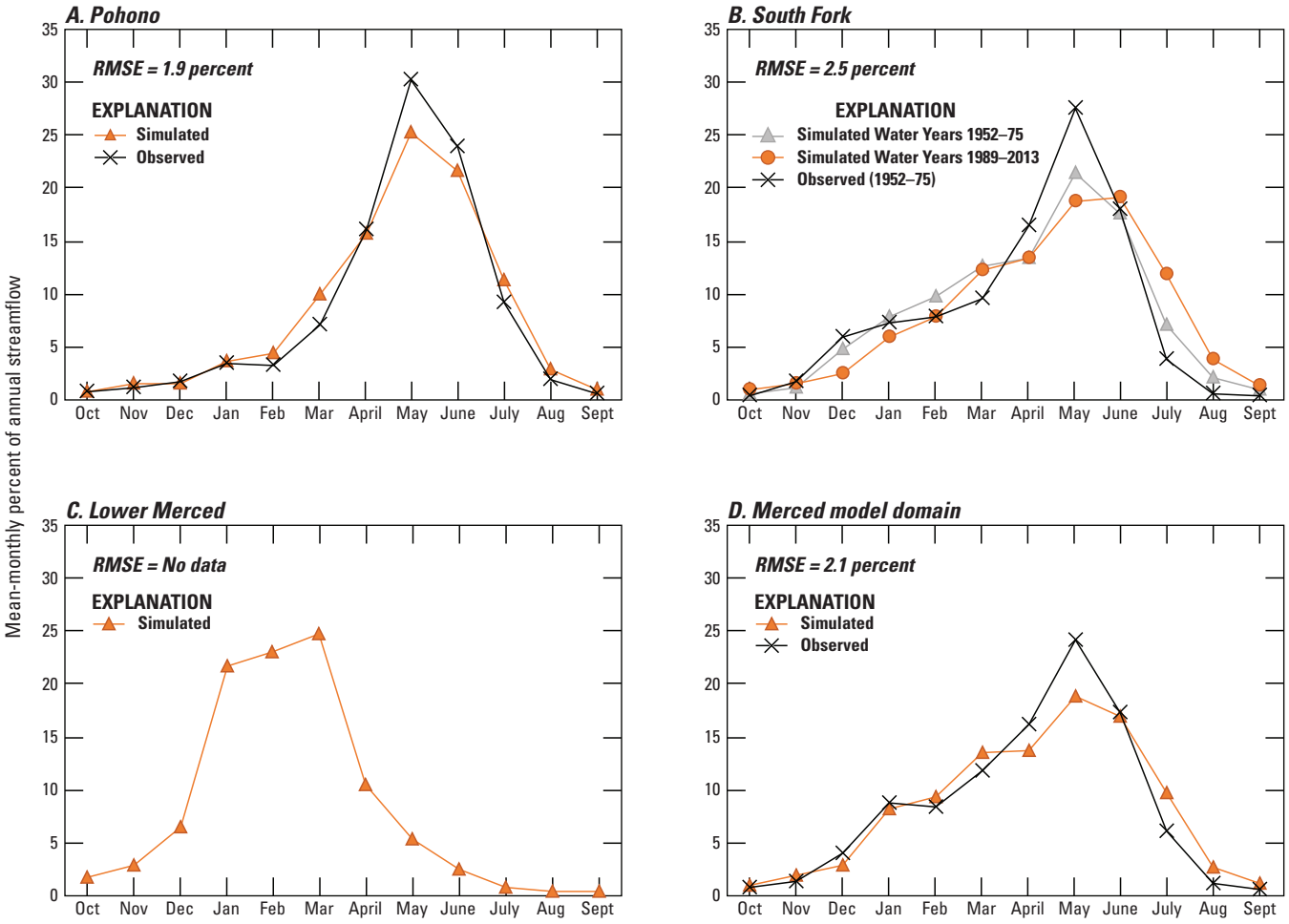

Figure 14. Mean-monthly percentages of annual streamflow for individual subbasins *A*, Pohono, *B*, South Fork, *C*, Lower Merced, and *D*, the model domain, water years 1989–2013. South Fork graph shows period of calibration/validation during water years 1952–75, and simulation during water years 1989–2013. (Observed streamflow is measured or reconstructed. RMSE, root-mean-square error. RMSE's were normalized by dividing by the annual total.)

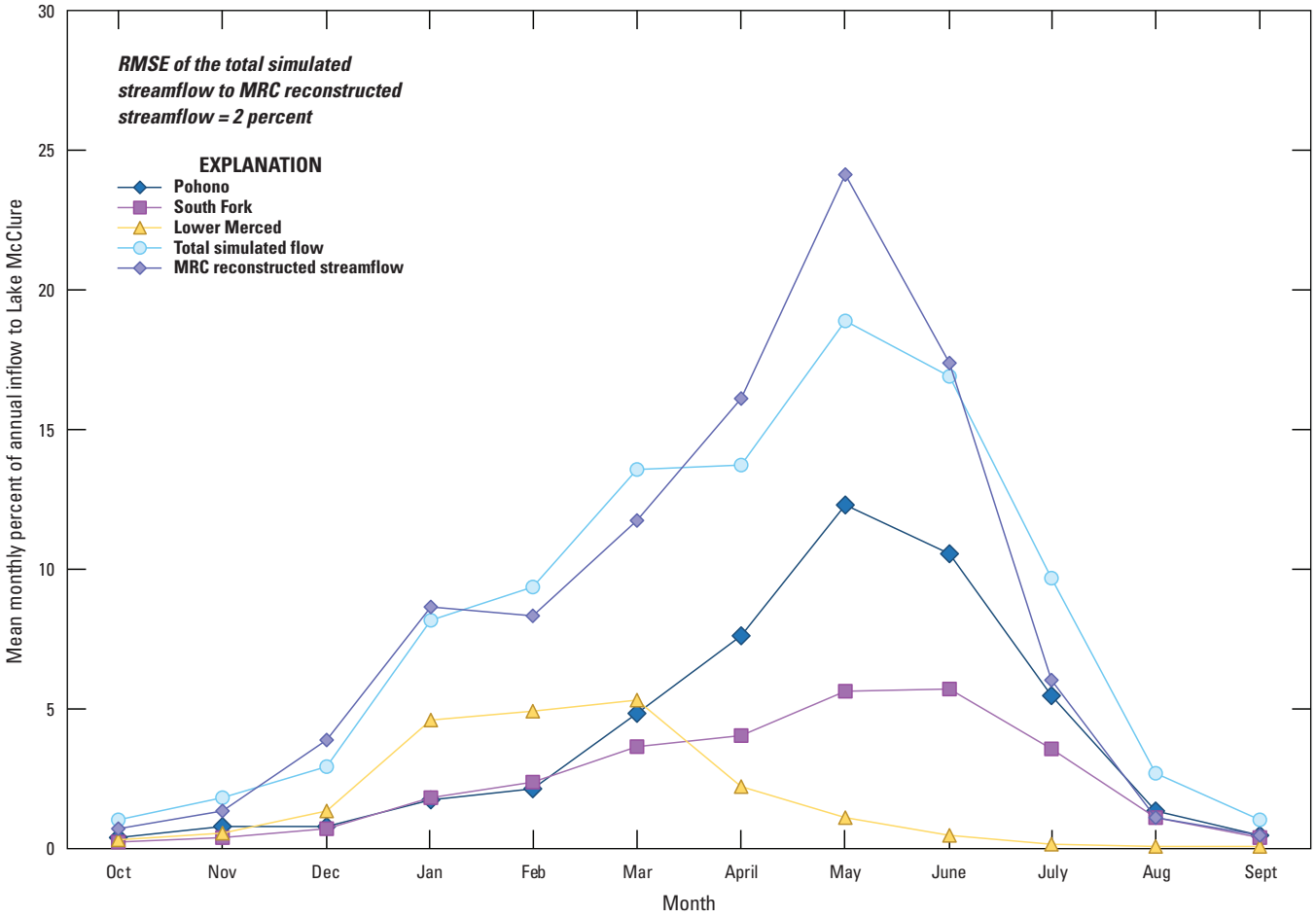

Figure 15. Mean-monthly percentages of simulated inflows to Lake McClure and Merced River near Merced Falls (MRC), water years 1989–2013. (RMSE, root-mean-square error. RMSE's were normalized by dividing to the annual total).

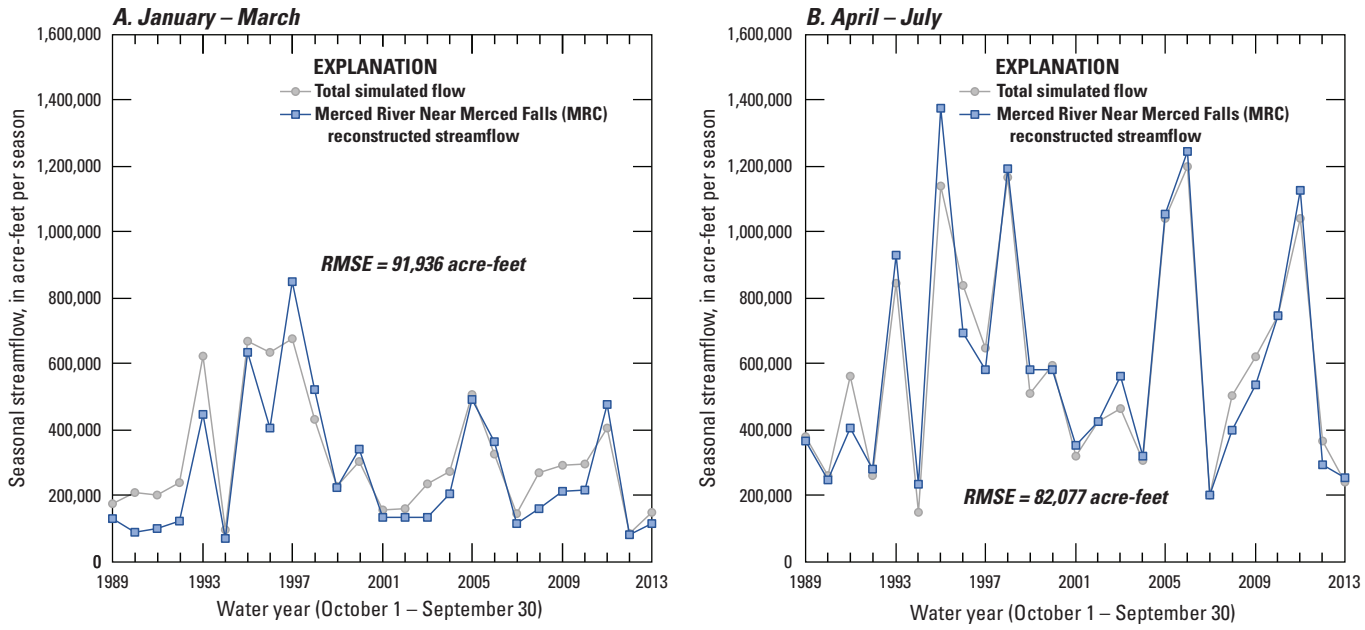

Figure 16. Seasonal inflows to Lake McClure, water years 1989–2013, including *A*, January–March and *B*, April–July. (RMSE, root-mean square error.)

Annual Inflows to Lake McClure

The graph of total annual simulated inflow volumes (water years 1989–2013; fig. 17) closely track the phase and volumes of MRC reconstructions for the model domain calibration (18 years; 1989–2006) and validation (7 years; 2007–13) water year periods (table 12). For the calibration water years 1989–2006, simulated volumes ranged from about 280,000 acre-feet (in 1994) to 2,050,000 acre-feet (in 1995), with an overestimation bias of +5.3 percent and relative error of less than +10 percent (table 14), indicating good agreement. Notably, these extremes in flow volumes are only a year apart, indicating an extreme year to year variability of climate and streamflow in the Sierra Nevada that is not unusual. For validation water years 2007–13, simulated volumes ranged about 383,000 acre-feet (in 2007) to 1,731,000 acre-feet (in 2011), positive bias was +8.4 percent, and relative error +14 percent, indicating good agreement (table 14). The difference in bias and relative error between the calibration and validation time periods reflects a possible change in climatic conditions.

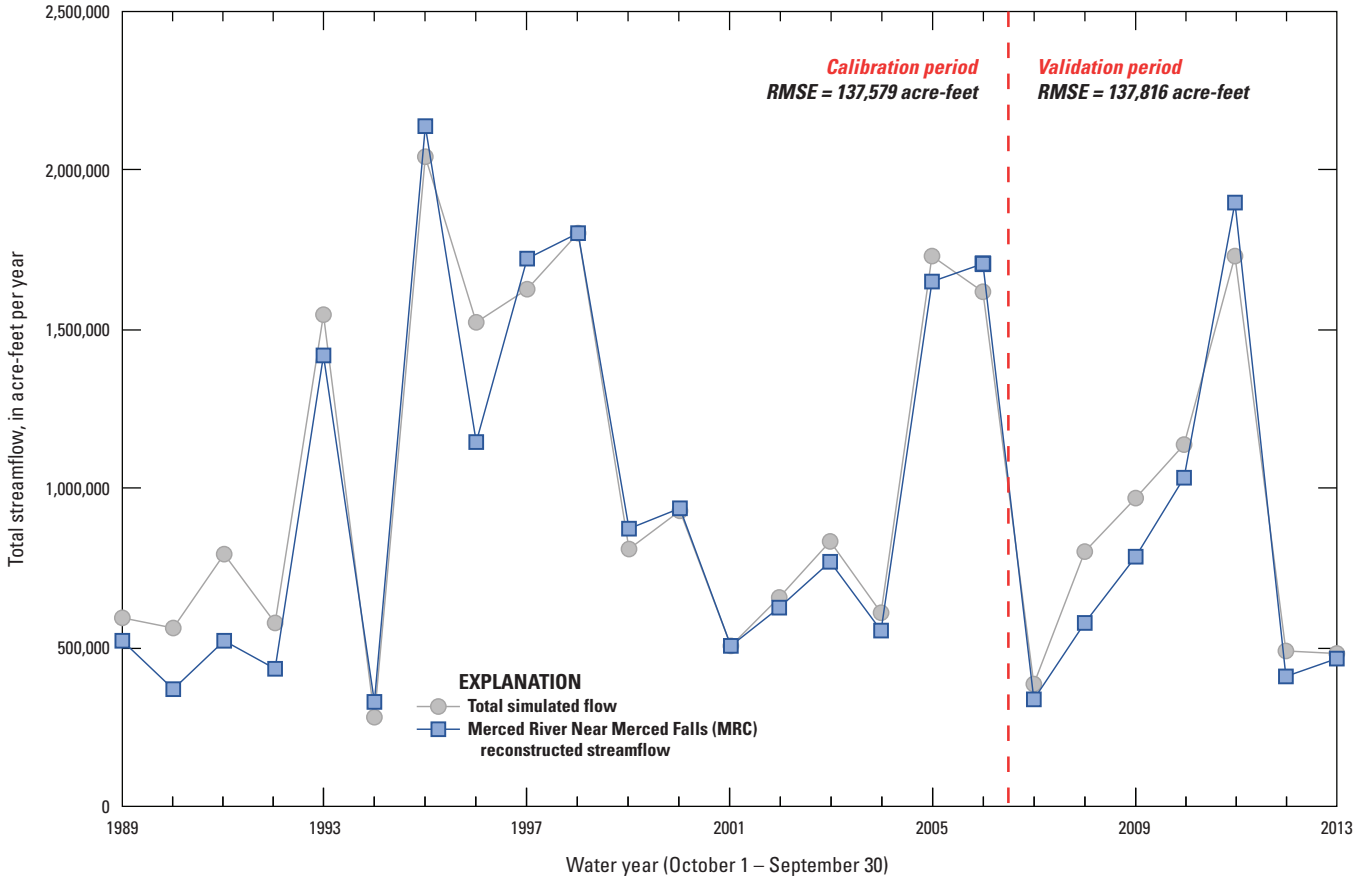

Figure 17. Total annual inflows into Lake McClure, water years 1989–2013. (RMSE, root-mean-square error.)

Applications

Output from the model was used to assess the basin's water balance in terms of components of streamflow and the hydrologic system. Furthermore, the prospects to use the model to make streamflow forecasts using ESP are discussed in the following sections.

Water-Balance Assessment

The major contributor of streamflow into Lake McClure is the Pohono Subbasin, contributing an average of about 50 percent of total annual streamflow past the streamflow station 11270900/MRC (table 15; figs. 8, 11). The model indicates that the simulated streamflow into Lake McClure is primarily from subsurface flow (60.5 percent) with little surface runoff (overland flow; 7 percent; table 16). The largest contribution to streamflow from groundwater is from the South Fork Subbasin (11 percent of the South Fork total streamflow; table 16; figs. 8, 11).

In the headwater subbasins of Pohono and South Fork, maximum streamflow occurs in May and is overwhelmingly from subsurface flow (fig. 18). However, in the lower altitude, Lower Merced Subbasin, maximum streamflow occurs in January–February (fig. 18), corresponding with the rainy season. From the headwater subbasins, subsurface flow (fig. 18) is greatest in May–June (deriving from melting snow and rainfall) and declines from June through July, with much lower rainfall and little or no snowmelt. Simulations of the Lower Merced Subbasin indicate that subsurface flows are greatest December–February, corresponding with the rainy season. Therefore, in June–July, streams flow at much lower rates. In late June–September, when subsurface flow is at its lowest, the major contributor to streamflow is groundwater, likely from the South Fork.

Simulations also indicate that on an annual basis approximately 50 percent of the water that enters the basin as precipitation leaves as streamflow to Lake McClure. Nearly all the rest leaves the basin as evapotranspiration (table 17; fig. 19).

The simulated annual water budgets for all subbasins and for the model domain are summarized in table 17. Storage is reported as an average of the series of last daily estimate in the months or years of interest; other budget items are reported as long-term averages. Subsurface and groundwater storage are highest in the Pohono Subbasin and substantially less in the Lower Merced Subbasin.

Mean-monthly and annual components of the water budget are shown in figure 19. Precipitation quickly increases from the summer lows to the highs of November–March. Evapotranspiration increases and decreases throughout the year governed by the availability of soil moisture and the vegetative life cycle (phenology). Evapotranspiration peaks by April–May in response to spring warming and vegetative growth. During the warmest months, evapotranspiration is limited by declines in precipitation and soil moisture. Storage in soil, subsurface, and groundwater reservoirs is greatest during January through March.

Snowmelt is an indirect contribution to streamflow. Meltwater moves from the snowpack to streams by way of surface, subsurface, and groundwater pathways. In the Merced River Basin, simulated maximum snowmelt occurs in May. By contrast, maximum snowmelt in the Lower Merced Subbasin varies from year to year in the months of January–March (fig. 19).

Table 15. Percentages of mean-annual inflow to Lake McClure from three subbasins, simulated or observed, water years 1989–2013.

Subbasin	Percent of simulated streamflow	Percent of observed streamflow
Pohono	49	[1]51
South Fork	30	[2]27
Lower Merced	21	[3]22

[1]Computed from water years 1989–2013 and total reconstructed streamflow past California Data Exchange Center (CDEC) station MRC.

[2]Computed from available measured data, water years 1952–75, and total simulated streamflow past CDEC station MRC.

[3]Estimated. This could not be directly computed, since a common observed period-of-record does not exist between the outlet station, MRC and the South Fork gage. Therefore, this was computed as the difference of 100 percent minus the Pohono and South Fork values.

Table 16. Average-annual simulated components of streamflow in the Merced River Basin, water years 1952–2013, as inches per year (equal to streamflow volumes divided by drainage areas).

Subbasin	Groundwater flow (inches)	Subsurface flow (inches)	Surface runoff (inches)
Pohono	6.6	20.5	1.0
South Fork	11.2	10.5	0.2
Lower Merced	2.2	3.7	1.9
Average cumulative inflow to Lake McClure	5.6 (32.5 percent of flow)	10.4 (60.5 percent of flow)	1.2 (7 percent of flow)

Table 17. Average-annual simulated water-budget analysis for the Merced River Basin, water years 1952–2013, with measured or reconstructed streamflow.

[N/A, not applicable]

Subbasin	Snowmelt[1] (inches)	Precipitation (inches)	Evapotranspiration (inches)	Storage, groundwater and subsurface[2] (inches)	Simulated streamflow (inches)	Measured or reconstructed streamflow (inches)
Pohono	41.2	50.2	22.1	11.9	28.0	[3]56.4
South Fork[4]	30.7	40.0	18.0	8.7	22.0	[4]19.8
Lower Merced	3.1	21.2	12.6	2.1	7.8	N/A
Average for the Model Domain	21.0	34.3	16.7	22.7	17.2	[5]17.9

[1]Snowmelt contributes to other parts of the water budget, including evapotranspiration, storage and runoff. It is shown here to illustrate that it is a principle component of the hydrologic cycle.

[2]Mean-daily storage water years 1952–2013.

[3]Measured at Merced River at Pohono Bridge near Yosemite, CA (USGS 11266500).

[4]South Fork Merced River near El Portal, CA (USGS 1126800) measured streamflow from water years 1952–75.

[5]Merced River Basin (California Data Exchange Center [CDEC] station MRC) reconstructed streamflow from water years 1967–2013 (including zero/low flows).

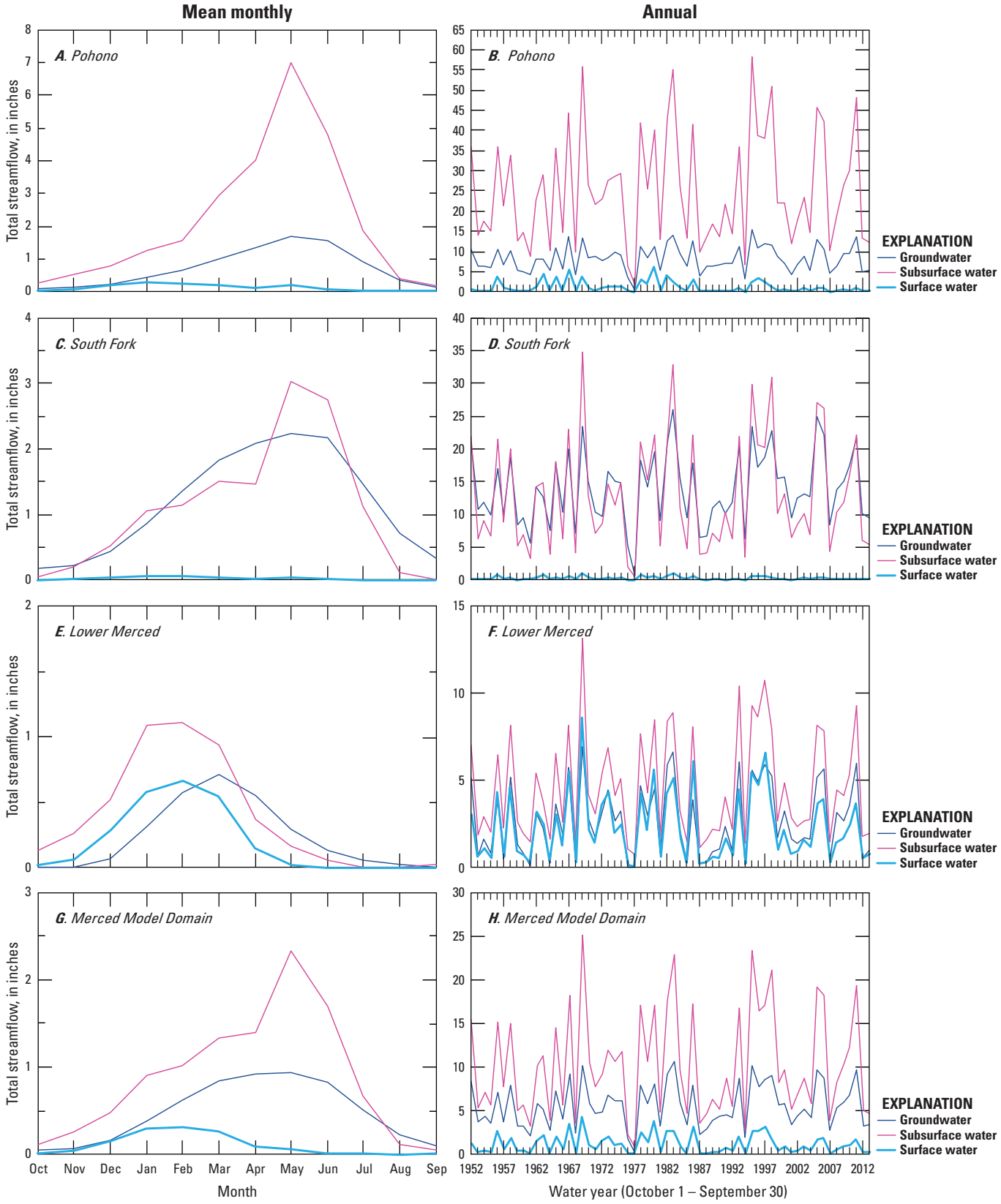

Figure 18. Components of streamflow by subbasin (*A–F*) and for model domain (*G–H*). Mean-monthly flow (left panels) and annual total flows (right panels), water years 1952–2013. (Ranges of vertical axes vary.)

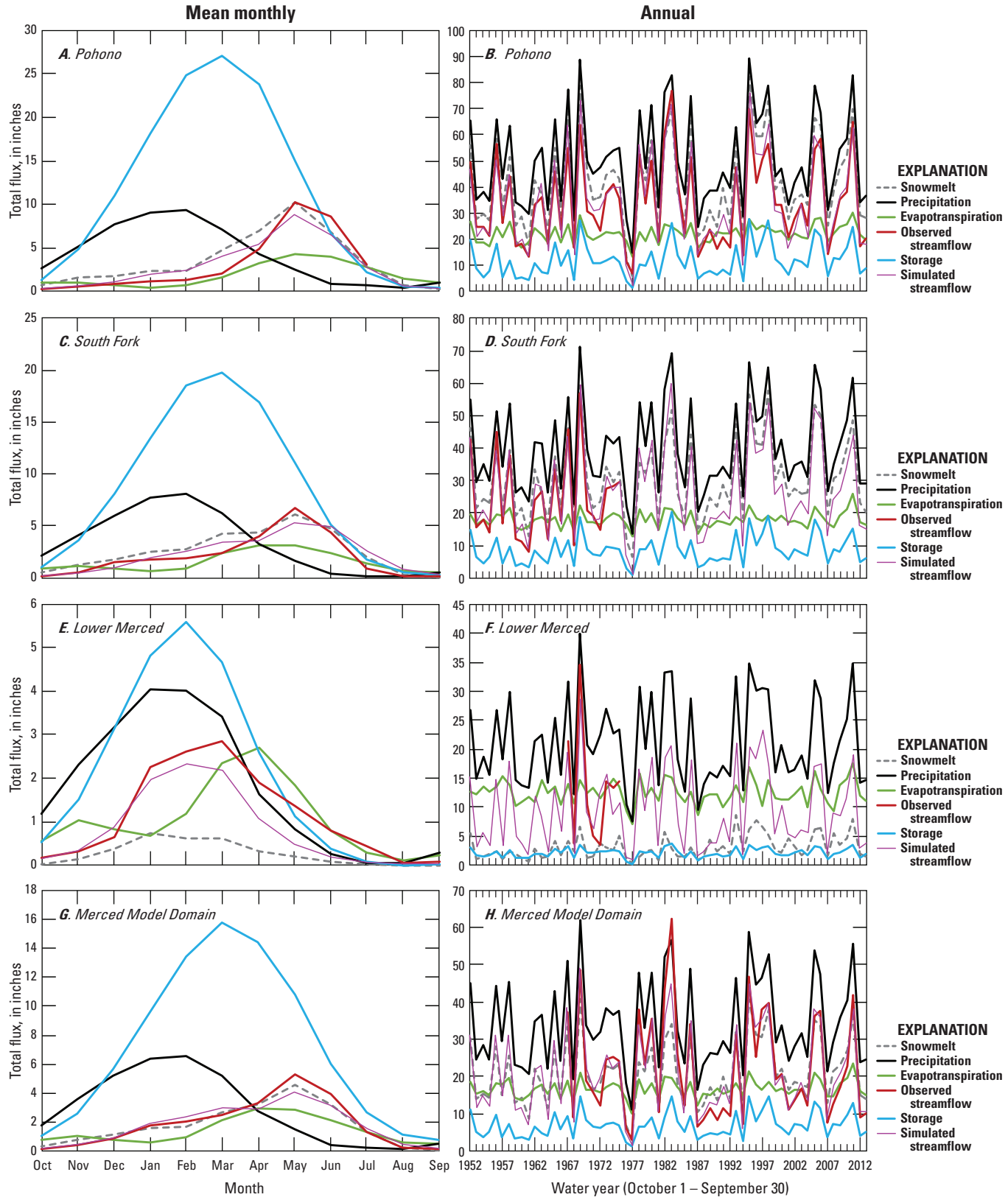

Figure 19. Water-budget components by subbasin (*A*–*F*) and for model domain: (*G*–*H*), mean-monthly (left panels) and annual total (right panels) values, water years 1952–2013. Storage values plotted are not fluxes, but rather are averages of the storage at the end of each month, in inches; other components reported as inches per year or inches per month. (Ranges of vertical axes vary. Observed streamflow is measured or reconstructed flow.)

Seasonal Forecast Modeling Using Ensemble Streamflow Prediction (ESP)

A modified version of the National Weather Service's forecast ensemble streamflow predictions (ESP) program (Day, 1985) has been coupled with the model through a customized Object User Interface (OUI; Markstrom and Koczot, 2008). The OUI is a map-based modeling framework for models, modeling data, and associated tools. It provides a common interface for running models as well as acquiring, browsing, organizing, and selecting spatial and temporal data, and in this case, producing single-run, routed, and ESP streamflow forecasts. The OUI is the platform that allows the user to operate the Merced River Basin PRMS model and perform ESP forecasts (Koczot and others, 2021; https://doi.org/10.5066/F7JH3KFR).

The ESP procedure uses historical or synthesized climate data to forecast future streamflow, starting with simulated initial hydrologic conditions at the beginning of the forecast period. When historical climate data are used, all past events from the historical record are treated as examples of possible future climatic events and used to drive the model to create an ensemble of possible outcomes for the forecast period. Optionally, future climate conditions, not yet witnessed in the historical record, can be included by adding synthesized climate data series, but this was not done for this study.

The current implementation of ESP for the model may be applied to predict streamflow for the April–July (snowmelt) season using historical data with a 3-year period for model warm up. Once initial conditions are established by simulating conditions up to the beginning of the forecast period, April–July streamflow is simulated using daily temperature and precipitation series from historical April–July periods (in this case, April–July 1949–2012 series data from the Draper CBH files). With each iteration, the model is re-initialized to use the initial conditions from the current March 31. Together, these simulations of the April–July streamflows compose an ensemble of streamflow predictions representing combinations of the current (forecast) year's hydrologic states and streamflows simulated from historical April–July weather conditions. Maximum daily flows, seasonal volumes, and dates on which the flow decreases to user-specified thresholds can be extracted from each prediction hydrograph and used to produce probabilistic forecasts.

As part of the functionality of the ESP tool, ESP simulations from the model are automatically evaluated and ranked according to the probability of occurance. Figure 20 shows the results of an ESP run for the Pohono Subbasin, forecast period April 1, 2013, to July 31, 2013, using the initial conditions for March 31, 2013, and the historical input series from El Niño years: 1958, 1966, 1969, 1977, 1982, 1983, 1987, 1991, 1992, 1993, 1994, 1995, 1997, and 1998. The ensemble of predicted flows was sorted to estimate the chance that a particular streamflow may occur. This likelihood is expressed as an exceedance-probability value: the probability that a flow level will be exceeded by the actual (observed) streamflow during the forecast period April–July 2013 is estimated by

$$P(exceedance) = i/(\mathrm{N}+1) \times 100 \quad (4)$$

where

i is the historical-trial rank order, in descending seasonal volume, and

N is the total number of historical trials.

The Merced River Basin OUI has been configured to produce ESP forecasts for all subbasin areas and stream-routing segments as described in the "Geospatial Fabric" section of this report. Simulated streamflows produced using ESP are stored as flat text files in the PRMS model output directory and are available for further analysis, as described in Markstrom and Koczot, 2008, and in the model-archive operating instructions (Koczot and others, 2021; https://doi.org/10.5066/F7JH3KFR).

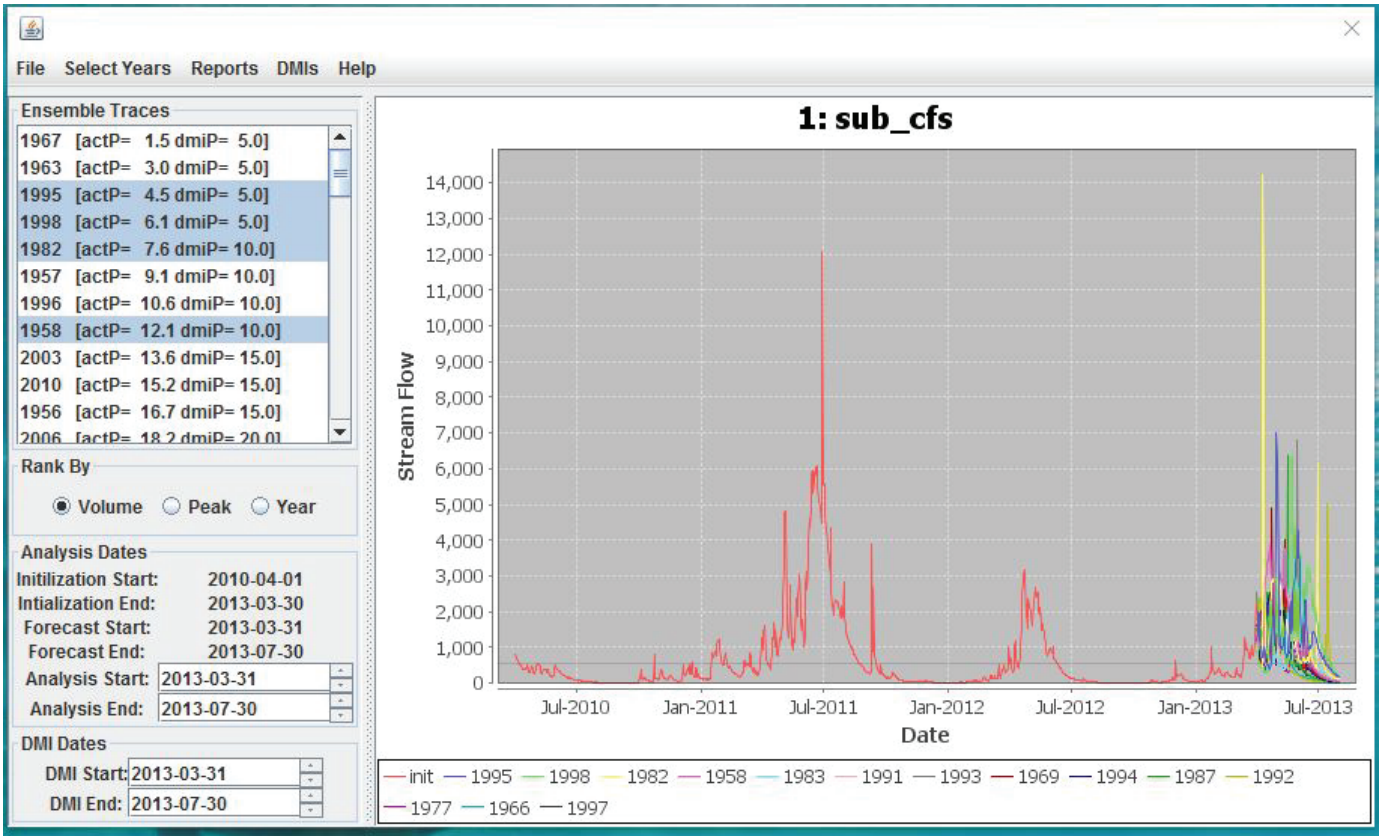

EXPLANATION

Pohono Subbasin, Merced River, Ensemble Streamflow Prediction, April 1, 2013, through July 31, 2013

Observed streamflow

2013 simulated streamflow

Streamflow prediction using historical climate data

1995 1998 1982 1958
1983 1991 1993 1969
1994 1987 1992 1977
1966 1997

Figure 20. Graphical User Interface screenshot of display from Object User Interface (OUI), showing Ensemble Streamflow Prediction (ESP) runs. (Selected historical El Niño years are plotted to illustrate simulated forecasts. OUI is described in Markstrom and Koczot, 2008.)

Model Limitations and Future Enhancements

Despite the uncertainty associated with the streamflow and climate information used in the development of this model, the Merced River Basin PRMS provides reasonable simulations from a preliminary calibration of the long-term flow into Lake McClure and past streamflow station 11270900/MRC, as well as at four important internal nodes. Specifically, the following model limitations may be major sources of uncertainty: (1) the accuracy of model simulations may be limited by the available streamflow records used for calibration targets; the reconstructions of low-flow periods at the model domain outlet were, in some cases, considered unreliable; (2) the narrow focus of the calibration on seasonal totals of flow, especially on April–July snowmelt season; (3) the lack of empirical data for truly unimpaired streamflow at the model domain outlet (CDEC station MRC); and (4) the number and location of real-time climate stations with long-term records available to make model-input files using the Draper Climate-Distribution Software. Climate stations were located mostly in lower to mid-altitudes of the model domain, so that available data likely are biased towards warmer and dryer measurements. A significant limitation especially for the South Fork Subbasin is (5) the relatively short period of streamflow records (record ending 1975; table 3), which prohibits calibration for a greater variety of climate events (both wetter wet spells and drier dry spells). Calibration and validation periods were different between the South Fork and the model domain outlet (11270900/MRC; table 12), and the climate regimes were different.

Further, this model was also constrained by (6) the lack of continuous time-series data in both streamflow and climate records, (7) the absence of more recent streamflows for use as calibration targets (table 3), and (8) physical characteristics, such as land-cover, that were held constant.

Another source of uncertainty arises from parameter estimations and adjustments made during calibration. After the upstream calibrations were completed for the Pohono and South Fork Subbasins, the Lower Merced Subbasin parameters were adjusted solely to achieve the best visual and statistical fit of simulations to observed flows at the model domain outlet (reconstructed flows at CDEC station MRC). This cascading parameter adjustment approach could put undue weight on the parameters associated with more upstream areas. Finally, the South Fork Subbasin parameters representing the contribution of groundwater to streams were adjusted as a calibration compromise to match lower flows, but in so doing, the subbasin may simulate too much baseflow for the geology of that area.

Uncertainty varies across space and time. Calibration and validation results vary in uncertainty from location to location, season to season, and across the historical time period evaluated. Calibration and validation statistics and the fit between model simulations and streamflow reconstructions or observations, as indicated in table 14 and shown in figures 14−17, may provide further insight into the uncertainly associated with simulations.

To improve model performance, future enhancements may include the following: (1) Reestablish gage operation at the South Fork Subbasin outlet to provide current streamflow data for use as a calibration target (SF Merced R NR El Portal CA, 11268000, offline since 1975; table 3). (2) Extend all streamflow calibration data to the present and recalibrate with more recent data. (3) Eliminate low streamflows from the target data and recalibrate only on medium-to-high streamflows to improve wet season simulations. This may eliminate adjustments to some groundwater parameters that were needed to match low-flow streamflow targets. (4) Improve the representation of daily precipitation and temperatures in the model by adding new telemetered gages, especially by gaining permission to establish additional high-attitude, accurate and reliable real-time sites in Yosemite National Park. This would yield a more comprehensive distribution and representation of real-time climate stations. (5) The current model configuration assumes a constant land surface and plant canopy throughout simulations. The model may also be adjusted to use different land-cover representations to test effects of changing land cover on streamflows, caused by, for example, forest fires.

Summary and Conclusions

This report documents the deterministic, distributed-parameter, physical-process-based PRMS model constructed for the Merced River Basin, California (also referred to as “the model”). The report also characterizes the Merced River Basin’s precipitation, temperature, snowpack evolution, and water and energy balances that determine streamflow rates and documents the performance of the model to assess the prospects for (physically based) predictability of seasonal inflows to Lake McClure.

The Merced River Basin, a tributary of the San Joaquin River in California and covering the southern half of Yosemite National Park, is part of a water-supply system managed for outdoor recreation, forest conservation, and fish-and-wildlife enhancements. This is a high-altitude basin (300–13,000 ft) with a Mediterranean/alpine climate from which most streamflow originates as snowmelt. This basin provides fresh water for downstream irrigation, domestic use and hydropower production, and plays an important role in downstream flood management. In addition, streamflow releases from Lake McClure, at the outlet of the basin, are managed for winter floods and summer streamflows during the April 1–July 31 snowmelt season, when 65 percent of the average annual streamflow occurs.

The Merced PRMS model was designed with a focus on prioritizing support for end-user decisions including watershed management and reservoir operations. It can be operated through a customized Object User Interface (OUI), coupled to an “ensemble streamflow prediction” (ESP) forecasting methodology and data-visualization tools, and includes daily-climate distribution preprocessing and climate input-file formatting tools.

The Merced PRMS model runs on a daily time step with precipitation and temperatures as inputs and simulates basin hydrologic response at a higher resolution than was available in previous Merced River Basin models. The Merced PRMS simulates basin hydrologic response at three spatial scales: (1) areas contributing runoff to 42 stream channels summed at 20 nodes (or gages) of interest, (2) 3 subbasins within which hydrologic characteristics were represented in terms of 653 hydrologic response units, and (3) as the sum of the hydrologic response units to represent overall basinwide outflow. In this configuration, climate data were preprocessed prior to the model runs, so that any climate adjustments were made outside of PRMS.

The model was calibrated (water years 1952–2013) primarily to simulate year-to-year variation of the April–July snowmelt-season total streamflow, secondly for monthly variation, and thirdly to simulate daily streamflow characteristics. The model does not necessarily capture all extreme high and low historical streamflow events. Model simulations were calibrated using manual and automated methods, against gridded data of solar radiation and potential evapotranspiration and at 5 streamflow gages, and evaluated statistically (bias, relative error, RMSE) and visually (table 14; figs. 13, 14, 15, 16, and 17). This model was especially sensitive to changes in temperature and precipitation in the input datasets, and to parameters describing transmission of water to (and from) the subsurface and groundwater reservoirs. Notably, uncertainty in calibration and validation results was found to vary across time and space, not only based on the timeframes selected for evaluation (daily, monthly, seasonal, and annual), but for different subbasins during that same timeframe.

Calibration and validation statistics indicated a good agreement of simulations to observations during the April–July snowmelt season (RMSE of 82,077 acre-ft with flow volumes ranging from 152,400 to 1,375,700 acre-ft; fig. 16*B*), but less so during other seasons, with some explainable exceptions. Because the model was designed to target higher flows, as expected, low-flow months and seasons had higher calibration/validation errors than high flow seasons. Although statistically sound, an overestimation of streamflows during February–March in some years resulted in early runoff and less snowpack available for April–May snowmelt. This possibly indicates that February–March storms were not accounted for adequately in the climate data used to drive the model.

Modeled simulations of the contributions of inflow to Lake McClure from surface runoff, subsurface and groundwater flow (table 16, fig. 17), and the basins' water budgets were quantified (table 17; fig. 18). The major contributors are the Pohono (49 percent) followed by the South Fork Subbasin (30 percent; table 15). Simulated streamflow is from subsurface (60.5 percent), groundwater (32.5 percent), and surface runoff (7 percent). In higher altitudes where snowpack forms, maximum streamflow (from subsurface flow) occurs in May–June. In lower altitudes maximum streamflow occurs in January–March corresponding with the rainy season. Storage is greatest in February–April. Evapotranspiration peaks by May/June in higher altitudes, and in April/May in lower altitudes. In late summer, with little to no snowmelt or rainfall, streams flow at much lower rates and originate from subsurface and groundwater.

With some refinements, this model may be applied not only for forecasting real-time streamflows but to assess future effects of climate and land-cover change in this watershed, and thus further inform watershed management strategies. This PRMS model could eventually join a suite of forecast tools to aid watershed managers in forecasting basin water yield, improving reservoir operations and watershed management. Techniques developed in this work may apply to studies of other basins in the Sierra Nevada and other montane environments.

References Cited

Anderson, E.A., 1973, National Weather Service river forecast system—Snow accumulation and ablation model: U.S. Department of Commerce, NOAA Technical Memorandum NWS-Hydro-17, 224 p., https://repository.library.noaa.gov/view/noaa/13507.

Anderson, J., Chung, F., Anderson, M., Brekke, L., Easton, D., Ejeta, M., Peterson, R., and Snyder, R., 2008, Progress on incorporating climate change into management of California's water resources: Climatic Change, v. 89, suppl. 1, p. 91–108, https://doi.org/10.1007/s10584-007-9353-1.

Bardini, G., Guillen, S., Pierotti, B., Rooks, H., and Sou, S., 2001, Climate change in California—Potential consequences and strategies to cope and adapt: California Department of Water Resources Report, 91 p.

Battaglin, W.A., Hay, L.E., Parker, R.S., and Leauesley, G.H., 1993, Applications of a GIS for modeling the sensitivity of water resources to alterations in climate in the Gunnison River Basin, Colorado: Journal of the American Water Resources Association, v. 29, no. 6, p. 1021–1028, https://doi.org/10.1111/j.1752-1688.1993.tb03265.x.

Beck, H.E., Zimmermann, N.E., McVicar, T.R., Vergopolan, N., Berg, A., and Wood, E.F., 2018, Present and future Köppen-Geiger climate classification maps at 1-km resolution: Scienfitic Data, v. 5, no. 180214, 12 p., https://www.nature.com/articles/sdata2018214#ref-link-section-1.

Black, P.E., 1996, Watershed hydrology: Chelsea, MI, Ann Arbor Press, Inc., 449 p.

Bonner, L.J., Elliott, P.E., Etchemendy, L.P., and Swartwood, J.R., 1998, Water resources data, Nevada, water year 1997: U.S. Geological Survey Water Data Report NV–97–1, 636 p., https://doi.org/10.3133/wdrNV971.

Bostic, R.E., Kane, R.L., Kipfer, K.M., and Johnson, A.W., 1997, Water resources data, Nevada, water year 1996: U.S. Geological Survey Water Data Report NV–96–1, 611 p., https://doi.org/10.3133/wdrNV961.

Brekke, L.D., Kiang, J.E., Olsen, J.R., Pulwarty, R.S., Raff, D.A., Turnipseed, D.P., Webb, R.S., and White, K.D., 2009, Climate change and water resources management—A federal perspective: U.S. Geological Survey Circular 1331, 66 p., https://doi.org/10.3133/cir1331.

Buer, S., 1988, Program manual—Headwater forecasting using HED71: Sacramento, Calif., California Department of Water Resources, Division of Flood Management, 48 p.

Burnash, R.J.C., Ferral, R.L., and McQuire, R.A., 1973, A generalized streamflow simulation system—Conceptual modeling for digital Ccomputers: Sacramento, Calif., U.S. Department of Commerce, National Weather Service, 204 p.

California Department of Water Resources, 2006, Progress on incorporating climate change into management of California's water resources: Department of Water Resources, Technical Memorandum Report, 338 p., https://www.waterboards.ca.gov/waterrights/water_issues/programs/bay_delta/california_waterfix/exhibits/docs/PCFFA&IGFR/PCFFA_22_DWRcc.pdf.

California Department of Water Resources, 2020a, Dams within jurisdiction of the State of California: State of California, California Natural Resources Agency, Division of Safety of Dams, 107 p., https://water.ca.gov/-/media/DWR-Website/Web-Pages/Programs/All-Programs/Division-of-Safety-of-Dams/Files/Publications/Dams-Within-Jurisdiction-of-the-State-of-California-Listed-Alphabetically-by-Name.pdf.

California Department of Water Resources, 2020b, Water conditions in California: California Cooperative Snow Surveys, Bulletin 120-2-20, 16 p., https://cdec.water.ca.gov/snow/bulletin120/index2.html.

Cayan, D.R., Kammerdiener, S.A., Dettinger, M.D., Caprio, J.M., and Peterson, D.H., 2001, Changes in the onset of spring in the western United States: Bulletin of the American Meteorological Society, v. 82, no. 3, p. 399–416, https://doi.org/10.1175/1520-0477(2001)082%3C0399:CITOOS%3E2.3.CO;2.

Christiansen, D.E., 2012, Simulation of daily streamflows at gaged and ungaged locations within the Cedar River Basin, Iowa, using a Precipitation-Runoff Modeling System model: U.S. Geological Survey Scientific Investigations Report 2012–5213, 20 p., https://doi.org/10.3133/sir20125213.

Daly, C., Neilson, R.P., and Phillips, D.L., 1994, A statistical-topographic model for mapping climatological precipitation over mountainous terrain: Journal of Applied Meteorology, v. 33, no. 2, p. 140–158, https://doi.org/10.1175/1520-0450(1994)033%3C0140:ASTMFM%3E2.0.CO;2.

Daly, C., Halbleib, M., Smith, J.I., Gibson, W.P., Doggett, M.K., Taylor, G.H., Curtis, J., and Pasteris, P.P., 2008, Physiographically sensitive mapping of climatological temperature and precipitation across the conterminous United States: International Journal of Climatology, v. 28, no. 15, p. 2031–2064, https://doi.org/10.1002/joc.1688.

Day, G.N., 1985, Extended streamflow forecasting using NWSRFS: Journal of Water Resources Planning and Management, v. 111, no. 2, p. 157–170, https://doi.org/10.1061/(ASCE)0733-9496(1985)111:2(157).

Dettinger, M., 2005a, Changes in streamflow timing in the western United States in recent decades: U.S. Geological Survey Fact Sheet 2005–3018, 4 p., https://doi.org/10.3133/fs20053018.

Dettinger, M.D., 2005b, From climate-change spaghetti to climate-change distributions for 21st Century California: San Francisco Estuary and Watershed Science, v. 3, no. 1, 15 p., https://doi.org/10.15447/sfews.2005v3iss1art6.

Dettinger, M., Alpert, H., Battles, J., Kusel, J., Safford, H., Fougeres, D., Knight, C., Miller, L., and Sawyer, S., 2018a, Sierra Nevada Summary Report: California's Fourth Climate Change Assessment, Publication number SUM-CCCA4-2018-004, 94 p., https://pubs.er.usgs.gov/publication/70201117.

Dettinger, M.D., Alpert, H., Battles, J., Kusel, J., Safford, H., Fougeres, D., Knight, C., Miller, L., and Sawyer, S., 2018b, Sierra Nevada Executive Summary Report: California's Fourth Climate Change Assessment, 5 p., accessed 2019 at https://climateassessment.ca.gov/regions/docs/20180827-SierraNevada.pdf.

Dettinger, M.D., and Cayan, D.R., 1995, Large-scale atmospheric forcing of recent trends toward early snowmelt runoff in California: Journal of Climate, v. 8, p. 606–623, https://doi.org/10.1175/1520-0442(1995)008%3C0606:LSAFOR%3E2.0.CO;2.

Dettinger, M.D., Battisti, D.S., Garreaud, R.D., McCabe, G.J., Jr., and Bitz, C.M., 2001, Interhemispheric effects of interannual and decadal ENSO-like climate variations on the Americas, chap. 1 *of* Markgraf, V., ed., Interhemispheric climate linkages: Academic Press, p. 1–16, https://doi.org/10.1016/B978-012472670-3/50004-5.

Dettinger, M.D., Cayan, D.R., Meyer, M.K., and Jeton, A.E., 2004, Simulated hydrologic responses to climate variations and change in the Merced, Carson, and American River Basins, Sierra Nevada, California, 1900–2099: Climatic Change, v. 62, no. 1–3, p. 283–317, https://doi.org/10.1023/B:CLIM.0000013683.13346.4f.

Dettinger, M.D., Kingtse, M., Cayan, D.R., and Peterson, D.H., 1998, Hindcasts and forecasts of streamflow in the Merced and American Rivers, Sierra Nevada, during recent El Niños: Eos, Trans. Amer. Geophy. Union (Washington, D.C.), v. 79, no. 45, p. 545–548.

Dettinger, M.D., Peterson, D.H., Diaz, H.F., and Cayan, D.R., 1997, Forecasting spring runoff pulses from the Sierra Nevada: Interagency Ecosystem Program Newsletter, v. 10, Summer 1997, p. 32–35, https://archive.usgs.gov/archive/sites/sfbay.wr.usgs.gov/publications/pdf/dettinger_1997_runoff.pdf.

Donovan, J.M., and Koczot, K.M., 2019, User's manual for the Draper climate-distribution software suite with data-evaluation tools: U.S. Geological Survey Techniques and Methods 7–C22, 55 p., https://doi.org/10.3133/tm7C22.

Driscoll, J.M., Hay, L.E., and Bock, A.R., 2017, Spatiotemporal variability of snow depletion curves derived from SNODAS for the conterminous United States, 2004–2013: Journal of the American Water Resources Association, v. 53, no. 3, p. 655–666, https://doi.org/10.1111/1752-1688.12520.

Duan, Q.Y., Gupta, V.K., and Sorooshian, S., 1993, Shuffled complex evolution approach for effective and efficient global minimization: Journal of Optimization Theory and Applications, v. 76, no. 3, p. 501–521, https://doi.org/10.1007/BF00939380.

Dudley, R.W., 2008, Simulation of the quantity, variability, and timing of streamflow in the Dennys River Basin, Maine, by use of a precipitation-runoff watershed model: U.S. Geological Survey Scientific Investigations Report 2008–5100, 37 p., https://doi.org/10.3133/sir20085100.

Environmental Systems Research Institute, Inc. (ESRI), 1992, Understanding GIS—The ARC/INFO method: Environmental Systems Research Institute Inc., Redlands, Calif., v. 1, variously paged.

Farnsworth, R.K., and Thompson, E.S., 1982, Mean monthly, seasonal, and annual pan evaporation for the United States—NOAA Technical Report NWS 34: Washington, D.C., National Oceanic and Atmospheric Administration, 85 p., www.dynsystem.com/netstorm/docs/NWS34EvapTables.pdf.

Farnsworth, R.K., Thompson, E.S., and Peck, E.L., 1982, Evaporation atlas for the contiguous 48 United States—NOAA Technical Report NWS 33: Washington, D.C., National Oceanic and Atmospheric Administration, 26 p., www.nws.noaa.gov/oh/hdsc/PMP_related_studies/TR33.pdf.

Fazel, K., King, J.J., Maher, K., DeGuzman, S., Fabbiani-Leon, A., Koczot, K.M., Fortner, M., and Risley, J.C., 2013, Precipitation Runoff Modeling System (PRMS) Data Development documentation, October 2013: California Department of Water Resources, Flood Emergency Response Program, Agreement no. 4600007756, Activity no. 139860.

Frankoski, L., 1994, Effect of spatial resolution on hydrologic model results: University of Colorado, Master's thesis, 104 p.

Freeman, G.J., 2002, Looking for recent climatic trends and patterns in California's Central Sierra: 2002 PACLIM Conference Proceedings, p. 35–47, http://almanorpost.com/tap/wp-content/uploads/2014/02/Freeman-Trends-Patterns-Central-Sierra-2002.pdf.

Freeze, R.A., and Cherry, J.A., 1979, Groundwater: Englewood Cliffs, N.J., Prentice-Hall, 604 p.

Goode, D.J., Koerkle, E.H., Hoffman, S.A., Regan, R.S., Hay, L.E., and Markstrom, S.L., 2010, Simulation of runoff and reservoir inflow for use in a flood-analysis model for the Delaware River, Pennsylvania, New Jersey, and New York, 2004–2006: U.S. Geological Survey Open-File Report 2010–1014, 68 p., https://doi.org/10.3133/ofr20101014.

Haan, C.T., Johnson, H.P., and Brankensiek, D.L., eds., 1982, Hydrologic modeling of small watersheds: American Society of Agricultural Engineers Monograph 5, 533 p.

Haj, A.E., Christiansen, D.E., and Viger, R.J., 2014, The effects of Missouri River mainstem reservoir system operations on 2011 flooding using a precipitation-runoff modeling system model: U.S. Geological Survey Professional Paper 1798–K, 33 p., https://doi.org/10.3133/pp1798K.

Haj, A.E., Christiansen, D.E., and Hutchinson, K.J., 2015, Simulation of daily streamflow for nine river basins in eastern Iowa using the precipitation-runoff modeling system: U.S. Geological Survey Scientific Investigations Report 2015–5129, 29 p., https://doi.org/10.3133/sir20155129.

Hay, L.E., Battaglin, W.A., Parker, R.S., and Leavesley, G.H., 1993, Modeling the effects of climate change on water resources in the Gunnison River basin, Colorado, *in* Goodchild, M.F., Parks, B.O., and Steyaert, L.T., eds., Environmental modeling with GIS: Oxford University Press, p. 173–181.

Hay, L.E., Leavesley, G.H., Clark, M.P., Markstrom, S.L., Viger, R.J., and Umemoto, M., 2006, Step wise, multiple objective calibration of a hydrologic model for a snowmelt dominated basin: Journal of the American Water Resources Association, v. 42, no. 4, p. 877–890, https://doi.org/10.1111/j.1752-1688.2006.tb04501.x.

Hay, L.E., Markstrom, S.L., and Ward-Garrison, C., 2011, Watershed-scale response to climate change through the twenty-first century for selected basins across the United States: Earth Interactions, v. 15, no. 17, p. 1–37, https://doi.org/10.1175/2010EI370.1.

Hay, L.E., and Umemoto, M., 2007, Multiple-objective stepwise calibration using LUCA: U.S. Geological Survey Open-File Report 2006–1323, 25 p., https://doi.org/10.3133/ofr20061323.

Huber, N.K., 1989, The geologic story of Yosemite National Park: Yosemite Association, Yosemite National Park, Calif., published in 1987 as U.S. Geological Survey Bulletin 1595, 64 p., https://doi.org/10.3133/b1595.

Intergovernmental Panel on Climate Change (IPCC), 2014, Climate Change 2014: Synthesis Report. Contribution of Working Groups I, II and III to the Fifth Assessment Report of the Intergovernmental Panel on Climate Change [Core Writing Team, R.K. Pachauri and L.A. Meyer (eds.)]: IPCC, Geneva, Switzerland, 151 p.

Jennings, C.W., Strand, R.G., and Rogers, T.H., 1977, Geological map of California: California Division of Mines and Geology, Sacramento, scale 1:750,000.

Jensen, M.E., and Haise, H.R., 1963, Estimating evapotranspiration from solar radiation—Proceedings of the American Society of Civil Engineers: Guangai Paishui Xuebao, v. 89, p. 15–41, https://eprints.nwisrl.ars.usda.gov/id/eprint/1248.

Jensen, M.E., Robb, D.C.N., and Franzoy, C.E., 1970, Scheduling irrigations using climate-crop-soil data—Proceedings of the American Society of Civil Engineers: Journal of the Irrigation and Drainage Division, v. 96, p. 25–38, https://eprints.nwisrl.ars.usda.gov/id/eprint/1207.

Jeton, A.E., 1999, Precipitation-runoff simulations for the Lake Tahoe Basin, California and Nevada: U.S. Geological Survey Water-Resources Investigations Report 99–4110, 61 p., https://doi.org/10.3133/wri994110.

Jeton, A.E., 2000, Precipitation-runoff simulations for the upper part of the Truckee River Basin, California and Nevada: U.S. Geological Survey Water-Resources Investigations Report 99–4282, 41 p., https://doi.org/10.3133/wri994282.

Jeton, A.E., Dettinger, M.D., and LaRue Smith, J., 1996, Potential effects of climate change on streamflow, eastern and western slopes of the Sierra Nevada, California and Nevada: U.S. Geological Survey Water-Resources Investigations Report 95–4260, 44 p., https://doi.org/10.3133/wri954260.

Jeton, A.E., and LaRue Smith, J., 1993, Development of watershed models for two Sierra Nevada basins using a geographic information system: Journal of the American Water Resources Association, v. 29, no. 6, p. 923–932, https://doi.org/10.1111/j.1752-1688.1993.tb03253.x.

Koczot, K.M., Jeton, A.E., McGurk, B., and Dettinger, M.D., 2005, Precipitation-runoff processes in the Feather River Basin, northeastern California, with streamflow predictability, water years 1971–97: U.S. Geological Survey Scientific Investigations Report 2004–5202, 92 p., https://doi.oeg/10.3133/sir20045202.

Koczot, K.M., Risley, J.C., Gronberg, J.M., Donovan, J.W., and McPherson, K.R., 2021, Archive of Merced River Basin Precipitation-Runoff Modeling System, with forecasting, climate-file preparation, and data-visualization tools: U.S. Geological Survey data release, https://doi.org/10.5066/F7JH3KFR.

LaFontaine, J.H., Hay, L.E., Viger, R.J., Markstrom, S.L., Regan, R.S., Elliott, C.M., and Jones, J.W., 2013, Application of the precipitation-runoff modeling system (PRMS) in the Apalachicola-Chattahoochee-Flint River Basin in the southeastern United States: U.S. Geological Survey Scientific Investigations Report 2013–5162, 118 p., https://doi.org/10.3133/sir20135162.

Leavesley, G., 2005, Rainfall-runoff modeling for integrated basin management, Part 11—Rainfall-runoff modeling, chap. 129 *in* Anderson, M.G., ed., Encyclopedia of hydrological sciences: J.W. Wiley, p. 2001–2006, https://doi.org/10.1002/0470848944.hsa136.

Leavesley, G.H., Lichty, R.W., Troutman, B.M., and Saindon, L.G., 1983, Precipitation-runoff modeling system—User's manual: U.S. Geological Survey Water-Resources Investigations Report 83–4238, 207 p., https://doi.org/10.3133/wri834238.

Leavesley, G.H., Markstrom, S.L., Restrepo, P.J., and Viger, R.J., 2002, A modular approach to addressing model design, scale, and parameter estimation issues in distributed hydrological modelling: Hydrological Processes, v. 16, no. 2, p. 173–187, https://doi.org/10.1002/hyp.344.

Leavesley, G.H., Restrepo, P.J., Markstrom, S.L., Dixon, M., and Stannard, L.G., 1996, The modular modeling system (MMS)—User's manual: U.S. Geological Survey Open-File Report 96–151, 142 p., https://doi.org/10.3133/ofr96151.

Leavesley, G.H., and Stannard, L.G., 1995, The precipitation-runoff modeling system—PRMS, *in* Singh, V.P., ed., Computer models of watershed hydrology: Highlands Ranch, Colo., Water Resource Publications, p. 281–310.

Lundquist, J.D., Dettinger, M.D., Stewart, I.T., and Cayan, D.C., 2009, Variability and trends in spring runoff in the western United States, *in* Wagner, F., ed., Climate warming in western North America—Evidence and environmental effects: Salt Lake City, Utah, University of Utah Press, p. 63–76, https://pdfs.semanticscholar.org/f4de/06327bf5b3df405fc7878e69cb3320d416bb.pdf.

Markstrom, S.L., Hay, L.E., Ward-Garrison, C.D., Risley, J.C., Battaglin, W.A., Bjerklie, D.M., Chase, K.J., Christiansen, D.E., Dudley, R.W., Hunt, R.J., Koczot, K.M., Mastin, M.C., Regan, R.S., Viger, R.J., Vining, K.C., and Walker, J.F., 2012, Integrated watershed-scale response to climate change for selected basins across the United States: U.S. Geological Survey Scientific Investigations Report 2011–5077, 134 p., https://doi.org/10.3133/sir20115077.

Markstrom, S.L., and Koczot, K.M., 2008, User's Manual for the object user interface (OUI)—An environmental resource modeling framework: U.S. Geological Survey Open-File Report 2008–1120, 39 p., https://doi.org/10.3133/ofr20081120.

Markstrom, S.L., Regan, R.S., Hay, L.E., Viger, R.J., Webb, R.M.T., Payn, R.A., and LaFontaine, J.H., 2015, PRMS-IV, the precipitation-runoff modeling system, version 4: U.S. Geological Survey Techniques and Methods, book 6, chap. B7, 158 p., https://doi.org/10.3133/tm6B7.

Markstrom, S.L., Hay, L.E., and Clark, M.P., 2016, Towards simplification of hydrologic modeling—Identification of dominant processes: Hydrology and Earth System Sciences, v. 20, no. 11, p. 4655–4671, https://doi.org/10.5194/hess-20-4655-2016.

McCabe, G.J., and Dettinger, M.D., 2002, Primary modes and predictability of year-to-year snowpack variations in the western United States from teleconnections with Pacific Ocean climate: Journal of Hydrometeorology, v. 3, p. 13–25, https://doi.org/10.1175/1525-7541(2002)003%3C0013:PMAPOY%3E2.0.CO;2.

Miller, N.L., Bashford, K.E., and Strem, E., 2001, Climate change sensitivity study of California hydrology, A report to the California Energy Commission: Lawrence Berkeley National Laboratory Technical Report no. 49110, 30 p.

Miller, N.L., Bashford, K.E., and Strem, E., 2003, Potential impacts of climate change on California Hydrology: Journal of the American Water Resources Association, v. 39, no. 4, p. 771–784, https://doi.org/10.1111/j.1752-1688.2003.tb04404.x.

Mote, P.W., Hamlet, A.F., Clark, M.P., and Lettenmaier, D.P., 2005, Declining mountain snowpack in western North America: Bulletin of the American Meteorological Society, v. 86, no. 1, p. 39–50, https://doi.org/10.1175/BAMS-86-1-39.

National Renewable Energy Laboratory (NREL), 1980, Reprocessed data converted from kilowatt-hours per square meter per day to Langleys per day: National Renewable Energy Laboratory, accessed December 30, 2015, at https://www.nrel.gov/gis/data-solar.html. Available from Geodata portal, Normal incident Solar Radiation Atlas, https://cida.usgs.gov/gdp/.

Peterson, D.H., Smith, R.E., Dettinger, M.D., Cayan, D.R., Hager, S.W., and Schemel, L.E., 1999, Forecasting spring discharge in the west—A step towards forecasting stream chemistry, *in* Section A of Morganwalp, D.W., and Buxton, H.T., eds., U.S. Geological Survey toxic substances hydrology program—Proceedings of the technical meeting, Charleston, South Carolina, March 8–12, 1999—Volume 2 of 3 (Part B): U.S. Geological Survey Water-Resources Investigations Report 99–4018B, p. 51–58, https://doi.org/10.3133/wri994018B.

Peterson, D.H., Smith, R.E., Dettinger, M.D., Cayan, D.R., and Riddle, L., 2000, An organized signal in snowmelt runoff over the western United States: Journal of the American Water Resources Association, v. 36, no. 2, p. 421–432, https://doi.org/10.1111/j.1752-1688.2000.tb04278.x.

Puente, C., and Atkins, J.T., 1989, Simulation of rainfall-runoff response in mined and unmined watersheds in coal areas of West Virginia: U.S. Geological Survey Water Supply Paper 2298, 48 p., https://doi.org/10.3133/wsp2298.

Risley, J.C., 1994, Use of a precipitation-runoff model for simulating effects of forest management on stream flow in 11 small drainage basins, Oregon Coast Range: U.S. Geological Survey Water-Resources Investigations Report 93–4181, 61 p., https://doi.org/10.3133/wri934181.

Risley, J.C., 2019, Predicting seasonal water availability in the Upper Klamath River Basin using the Precipitation-Runoff Modeling System: U.S. Geological Survey Scientific Investigations Report 2019–5044, 37 p., https://doi.org/10.3133/sir20195044.

Ryan, T., 1996, Development and application of a physically based distributed parameter rainfall runoff model in the Gunnison River basin—U.S. Bureau of Reclamation: Climate Change Response Program, 64 p.

Schmidt, K.M., and Webb, R.H., 2001, Researchers consider U.S southwest's response to warmer, drier conditions: Eos (Washington, D.C.), v. 82, no. 41, p. 475–478, https://doi.org/10.1029/01EO00284.

Simpson, J.J., Dettinger, M.D., Gehrke, F., McIntire, T.J., and Hufford, G.L., 2004, Hydrologic scales, cloud variability, remote sensing, and models—Implications for forecasting snowmelt and streamflow: Weather and Forecasting, v. 19, no. 2, p. 251–276, https://doi.org/10.1175/1520-0434(2004)019%3C0251:HSCVRS%3E2.0.CO;2.

Stewart, I.T., Cayan, D.R., and Dettinger, M.D., 2004a, Changes toward earlier streamflow timing across western North America: Journal of Climate, v. 18, p. 1136–1155, https://doi.org/10.1175/JCLI3321.1.

Stewart, I.T., Cayan, D.R., and Dettinger, M.D., 2004b, Changes in snowmelt runoff timing in western North America under a 'business as usual' climate change scenario: Climatic Change, v. 62, no. 1–3, p. 217–232, https://doi.org/10.1023/B:CLIM.0000013702.22656.e8.

Strahler, A.N., and Strahler, A.H., 1984, Elements of Physical Geography [3d ed.]: New York, John Wiley and Sons, 538 p.

Thorne, J.H., Wraithwall, J., and Franco, G., 2018, California's Changing Climate 2018: California's Fourth Climate Change Assessment, California Natural Resources Agency, Publication number: SUM-CCCA4-2018-013, https://www.climateassessment.ca.gov/.

Thornton, P.E., Thornton, M.M., Mayer, B.W., Wei, Y., Devarakonda, R., Vose, R.S., and Cook, R.B., 2018, Daymet—Daily surface weather data on a 1-km grid for North America, version 3: ORNL DAAC, Oak Ridge, Tenn., https://doi.org/10.3334/ORNLDAAC/1328.

Troutman, B.M., 1985, Errors and parameter estimation in precipitation-runoff modeling: Water Resources Research, v. 21, no. 8, p. 1195–1213, https://doi.org/10.1029/WR021i008p01195.

U.S. Department of Agriculture, 2013, Soil Survey Geographic (SSURGO) Database: Natural Resources Conservation Service, accessed January 13, 2013, at https://websoilsurvey.nrcs.usda.gov/.

U.S. Geological Survey, 2020, National Water Information System: U.S. Geological Survey web interface, accessed June 20, 2020, at https://doi.org/10.5066/F7P55KJN.

United States Global Change Research Program (USGCRP), 2017, Climate science special report—Fourth national climate assessment (NCA4), *in* Wuebbles, D.J., Fahey, D.W., Hibbard, K.A., Dokken, D.J., Stewart, B.C., and Maycock, T.K., eds., U.S. global change research program v. I: Washington, D.C., U.S. Global Change Research Program, https://doi.org/10.7930/J0J964J6.

Viger, J.J., Markstrom, S.M., and Leavesley, G.H., 1996, The GIS Weasel—An interface for the development of parameter inputs for watershed, *in* Shank, K.L., ed., Programs and Abstracts, U.S. Geological Survey National Computer Technology Meeting: Rancho Mirage, Calif., May 19–23, 1996, series 96-204, xiv, 65 p., https:/doi.org/10.3133/ofr96204.

Westerling, A.L., 2019, Wildfire simulations for the Fourth California Climate Assessment: Projecting Changes in Extreme Wildfire Events with a Warming Climate, California's Fourth Climate Change Assessment, California Energy Commission, https://www.energy.ca.gov/sites/default/files/2019-11/Projections_CCCA4-CEC-2018-014_ADA.pdf.

Westerling, A.L., Hidalgo, H.G., Cayan, D.R., and Swetnam, T.W., 2006, Warming and earlier spring increase western U.S. forest wildfire activity: Science, v. 313, no. 5789, p. 940–943, https://doi.org/10.1126/science.1128834.

Wieczorek, M.E., 2014, Area- and depth-weighted averages of selected SSURGO variables for the conterminous United States and District of Columbia: U.S. Geological Survey Data Series 866, https:/doi.org/10.3133/ds866.

Wilby, R.L., and Dettinger, M.D., 2000, Streamflow changes in the Sierra Nevada, California, simulated using statistically downscaled general circulation model scenario of climate change, *in* McClaren, S., and Kniveton, D.R., eds., Linking climate change to land surface change—Advances in global change research: Dordrecht, Springer, v. 6, p. 99–121, https://doi.org/10.1007/0-306-48086-7_6.

Appendix 1. Components of Reconstructed Natural Streamflow at CDEC Site MRC, the Merced River, California (Water Years 1950–2013), and a Simplified Schematic of the Merced Falls Project (FERC 2467, as of 2014)

Daily reconstructed streamflow (that is, full natural flows [FNF]) for Merced River near Merced Falls (CDEC MRC) is computed in cubic feet per second (ft^3/s) by the Merced Irrigation District as the sum of three components (fig. 1.1):

1. + Measured streamflow at Merced River near Merced Falls (USGS 11270900)
2. + Storage change in Lake McSwain
3. + Storage change in Lake McClure (Exchequer Reservoir).

Notes: Streamflow data have been further smoothed by DWR and provided as a calibration target for this study. From 1950 to 1964, the USGS measured daily streamflow above gage 11270900, Merced River at Exchequer (11270000). The dam at Lake McClure was completed in 1960 and enlarged in 1967, obstructing natural streamflow.

Monthly reconstructed streamflow at MRC is computed in acre-feet by DWR as the sum of

1. + Measured streamflow at Merced River near Merced Falls (USGS 11270900)
2. + Diversion at North Side Canal
3. + Evaporation at Lake McClure (also known as Exchequer Reservoir)
4. + Storage gain or loss in Lake McClure (also known as Exchequer Reservoir)
5. + Storage gain or loss in Lake McSwain

Notes: The equation for calculating monthly streamflow changed since 1957. In 1957, the flow below Exchequer, evaporation, and storage in Exchequer were used in the derivation of the monthly FNF. In 1965, the North Side Canal flows were added. Measured flows at 11270900 have been affected by the construction of Lake McSwain in 1966 and enlargement of Exchequer Reservoir (Lake McClure) in 1967. After the construction of Exchequer and Merced Falls Dam in 1967, the method of measuring streamflow shifted to reconstructing flows at a DWR's CDEC site MRC, which is co-located at USGS gage 11270900. In 1972, streamflow was measured below Lake McSwain rather than below Exchequer Reservoir (Lake McSwain was completed in 1966). Evaporation and storage change at Lake McSwain was added to the calculation. Evaporation values were considered a constant for a given month regardless of the storage for that month. So, for each year, the evaporation for January, as an example, was considered the same (Steve Nemeth, DWR Snow Survey Section, written commun., 2014).

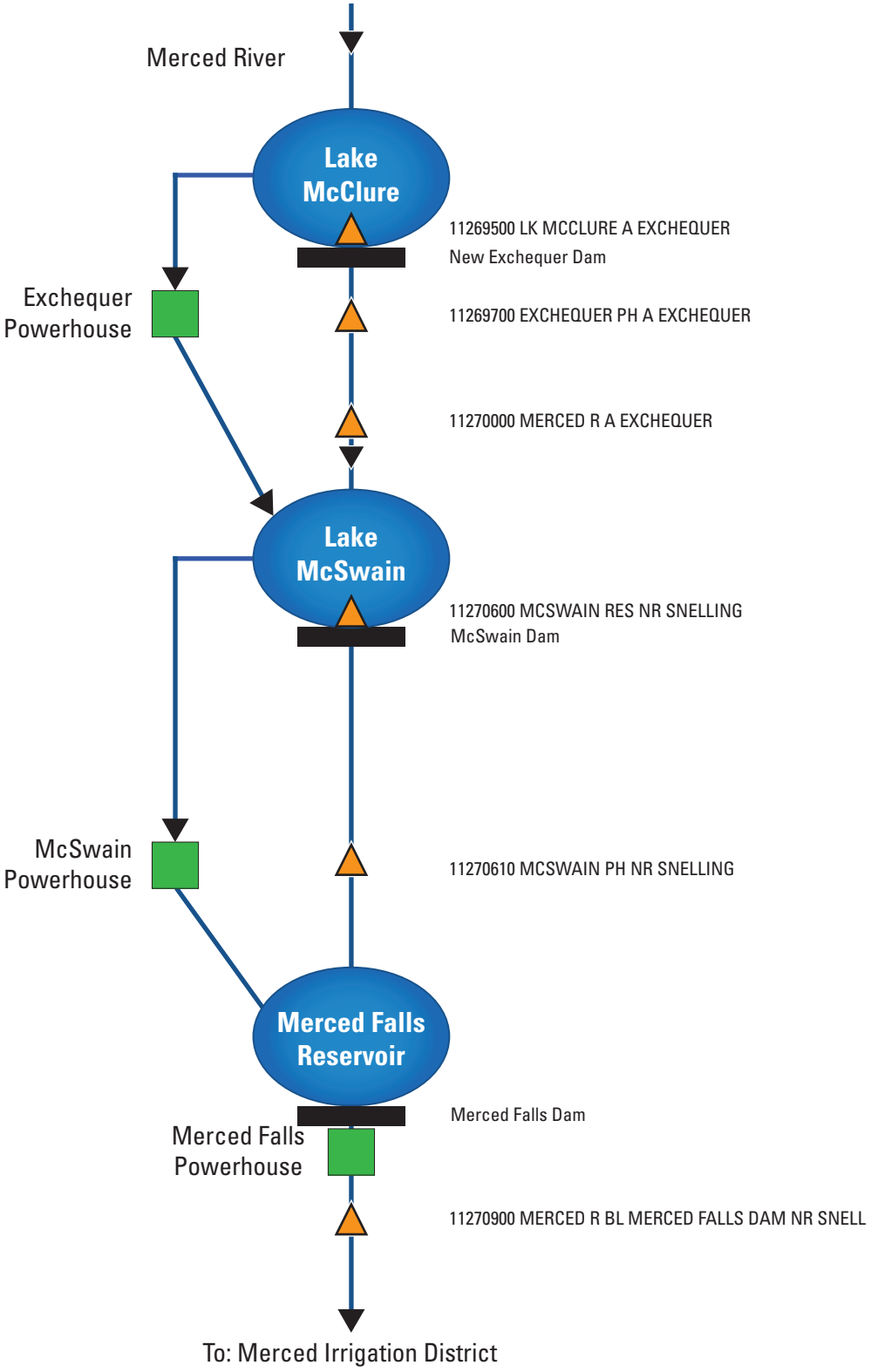

Figure 1.1. Simplified schematic of the Merced Falls Project (FERC 2467), including water supply, hydropower facilities and improvements downstream, and the locations of the U.S. Geological Survey streamflow stations from which monthly estimates of inflow to New Exchequer Reservoir (also known as Lake McClure [MID]) are derived.

For more information concerning the research in this report, contact the

Director, California Water Science Center
U.S. Geological Survey
6000 J Street, Placer Hall
Sacramento, California 95819
https://ca.water.usgs.gov

Publishing support provided by the

U.S. Geological Survey Science Publishing Network, Sacramento Publishing Service Center

ISSN 2328-0328 (online)
https://doi.org/10.3133/sir20205150